# ABSTRACT

Title of Document: CLASSIFICATION AND PROBABILISTIC MODEL DEVELOPMENT FOR CREEP FAILURES OF STRUCTURES: STUDY OF X-70 CARBON STEEL AND 7075-T6 ALUMINUM ALLOYS

Mohammad Nuhi Faridani, Master of Science, 2011

Directed By: Professor Mohammad Modarres
Department of Mechanical Engineering

Creep and creep-corrosion, which are the most important degradation mechanisms in structures such as piping used in the nuclear, chemical and petroleum industries, have been studied. Sixty two creep equations have been identified, and further classified into two simple groups of power law and exponential models. Then, a probabilistic model has been developed and compared with the mostly used and acceptable models from phenomenological and statistical points of view. This model is based on a power law approach for the primary creep part and a combination of power law and exponential approach for the secondary and tertiary part of the creep curve. This model captures the whole creep curve appropriately, with only two major parameters, represented by probability density functions. Moreover, the stress and temperature dependencies of the model have been calculated. Based on the Bayesian inference, the uncertainties of its parameters have been estimated by WinBUGS program. Linear temperature and stress dependency of exponent parameters are presented for the first time.

The probabilistic model has been validated by experimental data taken from Al-7075-T6 and X-70 carbon steel samples. Experimental chambers for corrosion, creep-corrosion, corrosion-fatigue, stress-corrosion cracking (SCC) together with a high temperature (1200 $^{0}$C) furnace for creep and creep-corrosion furnace have been designed, and fabricated. Practical applications of the empirical model used to estimate the activation energy of creep process, the remaining life of a super-heater tube, as well as the probability of exceedance of failures at 0.04% strain level for X-70 carbon steel.

# CLASSIFICATION AND PROBABILISTIC MODEL DEVELOPMENT FOR CREEP FAILURES OF STRUCTURES: STUDY OF X-70 CARBON STEEL AND 7075-T6 ALUMINUM ALLOYS

By

Mohammad Nuhi Faridani

Thesis submitted to the Faculty of the Graduate School of the
University of Maryland, College Park in partial fulfillment
of the requirements for the degree of
Master of Science
2012

***Advisory Committee:***
Professor Mohammad Modarres, (Advisor/Chair)
Professor Abhijit Dasgupta
Professor Hugh Bruck

# ACKNOWLEDGEMENTS

First and foremost, I would like to thank my advisor Prof. Modarres, for all the advice and support he has given me ever since I joined his group. I thank him for this willingness to listen to whatever I had to say, and his patient guidance over the years, which has enabled me to do this work. I would like to thank Prof. Dasgupta and Prof. Bruck for taking time off their busy schedules and reading my thesis, and serving on my thesis committee. I would like to thank my dear lab-mates Gary Paradee, Victor Luis Ontiveros, Kaushik Chatterjee and Reuel Smith for their help, and support.

Finally, I would like to acknowledge Petroleum Institute (PI) for the financial support I received during this research work.

# Table of Contents

**ACKNOWLEDGEMENTS** ..... ii

**Table of Content** ..... iii

**List of Tables** ..... viii

**List of Figures** ..... ix

**Motivation and Outline** ..... xvi

**Chapter 1: Creep and Classification of Creep Models** ..... 1

**1.1. Introduction and Definition of Creep** ..... 1

**1.2. Creep Curve** ..... 2

**1.3. Comparison of Creep Curve with Cumulative Failure** ..... 5

**1.4. Creep Mechanisms in Metals** ..... 7

**1.4.1. Dislocation Creep – (Climbs + Glides)** ..... 7

**1.4.2. Diffusion Creep** ..... 8

**1.5. Creep Deformation (Mechanisms) Map** ..... 10

**1.6. Factors Affecting the Creep Resistance of Materials** ..... 10

**1.7. Classification of Creep Relations Describing the Creep Curves** ..... 12

**1.7.1. Introduction** ..... 12

**1.7.2. Classification of creep models according to: (Strain-time-, Stress-, and Temperature-dependency)** ..... 15

**1.7.3. A New and Simple Classification of Creep Relations** ..... 19

**1.7.4. Classification of the Creep Models According to Three Parts of the Creep Model ..... 20**

**Chapter 2: Development of an Empirical Model and Testing Its Workability in Comparing with Acceptable Creep Models in the Literature ..... 22**

**2.1. Introduction ..... 22**

**2.2. A Review of Creep Models ..... 22**

**2.3. Development of a Probabilistic Model Based on Previous Work ..... 25**

**2.4. The Effect of Model Parameters on the Form of the Creep Curve ..... 27**

**2.5. Comparison of proposed Empirical Probabilistic Model with the Well-Known Creep Models ..... 30**

**2.5.1. Comparison with Theta-Projection Model ..... 30**

**2.5.2. Comparison with Kachannov-Rabotnov-Creep-Damage Model ..... 32**

**2.6. Statistical Consideration: Comparison of proposed Empirical Model with Theta Model for derivation of Residual Errors ..... 37**

**2.7. Model Comparison with Akaike Relation ..... 40**

**2.8. Model Uncertainty (Bayesian) Approach for Model Comparison ..... 43**

**Chapter 3: Specifying Stress and Temperature Dependencies of Creep Curve Parameters ..... 45**

**3.1.Specifying Stress Dependencies ..... 45**

**3.2. Results and Discussion ..... 47**

**3.3.Specifying Temperature Dependencies ..... 49**

**3.4.Results and Discussion** ..... **51**

**Chapter 4: Experimental Efforts for Al-7075-T6 and X-70 Carbon Steel** ..... **53**

**4.1.Experimental Efforts for creep tests** ..... **53**

**4.2.Introduction** ..... **53**

**4.3 Experimental Equipments Developed** ..... **53**

**4.4.Sample Preparations and Accompanied Problems** ..... **56**

**4.4.1. Al-7075-T6-Samples** ..... **56**

**4.4.2. X-70 Carbon Steel Samples** ..... **57**

**4.5. Preliminary Creep Experiments with Al-7075-T6 Alloys** ..... **61**

**4.6.Preliminary Creep Experiments with X-70 Carbon Steel Samples** ..... **66**

**4.7.Final Experiments on Al-7075-T6 Alloys** ..... **67**

**4.8.Final Experiments on X-70 Carbon Steel Alloys** ..... **74**

**Chapter 5: Estimation of the Proposed Empirical Model Parameters Using Bayesian Inference** ..... **82**

**5.1. Introduction** ..... **82**

**5.2. Estimation of Proposed Empirical Model Parameters for Al-7075-T6 Using Bayesian Inference** ..... **84**

**5.3. Estimation of Proposed Empirical Model Parameters for X-70 Carbon Steel Using Bayesian Inference** ..... **88**

**Chapter 6: Calculation of Rupture Analysis, Creep Activation Energy, and a Case Study 91**

**6.1. Introduction** ..... **91**

**6.2. Rupture Analysis for Al-7075-T6 and X-70 Carbon Steel** ..... **91**

**6.3. Creep Activation Energies for Al-7075-T6 and X-70 Carbon Steel** ..... **94**

**6.4. Practical Example:** ..... **96**

**6.4.1. Case Study I: Estimation of Remaining Life of Super-heater/Re-heater Tubes** ... **96**

**6.4.2. Case Study II: Estimation of Probability of Exceedance (PE) on 0.04% Strain Level** ..... **99**

**7.Coclusion** ..... **104**

**Appendix A. Creep Models Summarized from 1898 to 2007** ..... **106**

**Appendix B. References to creep models** ..... **121**

**Appendix C. MATLAB-Program for 7075-T6 Creep (Stress Dependency)** ..... **129**

**Appendix D. MATLAB-Program for Creep of X-70 Carbon Steel (Stress and Temperature dependency)** ..... **132**

**Appendix E. Example of a WinBUGs- Program for Creep of materials** ..... **137**

**Appendix F. Example of a WinBUGs- Program for Non-linear Regression of Creep of materials** ..... **137**

**Appendix G. Akaike Infromation Criterion** ..... **137**

**Appendix H. First Page of Published Papers** ..... **137**

**Regerences from Chapter 1 to 6** ..... **143-150**

# List of Tables

Table 1.1: Approximate max. service temperature T(max) of several materials under high mechanical stresses compared to their pure melting points T(m)……2

Table 1.2: Most important creep model that describe the whole creep curve from primary (P), to secondary (S) and tertiary part applied to [10 Cr Mo (9-10)] steel alloys [81] .....21

Table 2.1: AIC-values from comparison of different creep models for the given experimental data……42

Table 3.1: Data calculated with our model at T=600 C, evaluated under fifteen different stress conditions (a), and (b) for 2 ¼ Cr 1Mo pipeline steel……47

Table 3.2: Data calculated by Regression Analysis in Excel (a) and by WinBUGs (b) to develop our model , evaluated under seven different temperature conditions for Mo-V pipeline steelat a definite applied stress…….……51

Table 4.2: Numerical values for corresponding parameters of the proposed empirical model…….....78

Table 6.1: Probability and probability of exceedance on the 0.04 Strain level at different times…….…103

# List of Figures

Figure 1.1: Illustration of a typical creep curve showing three common regions of creep curve (left) and their stress and temperature dependencies (right) [1]……..4

Figure 1.2: Classification of creep damage from metallurgical point of view [3], formation of cavities at grain boundaries up to final creep fracture…….…....5

Figure 1.3: Strain and strain-rate versus time of a typical creep experiment (left hand) compared with the cumulative and failure rate in percent versus time in reliability (right hand) [4]…….....6

Figure 1.4: Dislocation creep mechanisms, by vacancy climb and climb and glide over obstacle, optical micrographs showing longitudinal section near the fracture surface, and TEM Picture from dislocations on the fracture surfaces [5, 6]…….....8

Figure 1.5: Different diffusional creep mechanisms (Nabarro-Herring and Coble), and grain growth, cavitations, intergranular and transgranular mode of rupture and rupture dynamic [5, 6]……..9

Figure 1.6.: Creep deformation map of pure Aluminium and Iron with given different fracture modes of Tran- and inter-granulare repture mechanisms [7, 8, 9]…….....10

Figure 1.7: Tri-planar optical micrographs showing microstructural features observed in 7075 Al. Top and typical creep curves showing their true tensile strain, as a function of time, t. Samples tested under uniaxial and the same conditions [11, 12] ……11

Figure 1.8: Schematic representation of the Kelvin-Voigt creep model…….....13

Figure 2.1: Graham–Walles approach is the superposition of three individual terms, schematically [17]…….……25

Figure 2.2: The effect of parameter A on creep curves…….27

Figure 2.3: The effect of n on behavior of creep curves……....28

Figure 2.4: The effect of n on behavior of creep curves……28

Figure 2.5: Scaling effect of m and p on creep curves…….……..29

Figure 2.6: Strain vs. time comparison of the theta and proposed models……31

Figure 2.7: Strain rate vs. time comparison of the theta and proposed models…….31

Figure 2.8: Kachanov's damage model (area loss ~ damage)……...32

Figure 2.9: Kachanov's strain-time relation….....34

Figure 2.10: Strain and strain rate fractions versus time for different materials…….....35

Figure 2.11: Kachanov's strain -time relation with and without primary strain…….……...36

Figures 2.12: Kachanov's strain-time model (blue) compared with the proposed empirical model (red)……...…….36

Figure 2.13: Creep curves for an Aluminum alloy tested at $100^0$C and340 MPa with the data of three models [15]……..38

Figure 2.14: Residual errors for theta (4) and theta (6) models…….39

Figure 2.15: Residual errors versus time…….…….….39

Figure 2.16:.Comparison of different creep models with the given experimental data…….....42

Figure 2.17:Comparing different model data as predicted strain model data with the measured data……..……...44

Figure 3.1: Stain versus Time relation for 2-1/4Cr-1Mo pipeline alloy under an appliedstresses of σ=138 MPa, and T=600 $^0$C in vacuum and air [12]…….…….46

Figure 3.2: Creep curves from data given in table 4.1 to estimate stress dependency of the parameters of the empirical model; series 1 to 15 correspond to 15 different stress conditions……..…….48

Figure 3.3: Creep test results for Mo-V steel for a stress [22]……...50

Figure 3.4: simulated creep test result for Mo-V steel……...50

Figure 4.1: The corrosion-fatigue chamber with the prototype Dog-bone specimen in MTS machine…….….54

Figure 4.2: The corrosion fatigue and SCC chamber installed in the MTS equipment. The top left and right bottom pipes are the inlet and outlet of corrosive liquid……...….55

Figure 4.3: The heating chamber for creep experiment during the temperature test before installing in the MTS machine…….…..56

Figure 4.4: Al-sample fixed in the threaded holders (left) and into the grips of MTS machine (right)…….……...….57

Figure 4.5: Al-sample with two threaded holders (left), in top or bottom view (right)…….…57

Figure 4.6: X70 carbon steel with top and bottom threaded grips…….……...58

Figure 4.7: X70 carbon steel fixed in the furnace (left) and connected to the MTS macine (right)……...…..58

Figure 4.8: X-70 samples with two long grips (top left), sample connected to the grips, real dimensions (top right), sample connected to grips in furnace (bottom left), and in MTS machine (bottom right)…….59

Figure 4.9: deformed CT samples and the threaded grip part before and after deformation……60

Figure 4.10: X-70 threaded dog bone samples, 4mm cross section diameter, and gauge length of 45mm with grips for installation in the creep furnace…….....61

Figure 4.11: Stress- Strain Curve of Al-7075-T6 Alloy left , and stress-strain curve of the same alloy from the literature with elongated grains (etched with 10% phosphoric acid)[1]…….....62

Figure 4.12: Stress-Displacement Curve for Al 7075-T6 (left), and Stress-Displacement Curve for Al 7075-T6 (Elastic Region) (right)……....…62

Figure 4.13: MTS Displacement vs. Time for Different Al-7075-T5 Alloys at Different Stresses……...63

Figure 4.14: Displacement-Time (creep curve) of Al-7075-T6 at 400°C……...….64

Figure 4.15: Ductile transgranular mode of rupture form of Al-creep sample at 400°C, with recrystallized grain growth form and compared picture given in the literature…….....65

Figure 4.16: X-70 threaded dog bone samples, 4mm cross section diameter, and gauge length of 45mm with grips for installation in the creep furnace]…….65

Figure 4.17: Stress-strain curve of X-70 carbon……....66

Figure 4.18: Ductile cup and cone form of rupture cross section of X-70 carbon steel, broken sample parts, and grain elongation toward the necking region …….....67

Figure 4.19: MTS-810 Material Test System equipped with creep furnace and data acquisition.68

Figure 4.20: Al-7075-T6 used in creep experiments with hardened grip holders…….68

Figure 4.21: Stress strain curve of Al-7075 at different temperature compared with the given stress strain curve at room temperature from the literature [1]…….….69

Figure 4.22: Creep curves of Al-7075 from experiment and fitted with the proposed empirical model by Excel…….....70

Figure 4.23: Creep curves of Al-7075-T6 at different temperature and stresses from data given in the above table (bulk) and additional predicted creep curves at proposed temperature and stresses (thin lines)……...…..73

Figure 4.24: PDF and CDF of parameter, A = LN (μ=19.79, σ=0.11)…….....…..…73

Figure 4.25: PDF and CDF of parameter, B= LN (μ=-131-47, σ=0.12)……..…....74

Figure 4.26: Three dog bone X-70 carbon steel samples with threaded parts at two ends made from a part of X-70 carbon steel pipe……....74

Figure 4.27: Dog boned X70 carbon steel samples used for the creep experiment…….…..…75

Figure 4.28: Broken sample at room temperature with cup and cone ductile breakage (left) and two X70 carbon steel samples after creep experiment with brittle fracture types (right)……..75

Figure4.29: creep curve of X70 carbon steel at T=450°C and σ= 348MPa,(left) and predicted creep curve at 418°C both fitted with proposed empirical equation……..…76

Figure 4.30: Creep curves of X-70 carbon steel from experiment and fitted with the proposed empirical model by Excel…….....77

Figure 4.31: Creep curves of X-70 carbon steel at different T and σ from data in the above table (bulk) and predicted creep curves at proposed temperature and stresses (thin lines)……....80

Figure 4.32: PDF and CDF of parameter A = LN (μ=38.47, σ=0.11)…….....80

Figure 4.33: PDF and CDF of parameter B= LN (μ= -17.94, σ=0.12)……..……..…...81

Figure 5.1: (Top) Algorithm for the Bayesian approach and (Bottom) the corresponding posterior distributions of A, B and s……...….86

Figure 5.2: Values of node statistics for Al-7075-T6 model parameters taken from WinBUGs program……..…87

Figure 5.3: (Top) Algorithm for the Bayesian approach and (Bottom) the corresponding posterior distributions of A, B and s……...…..89

Figure 5.4: Values of node statistics for X-70 carbon steel model parameters taken from WinBUGs program……90

Figure 6.1:Creep curve, prepared for estimation of Monkman-Grant relation……92

Figure 6.2: Creep curve of Al-7075-T6 samples at T= 400°C and σ = 100Mpa, after 44.3 hrs = 1.84 days……..……...…...93

Figure 6.3: Creep curve of X70carbon steel at T=450°C and predicted at T= 418°C and σ=348.8 MPa, fitted by our proposed model……...94

Figure 6.4: The remaining life is lognormal distributed with a mean of 49600 hrs. Calculated by MATLAB program……...….98

Figure 6.5: The remaining life is lognormal distributed with a mean of 49600 hrs. calculated by Weibull++ program……99

Figure 6.6: Lognormal distributions estimated on 0.04 % strain with their corresponding probability of exceedance (filled brown area……..…100

Figure 6.7: Lognormal PDF's calculated with MATLAB code for 0.04 % strain level (practical strai limit in service) for X-70 carbon steel……101

Figure 6.8: Lognormal cumulative distributions calculated by Weibull++ for 0.04 % strain level (practical strain limit in service) for X-70 carbon steel……...101

Figure 6.9: Lognormal PDF's calculated byEXCEL, and drawn by Weibull++ for 0.04 % strain level for X-70 carbon steel……...102

Figure A.1: Schematic presentation of three parts of the creep curve (a), and strains generated during the loading in a creep test [8]…….……..120

Figure C1: MATLAB-picture from the above program for stress dependency of Al-7075-T6……131

Figure D1: MATLAB-picture from the above program for stress dependency of X-70 carbon steel……..136

# Motivation and Outline

Thermal power plants and refineries around the world share many of the same problems, namely aging equipment, high costs of replacement, and the need to produce more efficiently while being increasingly concerned with issues of safety and reliability. For equipment operating at high temperature, there are many different mechanisms of degradation, some of which interact with each other, and the rate of accumulation of damage is not simple to predict.

The principal deterioration mechanisms in high temperature plant are creep damage, micro-structural degradation, high temperature fatigue, creep-fatigue, hydrogen embrittlement, thermal shock, erosion, and high temperature corrosion of various types. Besides, although stress corrosion cracking and aqueous corrosion are not generally expected in high temperature components, they may cause problems during the components cooling while liquid is still present.

Creep is one of the most serious high temperature damage mechanisms. It involves time-dependent deformation. High temperature creep cracking generally develops in components that fail over an extended time such as boiler super-heater, petro-chemical furnace, reactor vessel components and gas turbine blades, and all other components operating at high temperature. In addition, local overheating at high temperatures may cause local deformation with large plastic strains and local wall thinning. In-service degradation with creep is one of the most critical factors determining the structural integrity of elevated temperature components in power plants, chemical plants, and oil refineries. Therefore study of creep, fatigue, corrosion and their effects on life time of materials subjected to high stress at high temperature is necessary. To investigate the pipeline health, risk and reliability, it is highly important to model creep and creep-corrosion phenomenon to characterize the observed deformation and fracture with respect to time.

In order to make such assessments on a sound basis, this thesis intends to address in detail the issues related creep relations and classifications to develop a probabilistic model derived from a physics of failure approach.

In chapter one, the general definition of creep and creep mechanisms from phenomenological point of view is provided. Besides, a classification of creep relations describing the creep curves is given together with the classification of creep models according to strain-time-, stress-, and temperature dependency; another classification is provided with respect to three parts of the creep curve.

In chapter two, a physically informed empirical model is developed and justified in its comparison with the mostly used and acceptable models from phenomenological and statistical points of view. This model that based on a power law approach for the primary creep part and a combination of power law and exponential approach for the secondary and tertiary part of the creep curve captures the whole creep curve appropriately. Besides, stress and temperature dependencies of our model are presented.

In chapter three stress and temperature dependencies of parameters of creep model from published data are specified.

In chapter four, the new probabilistic model is validated by experimental data taken from Al-7075-T6 and X-70 carbon steel samples. The details of experimental designs of chambers for corrosion, creep-corrosion, corrosion-fatigue, stress-corrosion cracking (SCC) (to do the experiments both on CT and dog-boned steel and Aluminum samples), and a high temperature (1200 $^{0}$C) furnace for creep and creep-corrosion (gas pressure) furnace both for CT and dog-boned samples are provided.

In chapter five, uncertainties of the mechanistic models as well as their parameters were estimated by WinBUGS program based on Bayesian Inference.

In chapter six practical applications of the empirical model to estimate the activation energy of creep process were provided, and two case studies to estimate the remaining life of a super heater tube, and probability of exceedance of failures at 0.04% strain level for X-70 carbon steel were given.

# Chapter 1: Creep and Classification of Creep Models

## 1.1. Introduction and Definition of Creep

Creep is the occurrence of time dependent strain in material under constant stress, normally at elevated temperature. Creep occurs as a result of the competing processes of work hardening caused by the applied force (tensile or compressive stress) and of annealing due to high temperature. Creep usually attributed to vacancy migration in grains of bulk materials or along the grain boundaries in direction of applied stresses, (Nabarro-Herring, and Coble mechanisms), and causing grain boundary sliding and separation, and dislocation climb and cross-slip.

Creep deformation also continues until the material fails because of creep rupture. Creep occurs usually at high temperatures typically at 40-50% of the melting point of the material ($T_m$) in Kelvin. In crystalline materials the activation energy Q is approximately equal to the activation energy of the self-diffusion of the material. Diffusion of atoms and vacancies at grain boundaries and in grains in direction of applied tensile stress result in an elongation and in a decrease in cross section of materials in a creep experiment. Besides, since enthalpy of vacancy formation is correlated with the binding forces in the material and thus with the melting temperature, then the homologous temperature ($T/T_m$) is used as a parameter to characterize the creep properties [1].

High temperature materials have a large value of binding energy and so they need a large amount of energy to create and move vacancies. A rule-of-thumb is the maximum service temperature of mechanically highly stressed materials with $T/T_m$=0.5. Approximate maximum service temperature $T_{max}$ of several materials compared to their pure melting points $T_m$ are given

in Table 1.1 [1]. Exceptions to the rule are Ni-based super-alloys with higher service temperatures used as aero engines.

**Table 1.1: Approximate maximum service temperature T(max) of several materials under high mechanical stresses compared to their pure melting points T(m) [1]**

| Material | $T_m$[K] | $T_{max}$[K] | $T_{max}/T_m$ |
|---|---|---|---|
| Al-alloys | 933 | 450 | 0.48 |
| Mg-alloys | 923 | 450 | 0.49 |
| Ferritic steels | 1811 | 875 | 0.48 |
| Ti-alloys | 1943 | 875 | 0.45 |
| $Al_2O_3$ | 2323 | 1200 | 0.52 |
| SiC | 3110 | 1650 | 0.53 |
| Ni-based superalloys | 1728 | 1728 | 0.75 |

Creep tests are usually made by deformation of material as a function of time when material is under constant or variable stresses at a constant elevated temperature.

The standard practice for creep experiments of metallic materials is specified in ASTME139 [2], and the test may proceed for a fixed time and to a specified strain. It is usually not practical to conduct full-life creep tests, because such a test takes a long time.

## 1.2. Creep Curve

The basic record of creep behavior is a plot of strain (ε) versus time (t). It is often useful to differentiate this data numerically to estimate the creep rate dε/dt vs. time. The shape of the creep curve is determined by several competing mechanisms, including:

1. **Strain Hardening:** With increasing strain, creep rate gradually decreases. This hardening transient is called "primary creep". Then the creep rate reaches a nearly constant value known as the steady state creep rate or minimum creep rate $\dot{\varepsilon}_m$. This value is usually used to characterize the creep resistance of materials and to identify the controlling mechanisms of the creep.

2. **Softening process:** While strain hardening decreases the creep rate the softening process increases the creep rate. So the balance between these factors and the damaging process determines the shape of the creep curves and results in a constantly increasing creep rate known as "secondary creep". This process includes processes like recovery, re-crystallization, strain softening and precipitate over-aging (in precipitation hardened materials). The extension of the steady state part (secondary creep) is material dependent. This part is longer for solid solution alloys and shorter in particle strengthening alloys [12].

3. **Damaging Processes:** As strain continues, micro-structural damages continue to accumulate and the creep rate continues to increase. This final stage, or "tertiary creep", results in final failure of the material (gradual or abrupt rupture of the specimen). This process includes cavitations (such as voids at grain boundaries), necking of the specimen and cracks in grains and grain boundaries.

Therefore, every creep curve is comprised of three different parts. These three parts with their stress and temperature dependencies are given in the following figure.

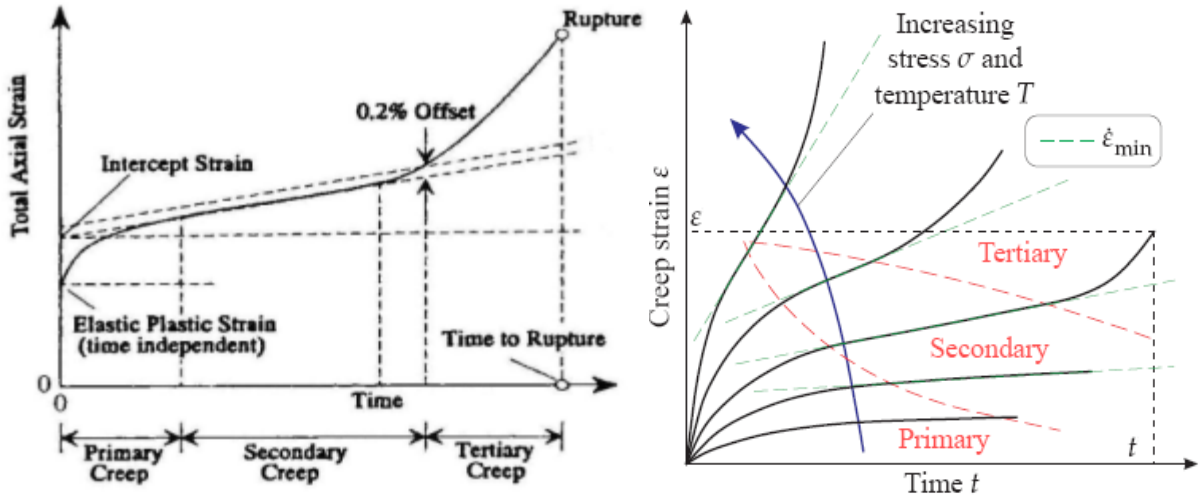


**Figure 1.1: Illustration of a typical creep curve showing three common regions of creep curve (left) and their stress and temperature dependencies (right) [1,2]**

Studying three parts of creep curve helps in understanding the whole process.

As the creep deformation begins to proceed in time, by applying a constant stress, the number of dislocations in material increases and the material get harder (hardening process).

The increase of the dislocation density has a limit; as the result of keeping the material at an elevated temperature, the dislocations can change their places (by climbing) and re-arrange themselves in an energetically more favorable configuration or condition, called recovery. In other words, there is a competition between additional generation of dislocations (as the result of plastic deformation), and cancellation in the recovery process. Therefore, the creep rate becomes nearly constant as a result of such equilibrium and so the secondary part is built. In this part of the curve, local stress concentrations at grain boundaries help the formation of cavitations and pores.

In tertiary creep, the creep rate increases again as a result of massive structural damages. At high stresses, the material fails due to formation of micro-cracks and cavitations at grain boundaries or because of inter-crystalline fractures [1, 2].

The secondary and tertiary parts of the creep curve are accompanied by a morphological change in materials. This morphological change starts from voids formation in the secondary parts; the aggregation of voids results in micro-cracks formation, which leads to complete rupture and fracture. Figure 1.2 shows these morphological changes for a steam generator schematically [3].

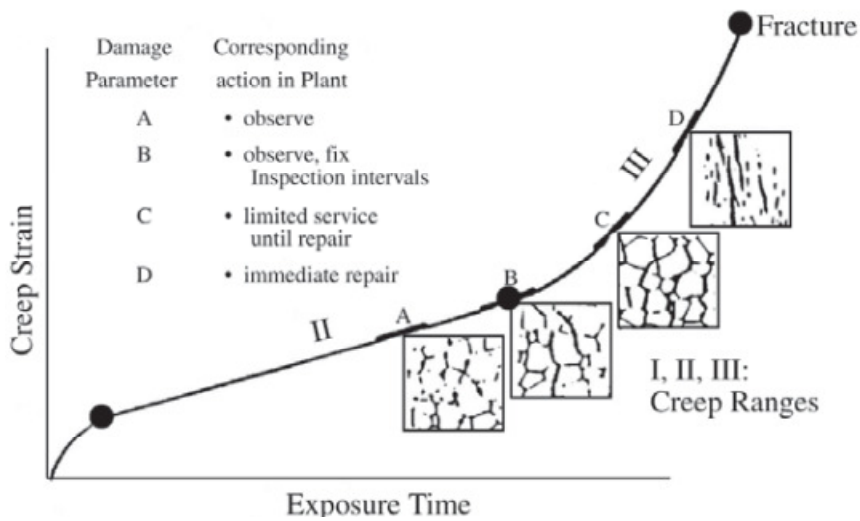


**Figure 1.2: Creep life assessment based on classification of creep damage from metallurgical point of view [3], formation of cavities at grain boundaries up to final creep fracture**

### 1.3. Comparison of Creep Curve with Cumulative Failure

A typical schematic plot of strain and strain-rate versus time for an ideal material is given in the left side of Figure 1.3. As it can be seen in Figure 1.3, the counterpart of creep strain versus time is the cumulative failures versus time in reliability. Besides, the counterpart of the

strain-rate versus time in creep is the failure rate percentage versus time (Bathtub curve) in reliability. Therefore, a cumulative degradation process can represent the creep experiment in time.

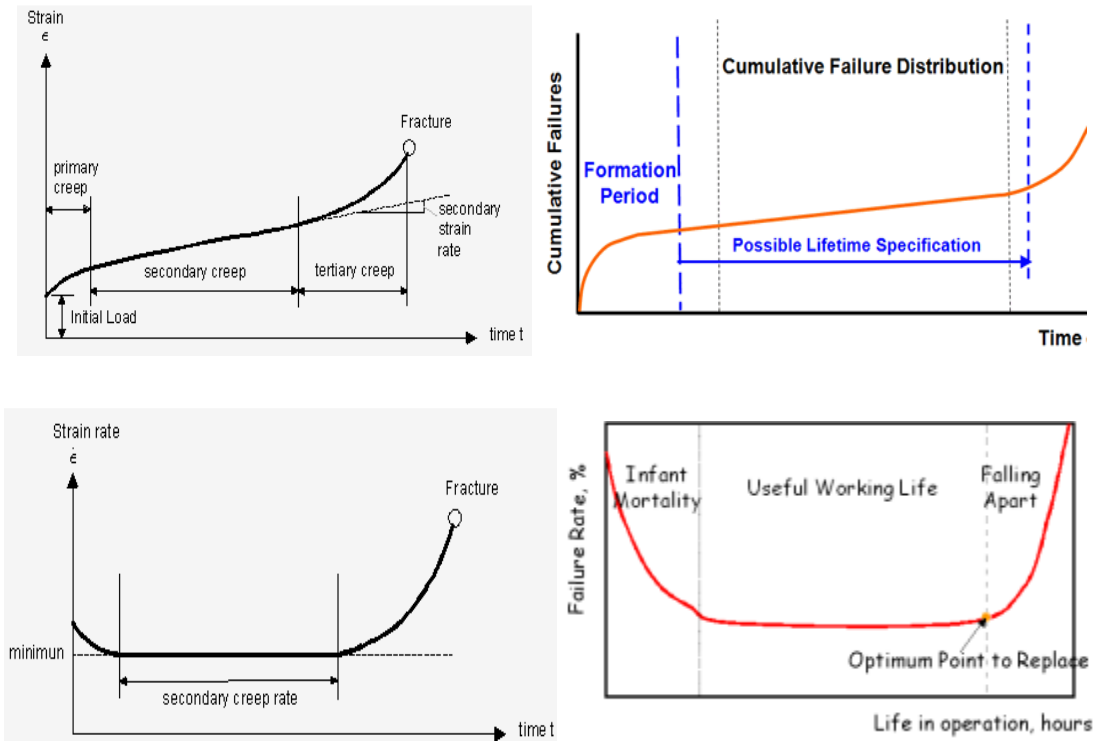


**Figure 1.3: Strain and strain-rate versus time of a typical creep experiment (left hand) compared with the cumulative failures and failure rate in percent versus time in reliability (right hand) [4]**

In the primary (transient) part of creep curve, strain (cumulative failure in reliability) increases, while the strain rate (failure rate) decreases continuously. In the secondary part, the strain increases nearly with a constant rate; this is also called the steady state creep, which can be compared with the constant failure rate part in reliability bathtub curve. In tertiary part, the creep rate strongly increases until the final fracture happens. This part is accompanied by a massive inter-structural damage of the material (comparable with the wear out of bathtub curve).

## 1.4. Creep Mechanisms in Metals

The response of a metallic body to mechanical stress σ below the yield stress of the metal results in an instantaneous elastic strain $\varepsilon_{el}$. The yield stress cannot be defined as a sharp limit. However, it can be stated that applied stress above the yield stress causes immediate plastic deformation. Creep in metals, i.e. the time-dependent plastic deformation of metals may occur at mechanical stress well below the yield stress. The creep strain rate $\dot{\varepsilon}$ is described and calculated as a function of temperature T, stress σ, structural parameters $S_i$ (such as dislocation density and grain size) and material parameters $M_j$ (such as diffusion constants or the atomic volume).

$$\dot{\varepsilon}_t = (T, \sigma, t, S_i, M_j) \tag{1.1}$$

There are three basic mechanisms that play significant role in both creep process and time-depending plastic deformation characterization; these three mechanisms are:

- Dislocation creep –(climb + glides)
- Diffusion creep: Nabarro Herring (volume diffusion- : interstitial and vacancy-diffusion)
- Diffusion creep: Coble (grain boundary diffusion

### 1.4.1. Dislocation Creep – (Climbs + Glides)

High stress below the yield stress causes creep by motion of dislocations, i.e. glide of dislocations. This motion of dislocations is hindered by the crystal structure itself (i.e. the crystal resistance). Further, discrete obstacles like single solute atoms, segregated particles or other dislocations block the motion of gliding dislocations. At high temperatures obstacle blocked dislocations can be released by dislocation climb. The diffusion of vacancies through the lattice or along the dislocation core into or out of the dislocation core drives the dislocation to change

its slipping plane and to pass by the obstacle. Atoms diffuse into or out of dislocation core, lead to dislocation climb and dislocation climb-and-glide leads to creep [5, 6]. Dislocation mechanism, optical microscopic and TEM pictures are given in the Figure 1.4.

Dislocation rate of such a mechanism is given by:

$$\dot{\varepsilon}_D = A\frac{DGb}{kT}\left(\frac{\sigma}{G}\right)^n \tag{1.2}$$

where A is a material parameters, D is the diffusion coefficient, G is shear modulus, b is Burgers vector, σ is the applied stress, n is a material dependent constant, k is the Boltzmann constant, and T is the temperature given in Kelvin.

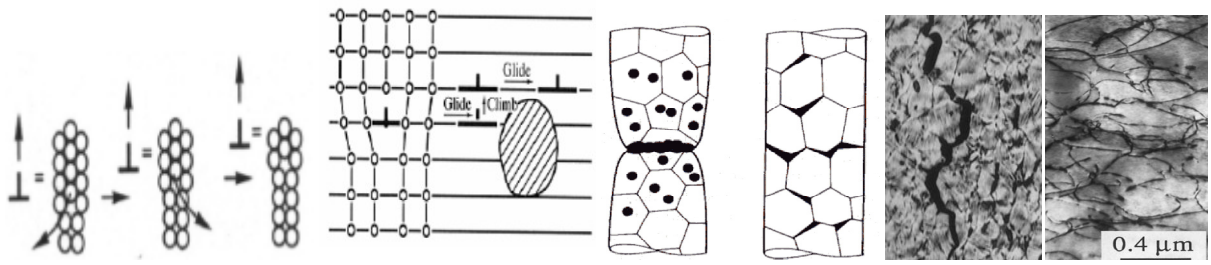


**Figure 1.4: Dislocation creep mechanisms, by vacancy climb and climb and glide over obstacle, optical micrographs showing longitudinal section near the fracture surface, and TEM Picture from dislocations on the fracture surfaces [5, 6]**

### 1.4.2. Diffusion Creep

Diffusion creep is significant at low stress and high temperature. Under the driving force of the applied stress, atoms diffuse from the sides of the grains to the tops and bottoms. The grain becomes longer as the applied stress is applied, and the process will be faster at high temperatures due to presence of more vacancies. Atomic diffusion in one direction is the same as vacancy diffusion in the opposite direction. This mechanism is called Nabarro-Herring creep [5].

The jump frequency of atoms and vacancies are higher along the grain boundaries. This mechanism is called Coble creep [5, 6]. The rate controlling mechanisms in both cases are vacancy diffusion, or self-diffusion. These two mechanisms are shown in Figure 1.5.

Strain rate of these mechanisms are given by:

$$\dot{\varepsilon}_{NH} = A_{NH}\frac{D_V}{d^2}\frac{\sigma\Omega}{kT} \qquad \dot{\varepsilon}_C = A_C\frac{\delta D_{gb}}{d^3}\frac{\sigma\Omega}{kT} \tag{1.3}$$

where, d is the grain diameter, Ω is the volume of a vacancy; δ is the grain boundary thickness, σ is the external stress, $D_V$ is the diffusion coefficient for the self-diffusion through the bulk material, and $D_{gb}$ is the diffusion coefficient for the self-diffusion along the grain boundary.

So it is possible to use these relationships to determine which mechanism is dominant in a material; varying the grain size and measuring how affect the strain rate.

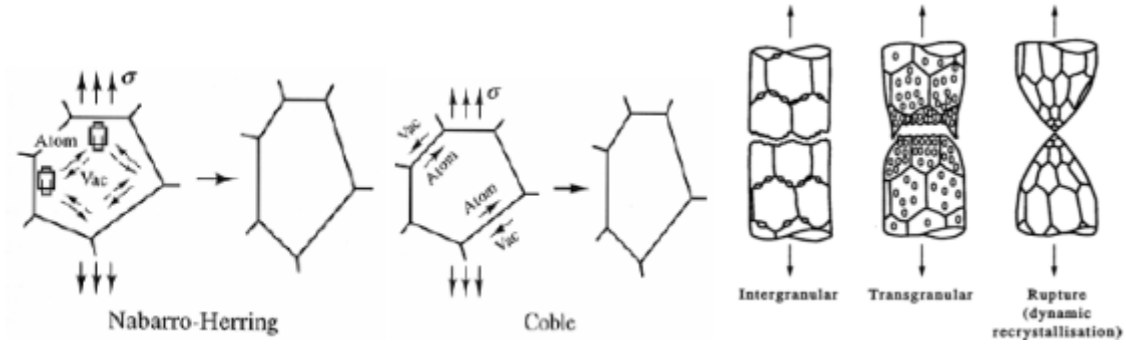


**Figure 1.5.: Different diffusional creep mechanisms (Nabarro-Herring and Coble), and grain growth, cavitation, inter-granular and trans-granular mode of rupture and rupture dynamic [5, 6]**

## 1.5. Creep Deformation (Mechanisms) Map

Deformation and fracture mechanism map, developed by Ashby and Mohamed and Langdon, is a useful tool to characterize the type of deformation and the relevant fracture mechanisms [7, 8]. The deformation map helps to find the mode of fractures (inter-granular or trans-granular) of that special material. The maps of pure Aluminum (for 7075-T6 Aluminum), and iron (for X-70 carbon steel), used for experiments of this thesis, are given in Figure 1.6.

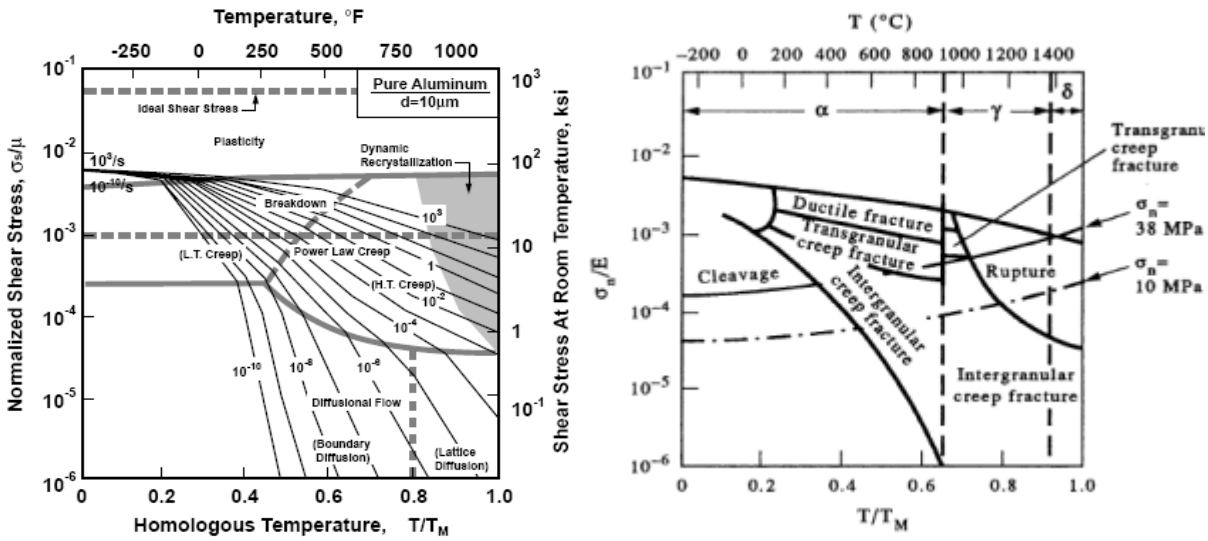


**Figure 1.6.: Creep deformation map of pure Aluminium and Iron with given different fracture modes of Tran- and inter-granulare rupture mechanisms [7, 8, and 9]**

Creep experiments can be conducted according to the given temperatures and applied stresses given above for aluminum and steel alloys, and so it is possible to prove the inter-granular or trans-granular mode of fracture of the samples accordingly.

## 1.6. Factors Affecting the Creep Resistance of Materials

It is very important to note that factors such as heat treatments, grain orientation and solution treatment significantly affect the creep curve in its primary, secondary and tertiary parts.

The creep curve is not only dependent on the heat treatment but also on the grain orientation of the material under test because the fracture toughness of a material commonly varies with grain direction.

Figure 1.7 shows the creep curves of Al7075 subjected to one stress (8.8 MPa) and one temperature (648K) in different orientations and previous heat treatments. As it can be seen, the creep curve forms are highly affected by the above-mentioned factors [10-12].

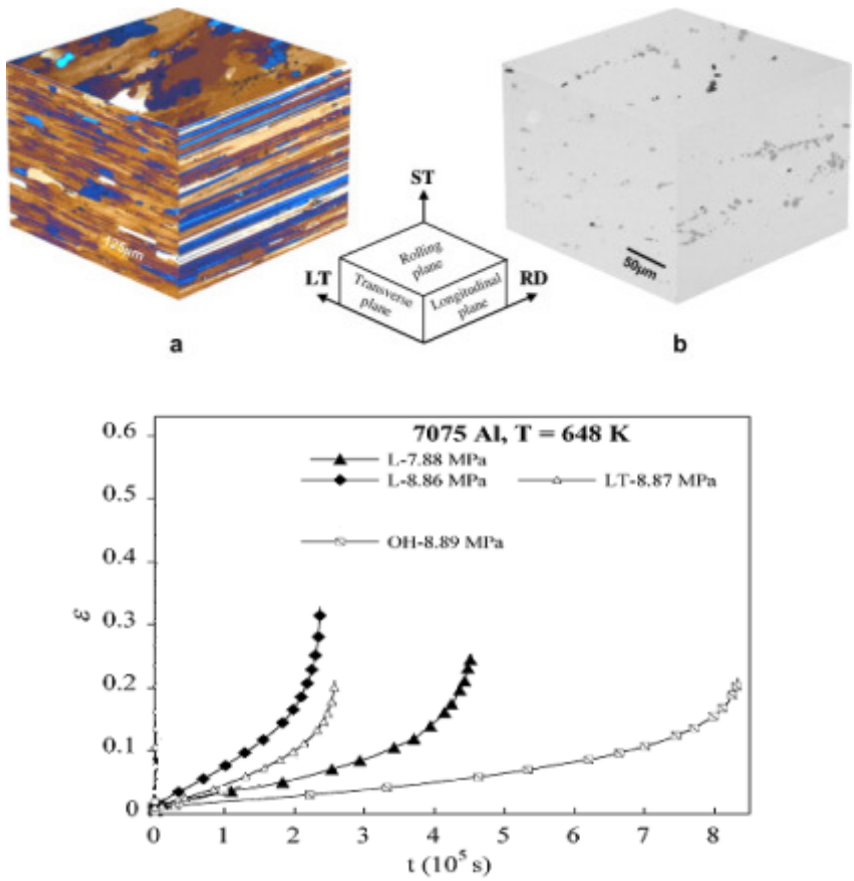


**Figure 1.7: Tri-planar optical micrographs showing micro-structural features observed in 7075 Al. Top and typical creep curves showing their true tensile strain, as a function of time. samples tested under uniaxial and the same conditions [11,12]**

## 1.7. Classification of Creep Relations Describing the Creep Curves

### 1.7.1. Introduction

More than sixty-two creep relations (Appendix) from Kelvin-Voigt creep model (1898) [13] to Holmström- Auerkari- Holdsworth (Logistic Creep Strain Prediction model (2007) [14], by searching the literature were identified. Thirty-three of these models describe the creep process according to power low and twenty-eight of them are based on the exponential approach (Appendix). Logarithmic approach was considered as power law and sine hyperbolic and cosine hyperbolic relations as exponential approach.

It should be mentioned that nearly all of the exponential approaches are based on the idea of the Kelvin-Voigt of visco-plastic deformation of creep in materials. Recent investigation shows that this approach is unable to describe the primary part of the creep curve; in addition, recent Evan's attempt to extend his 4-theta to 6-theta model [15] (by addition of more parameters) shows that exponential approach is not an adequate approximation for describing the creep process.

First the idea behind the visco-plastic creep approach of Voigt model is described. Description of creep process as a visco-plastic process goes back to the Kelvin–Voigt model [13] around 1898, known as the Voigt model, which consists of a Newtonian viscous damper (dashpot = D) and Hookean elastic spring (S) connected in parallel. Since the two components of the model are arranged in parallel, the strains in each component are identical.

$$\varepsilon_t = \varepsilon_D = \varepsilon_S \tag{1.4}$$

The total stress is the sum of the stresses of each component.

$$\sigma_t = \sigma_D + \sigma_S \tag{1.5}$$

where $\sigma_D = \eta \cdot \frac{d\varepsilon}{dt}, and\ \sigma_S = E \cdot \varepsilon\ with\ \eta = viscosity, E =$ materials Young's Modulus

Schematic representation of Kelvin-Voigt model is given in the Figure 1.8.

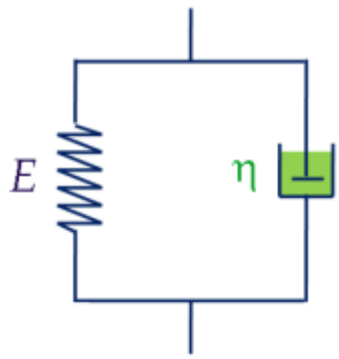


**Figure 1.8: Schematic representation of the Kelvin-Voigt creep model**

This model represents a solid that undergoes reversible, viscoelastic strain. By applying a constant stress, the material deforms at a decreasing rate, and approaches a steady-state strain. When the stress is released, the material relaxes to its un-deformed state. At constant stress (creep), the model predicts a strain that tends to σ/E.

This model is described as a first order differential equation for stress to explain the creep behavior.

$$\sigma(t) = E \cdot \varepsilon(t) + \eta \frac{d\varepsilon}{dt} \tag{1.6}$$

Solving this differential equation leads to the following relation:

$$\varepsilon(t) = \frac{\sigma_0}{E} \cdot [\mathbf{1} - \mathbf{exp}\left(\frac{-\boldsymbol{E}}{\boldsymbol{\eta}} \cdot \boldsymbol{t}\right)] \tag{1.7}$$

This model is more applicable to materials such as polymers and wood for applying a small amount of stress [5].

Garofalo's empirical equation [16] can be represented by:

$$\varepsilon = \varepsilon_0 + \boldsymbol{\varepsilon_t}[\mathbf{1} - \mathbf{exp}\left(-\frac{\boldsymbol{t}}{\boldsymbol{t_r}}\right)] + \dot{\varepsilon}_s \cdot t \tag{1.8}$$

where $\varepsilon_0$ corresponds to initial time independent strain that contains elastic and plastic parts, $\varepsilon_t$ is the transient creep strain, $t_r$ by Garofalo represent the transient time between the primary and secondary parts and $\dot{\varepsilon}_s$ is the strain rate of the secondary part.

Evans complicated 4-Theta model [17] could be written as:

$$\varepsilon_f = \theta_1[1 - \exp(-\theta_2 \cdot t)] + \theta_3[\exp(\theta_4 \cdot t) - 1]] \tag{1.9}$$

$$\log(\theta_i) = a_i + b_i \cdot T + c_i \cdot \sigma + d_i \cdot \sigma \cdot T \tag{1.10}$$

$$\varepsilon_f = A + B \cdot T + C \cdot \sigma + D \cdot \sigma \cdot T \tag{1.11}$$

where $\theta_i$, $a_i$, $b_i$, $c_i$, $d_i$, and A, B, C, D are constants estimated by curve fitting and regression analysis.

Garofalo's empirical equation (1.8) and Evan's model (Equation (1.9)) contain the following term for describing the primary creep

$$[1 - \exp(-\alpha \cdot t)] \tag{1.12}$$

which is exactly the same term in the Voigt's (Equation (1.7)) for describing the creep process.

Sawada et al. [18] criticized the exponential relations describing the primary part of creep curve, and show that the power law is better representation of that part of curve (this is the reason that our empirical model uses a power law to account for the primary part of the creep process).

### 1.7.2. Classification of creep models according to: (Strain-time-, Stress-, and Temperature-dependency)

At first almost all of sixty-two creep relations (62 creep relations) were investigated and according to their strain-time relations, their stress-and temperature- dependencies were categorized.

In the first approach strain-time relations are divided in exponential, logarithmic, sinus-hyperbolic, and power law approach. Stress-dependency has exponential, power law and sine hyperbolic subdivisions and temperature-dependency is subdivided by power law, sine hyperbolic and linear forms. This classification is given below:

**I. Strain-time- models**

**1. Exponential-time Approach**

- **Kelvin- Voigt (visco-plastic creep) model [1898],[1]**

$$\varepsilon(t) = \frac{\sigma_0}{E}[1 - \exp(-(E/\eta) \cdot t)] \tag{1.13}$$

Where $\eta$ is the viscosity, E is the elastic modulus, and $\sigma_0$ is the applied initial stress

- **Evans and Wilshire-(Theta-Projection)-model [1985]**

$$\varepsilon_f = \theta_1[1 - \exp(-\theta_2 \cdot t)] + \theta_3[\exp(\theta_4 \cdot t) - 1]]$$

$$\log(\theta_i) = a_i + b_i \cdot T + c_i \cdot \sigma + d_i \cdot \sigma \cdot T$$

$$\varepsilon_f = a + b \cdot T + c \cdot \sigma + d \cdot \sigma \cdot T \tag{1.14}$$

where $\theta_i$ are material constants dependent on stress and temperature like the final

strain $\varepsilon_f$. Parameters *a, b, c, d* and $a_i$, $b_i$, $c_i$, *and* $d_i$ are constants.

- **Garofalo-model [1965]**

$$\varepsilon_t = \varepsilon_{0'}[1 - \exp(-b \cdot t] + \dot{\varepsilon}_{f_{min}} \cdot t \tag{1.15}$$

where $\dot{\varepsilon}_{f_{min}}$ is the minimum creep rate, b is a constant, and $\varepsilon_{0'}$ is the primary strain

**2. Logarithmic-time Approach**

- **Phillips model [1905]**

$$\varepsilon = \varepsilon_0 + A \log(1 + B \cdot t) \tag{1.16}$$

Where A, B, $\varepsilon_0$ are constants

- **Mott and Nabarro [1948]**

$$\varepsilon = A \cdot [\log(1 + B \cdot t)]^{2/3} \tag{1.17}$$

**3. Sinus-hyperbolic-time Approach**

- **Parker model [1958]**

$$\varepsilon^c = A + B \cdot \sinh\left[C \cdot \left(\frac{t}{t_0}\right)^{\frac{1}{3}}\right] \tag{1.18}$$

where A, B, C, and $t_0$ are constants

**4. Polynomial-time Approach**

- **Norton-Bailey-model [1929-1935], Simple**

$$\boldsymbol{\varepsilon_f = A \cdot \sigma^n \cdot t^p} \tag{1.19}$$

Where A, n, and p are constants

- **Graham-Walles model [1953], Simple Polynomial**

$$\varepsilon_f = a_1 \cdot t^{1/3} + a_2 \cdot t + a_3 \cdot t^3 \tag{1.20}$$

where $a_i$ are constants

- **Rabotnov-Kackanov-model [1986] Complexe Polynomial, Structure deformation oriented (Continuum Damage Model)**

$$\varepsilon_c = \varepsilon_R \left[1 - \left(1 - \frac{t}{t_R}\right)^{\frac{1}{\lambda}}\right], \quad \lambda = \frac{\varepsilon_R}{\dot{\varepsilon}_0 \cdot t_R} \tag{1.21}$$

where $\varepsilon_R$ is the rupture strain, $t_R$ is the rupture time, and λ is a constant.

**5. Anderade's 1/3 model [1910], Combination of Power-exponential-time-model, [3]**

$$\varepsilon_c = A \cdot [1 + B(t/t_0)^{\frac{1}{3}}] \cdot \exp(-k \cdot t) \tag{1.22}$$

where A, B, and k are constants.

**II. Stress Dependencies of the Creep Models**

**1. Power Law model**

- **Norton-Bailey model [1929-1935, 2003]**

$$\varepsilon_f = A \cdot \sigma^n \cdot t^p \tag{1.23}$$

**2. Exponential model**

- **Bartsch-model [1986-1995], [56, 57]**

$$\varepsilon_f = A \cdot \sigma \cdot \exp(-Q_{A_1}/RT) \cdot \exp(-B \cdot \sigma) \cdot t^p +$$

$$C \cdot \sigma \cdot \exp(-Q_{A_2}/RT) \cdot \exp(-D \cdot \sigma) \cdot t \tag{1.24}$$

where A, B, C, D, and p are constants. $Q_{A_1}$, and $Q_{A_2}$ are activation energies.

- **BJF (Jones and Bagley)-model [1995-1996], [59]**

$$\epsilon_f = A[1 - \exp(-t)]^{\beta} + Bt, and\ t = (\sigma/A_1)^n \cdot \exp(-Q/RT) \tag{1.25}$$

where A, $A_1$, B, β, and n are constants.

**3. Sine Hyperbolic model**

- **Prandtl model [1928], [4]**

$$\varepsilon = B \cdot \sinh\left(\frac{\sigma}{C}\right) \tag{1.26}$$

where B, and C are constants

- **Nadai model [1938], [11]**

$$\dot{\varepsilon}_s = \dot{\varepsilon}_0 \cdot \sinh\left(\frac{\sigma}{\sigma_0}\right) \cdot \exp\left(-\frac{\Delta H}{RT}\right) \tag{1.27}$$

where $\dot{\varepsilon}_0$ , $\sigma_0$ are initial strain rate , and initial applied stress. ΔH is the activation enthalpy.

**III. Temperature Dependencies of the Creep Models**

**1. Exponential**

- **Modified Norton model [1929-1935, 1974], [6]**

$$\dot{\varepsilon}_{tmin} = A \cdot \sigma^n \exp(Q_A/RT) + B \cdot \sigma^n \exp(Q_B/RT) \tag{1.28}$$

where A, B, and n are constants. $Q_A$, and $Q_B$ are activation energies

- **Weertman model [1955], [24]**

$$\dot{\varepsilon} = A \cdot \sigma^n \cdot \exp\left(-\frac{Q_A}{kT}\right) \tag{1.29}$$

**2. Sine Hyperbolic**

- **Modified Nadai (by Conway) model [1967], [36]**

$$\dot{\varepsilon}_s = A \cdot \sinh(B \cdot \frac{\sigma}{RT})^n \cdot \exp\left(-\frac{\Delta H}{RT}\right) \tag{1.30}$$

**3. Linear (or Power Law)**

- **Davis model [NASTRAN]-NASA-STRuctural-ANalysis-finite element Program [1976], [40]**

$$Ln(\varepsilon_{ijCr}) = A + B \cdot T + C \cdot \sigma^2 + D \cdot \ln(\sigma) + E \cdot \ln(T) + \cdots \tag{1.31}$$

where A, B, C, D, and E are constants. $\varepsilon_{ijCr}$, is the tensoriel strain in the complex program.

- **Evans and Wilshire-(Theta-Projection)-model [1985], [44]**

$$\varepsilon_f = A + B \cdot T + C \cdot \sigma + D \cdot \sigma \cdot T \tag{1.32}$$

- **Larson-Miller Type**

$$\boldsymbol{\varepsilon \cong f[T(A + log(t)]} \ \ \boldsymbol{or} \ \ \boldsymbol{\varepsilon = A \cdot [t \cdot exp\left(-\frac{Q_A}{RT}\right)]^n} \tag{1.33}$$

### 1.7.3. A New and Simple Classification of Creep Relations

According to the classification given in previous part, strain-time models are categorized as exponential, logarithmic, sine hyperbolic and polynomial. The only power law-exponential form belongs to Anderade [Appendix, number 3] that can describe only one part (or region) of the creep curve.

In this part, a new kind of classification is given, that considers the logarithmic subdivision as power law and the sine hyperbolic as exponential; and then the strain-time models are reduced to only power law and exponential.

This classification helps us to develop a probabilistic model based on power law for the primary region and a combination of power law and exponential approach for the secondary and tertiary part. This relation has the following form:

$$\varepsilon_c = \varepsilon_P + \varepsilon_{S/T} = At^n + Bt^m \exp(pt) \tag{1.34}$$

Where $\varepsilon_P$ is the primary strain, $\varepsilon_{S/T}$ is the secondary and tertiary strain. Parameters n, m, and p are material constants.

The proposed probabilistic empirical model is able to estimate the uncertainties in material parameters A, n, B, m, and p. Parameters A, and B are lognormally distributed (also not deterministic), and they can be refined by updating with experimental field data. Parameters n, m, and p are temperature and stress dependent.

### 1.7.4. Classification of the Creep Models According to Three Parts of the Creep Model

Most of the sixty-two creep relations are not capable to describe the three parts of the creep curve. Some of them capture only the primary and most of them are developed to explain the creep behavior of the secondary region. Only a few are capable to describe the whole creep curve.

The proposed probabilistic empirical model belongs to the last class of relation that can capture the whole creep curve. Then, the proposed empirical probabilistic model is compared with acceptable and important creep relations not only in its phenomenological form but from statistical point of view (chapter 4). Table 1.2 summarizes the most important creep relations that capture the whole creep curves.

**Table 1.2: Most important creep model that describe the whole creep curve from primary (P), to secondary (S) and tertiary part applied to [10 Cr Mo (9-10)] steel alloys [81]**

| Model Equation | Model | Creep Range | References |
|---|---|---|---|
| Graham-Walles [1955] | Power law | P/S/T | [23] |
| Evans and Wilshire Theta model [1985] | Exponential | P/S/T | [44] |
| Modified Theta model [1985] | Exponential | P/S/T | [47] |
| Kachanov-Robotnov [1986] Robotnov | Power law | P/S/T | [48-51] |
| Bolton [1994] | Power law * | P/S/T | [54,55] |
| Dyson-McLean [1998] | Exponential | P/S/T | [60] |
| Modified Garofalo [2001] | Exponential | P/S/T | [61] |
| Holmström- Auerkari-Holdsworth (LCSP) [2007] | Power law * | P/S/T | [72] |
| Probabilistic. Model [2011] | Power law | P/S/T | [ ] |

(*) Power law is given in a complex form. For references given in the table see Appendix.

# Chapter 2:

# Development of an Empirical Model and Testing Its Workability in Comparing with Acceptable Creep Models in the Literature

## 2.1. Introduction

In this chapter brief review over the most well-known and acceptable creep models and describe their strengths and shortcomings will be discussed. Then, a probabilistic empirical model according to power law for the primary part of the creep curve, and power law and exponential for the secondary and tertiary parts will be proposed. Finally, the proposed models will be validated and their parameters estimated with the experimental data and show that not only it has all the advantages of the well-known creep models, but also it is more flexible and accurate in presenting the experimental data.

## 2.2. A Review of Creep Models

Although a number of significant theoretical descriptions of creep have been presented, current knowledge is based primarily on finding a correlation between experimental results and micromechanical models. In the simplest form, the creep of different materials can be described by a phenomenological rate relation such as [1]:

$$\dot{\varepsilon} = A \cdot \sigma^n \cdot \exp\left(\frac{-Q_c}{RT}\right) \tag{2.1}$$

where A and n are material constants and $Q_c$ is the activation energy of the creep process. The external variables are temperature, T, and stress, σ, while specific values for n and $Q_c$ are associated with specific creep mechanisms.

In 2009, Sawada et al [2] selected four constitutive creep equations that are widely accepted as basic equations [3, 4], and examined long term creep curve behavior up to the secondary stage (for time >105 hr) for carbon steels and other materials. Sawada et al. found these curves could be best described by the following widely accepted constitutive creep equations:

Power Law: $\varepsilon = \varepsilon_i + a \cdot t^b + \dot{\varepsilon}_M \cdot t$ (2.2)

Exponential Law: $\varepsilon = \varepsilon_i + a[1 - \exp(-b \cdot t)] + \dot{\varepsilon}_M \cdot t$ (2.3)

Logarithmic Law: $\varepsilon = \varepsilon_i + a \cdot \ln(1 + bt) + \dot{\varepsilon}_M \cdot t$ (2.4)

Blackburn'sEquation:

$$\varepsilon = \varepsilon_i + a[1 - \exp(-b \cdot t)] + c[1 - \exp(dt)] + \dot{\varepsilon}_M \cdot t \quad (2.5)$$

In the above equations, a, b, and c are constants, $\varepsilon_i$ is the initial strain, and $\dot{\varepsilon}_M$ is minimum strain rate , t is time and $\varepsilon$ is the creep strain

Sawada et al.[2] determined that the power law equation best fitted the actual long term creep curves for all steel materials, whereas the exponential law, logarithmic law and Blackburn's equation did not represent the beginning of primary creep during long term testing [2].

Recently Holdsworth et al. [4, 15] reviewed some of the strain equations of interest to the European Creep Collaborative Committee (ECCC) and gave four important relations for secondary and tertiary creep in Ni-based alloys (applicable to another alloys too). These relations are listed below:

1) Norton secondary creep equation[1]:

$$\dot{\varepsilon_s} = A \cdot \sigma^n \cdot \exp\left(-\frac{Q}{RT}\right) \quad (2.6)$$

Where A, and n are constants, Q is the activation energy, R is the gas constant , T is the temperature

2) The Garofalo transient –secondary creep equation[5]:

$$\varepsilon = \varepsilon_0 \cdot [(1 - \exp(-b \cdot t)] + \dot{\varepsilon}_M \cdot t \tag{2.7}$$

where $\varepsilon_0$ , b, $\dot{\varepsilon}_M$ are constants, t is time and ε is the strain.

3) The theta transient-tertiary creep equation (Evans-Wilshire)[6]:

$$\varepsilon_f = \theta_1[1 - \exp(-\theta_2 \cdot t)] + \theta_3[\exp(\theta_4 \cdot t) - 1]] \tag{2.8}$$

where $\theta_1$-$\theta_4$ are constants, t is time and ε is the strain.

4) The Dyson and McLean constitutive model[7]:

$$\dot{\varepsilon} = \dot{\varepsilon}_0(1 + D_d) \exp\left(\frac{-Q}{RT}\right) \sinh[\sigma(1 - H)/\sigma_0(1 - D_d)\,(1 - \omega)] \tag{2.9}$$

where $D_d$ , $D_p$, and ω are damage parameters whose values range from 0 to 1, H is a hardening parameter.

Holdsworth et al. [4] suggested that the damage model may be considered as a strong candidate for a unified creep model which would represent both the plasticity and the creep behavior of the material.

Besides all of the models previously mentioned, there are some models that are used for design, inspection and life assessment of components in high temperature facilities like the Graham-Walles [8], or modified Graham-Walles model [9]. This model is composed of four terms of a polynomial series that can be used to accurately describe any creep behavior. These four terms are shown below in the following relation:

$$\varepsilon_c = \sum_{i=1}^{n} C_i \cdot \sigma^{\alpha_i} \cdot t^{\beta_i} = C_1 \cdot \sigma^{\alpha_1} \cdot t^{1/3} + C_2 \cdot \sigma^{\alpha_2} \cdot t + (C_3 \cdot \sigma^{\alpha_3} + C_4 \cdot \sigma^{\alpha_4}) \quad (2.10)$$

where $\varepsilon_c$ = strain, $C_i$ and $\alpha_i$ are constants, σ is the stress and t is the time.

Graham-Walles superposition of the three individual terms shown in the equation above is given in Figure 2.1.

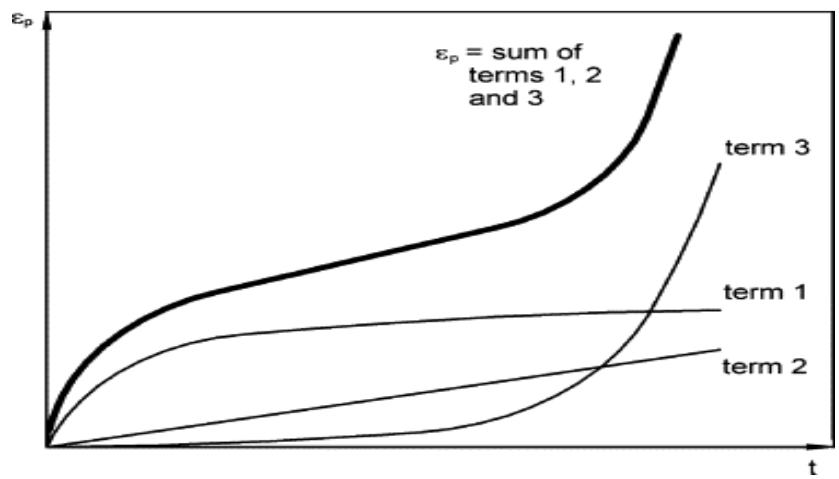


**Figure 2.1: Graham–Walles approach is the superposition of three individual terms, schematically [17]**

## 2.3. Development of a Probabilistic Model Based on Previous Work

Among all of the creep models, the Theta-projection model (from Evans and Wilshire), modified Theta model (Murayami and Oikawa by setting $\theta_2 = \theta_4$) [10, 11], and Graham Walles model were selected because of their accuracy of fitting the three stages of the creep curve [4, 9-15]. The theta model gives us a good physics based behavior of the creep process as a competing mechanism between hardening and softening of materials in the creep process.

The theta projection model is based originally on the Kelvin-Voigt model (or hardening-softening principle) and later by the Garofalo Model. This model is composed of two parts: primary and tertiary parts. The primary part is described by the relation shown below and

assumes that secondary creep remains constant after prolonged time. This model ignores the fact that a power law fit best describes primary creep.

$$\varepsilon_p = \theta_1(1 - \exp(-\theta_2)) \tag{2.11}$$

This model can not describe creep accurately; moreover, due to its wide range of parameters to describe creep process, the calculation is very complex. Besides, the tertiary part is described by the following relation ignores the abrupt breaking of the sample described by the Kachanov-Rabotnov–constitutional Damage model [12- 14]:

$$\varepsilon_p = \theta_3(\exp(\theta_4) - 1) \tag{2.12}$$

Current damage based models include both the plasticity and creep behavior of materials which make them more representative models, but these models contain too many parameters and require complex numerical integration.

On the other hand, although Graham-Walles model [8], is purely polynomial and reflects the physical behavior well, it ignores the exponential behavior of the tertiary creep region.

It has been shown previously that it is a power law expression that can describe primary creep very well. Therefore, if a power law expression for the primary part is combined with a power/exponential expression for the secondary and tertiary creep, the resulting expression is believed to provide a better picture of the Physics of Failure (PoF) based behavior of creep as well as a better curve fitting. The combined probabilistic empirical equation is a superposition of the primary and the secondary/tertiary parts that accurately describes the abrupt failure of a given material during creep. The combined model can be described by the following relation.

$$\epsilon_c = \epsilon_{P+}\epsilon_{S/T} = At^n + Bt^m \exp\,(p \cdot t) \tag{2.13}$$

where the variables A and B contain stress and temperature dependencies like the Norton equations and n, *m* and *p* are material constants.

The creep rate function of the model is defined by the following relation:

$$\frac{d\epsilon_c}{dt} = nAt^{n-1} + B \cdot t^{m-1}e^{pt}(m + p \cdot t) \tag{2.14}$$

## 2.4. The Effect of Model Parameters on the Form of the Creep Curve

First, the effect of changing parameters A and n on the shape of the creep curves is studied. The primary part is given by $\varepsilon_p = A\ t^n$ where the coefficient A represents the scaling (up and down) and n is responsible for the changes in curvature of the creep curves as shown in Figure 2.2, and 2.3.

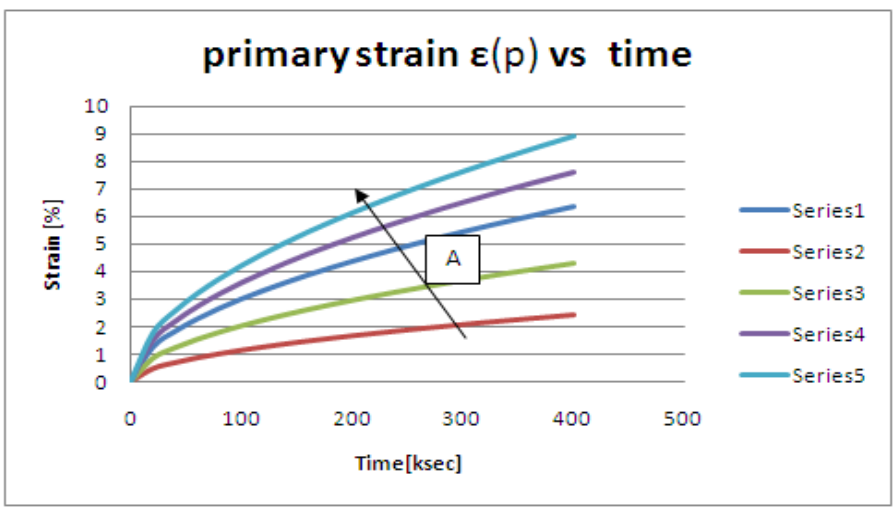


**Figure 2.2: The effect of parameter A on creep curves**

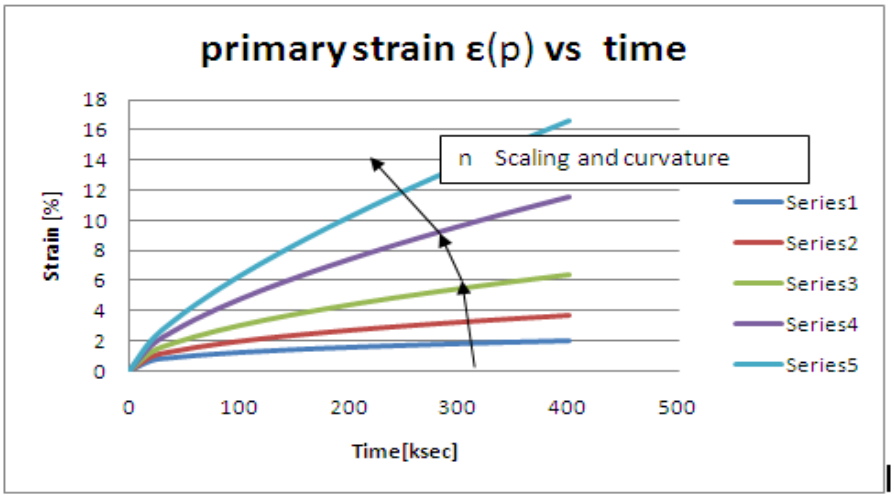


**Figure 2.3: The effect of n on behavior of creep curves**

Next the effect of parameter B on the resulting creep curves is studied. Changing the parameter B scales the creep curves (up and down) from the deflection point as shown in Figure 2.4.

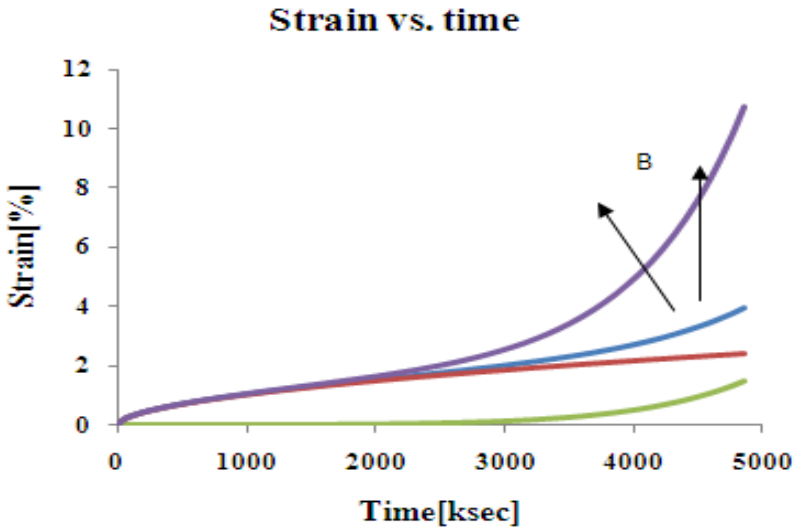


**Figure 2.4: The effect of parameter B on creep curves**

Next the effect of changing the power exponent m and the exponential p in the combined equation on the resulting creep curves was studied. Changing the m and p parameter result in

changes in the curvature of the creep curves as shown in Figure 2.5. Changes in m values result in sharp curvature changes while changes in p values result in gradual changes in the curvature of the creep curves.

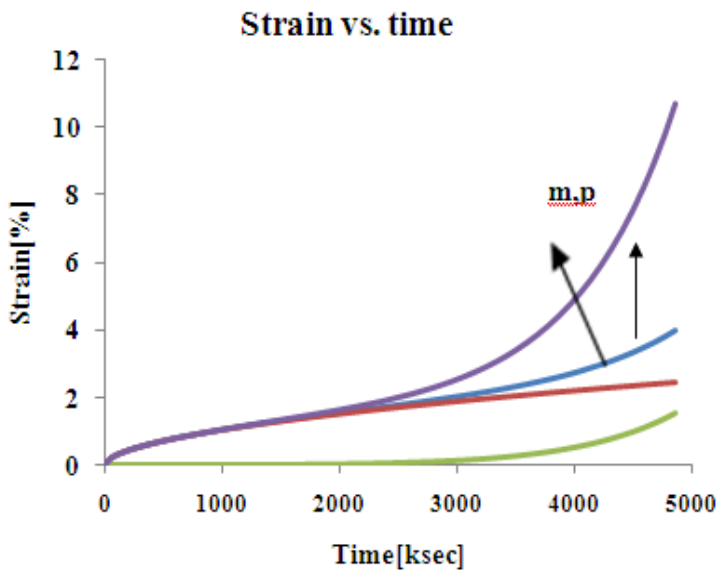


**Figure 2.5: Scaling effect of m and p on creep curves**

The proposed empirical probabilistic model gives the possibility of changing the scale as well as the curvature of the creep curves just like the Evans and Wilshire model. We are additionally able to change the curvature with sharper curvature changes like those observed by the Kachanov and Robotnov constitutional damage model. An additional advantage of this model is that the parameters A and B can be described probabilistic and therefore it is possible to capture the uncertainty in experimental data and updating it with new experimental data.

## 2.5. Phenomenological Comparison of proposed Empirical Probabilistic Model with the Well-Known Creep Models

### 2.5.1. Comparison with Theta-Projection Model

Evans and Wilshire [6] applied the Theta-projection model to polycrystalline copper with the use of the following parameters:

$$\theta_1 = 2.408 \times 10^{-3}\,, \theta_2 = 2.306 \times 10^{-5}, \theta_3 = 1.08 \times 10^{-3}, \theta_4 = 1.706 \times 10^{-5} \tag{2.15}$$

By using these parameters, the resulting strain-time expression looks like:

$$\varepsilon_c = 0.002408 \cdot (1 - \exp(-2.306 \times 10^{-5} \cdot t)) + 0.00108 \cdot (\exp(1.706 \times 10^{-5} t) - 1 \tag{2.16}$$

The resulting Strain Rate-Time expression has the following form:

$$d\varepsilon/dt = 5.6 \times 10^{-8} \exp(-0.0020408t) + 1.8 \times 10^{-8} \exp\,(1.706 \times 10^{-5} \tag{2.17}$$

It is shown that the proposed empirical model yields similar expressions to the ones developed by Evans and Wilshire for strain-time and strain rate-time. The strain-time and strain rate-time expressions of our model are given as:

$$\varepsilon_c = 5 \times 10^{-7} t^{0.745} + 3.86 \times 10^{-6} t^{0.469} \exp\,(1.612 \times 10^{-5} t) \tag{2.18}$$

$$\dot{\varepsilon} = 3.725 \times 10^{-7} t^{-0.255} + 1.81034 \times 10^{-6} t^{-0.531} \exp(1.612 \times 10^{-5} t)\,[1 + 3.4371 \times 10^{-5} t] \tag{2.19}$$

Figure 2.6 and 2.7 compare the resulting expressions of both models by plotting the strain versus time and strain rate versus time respectively.

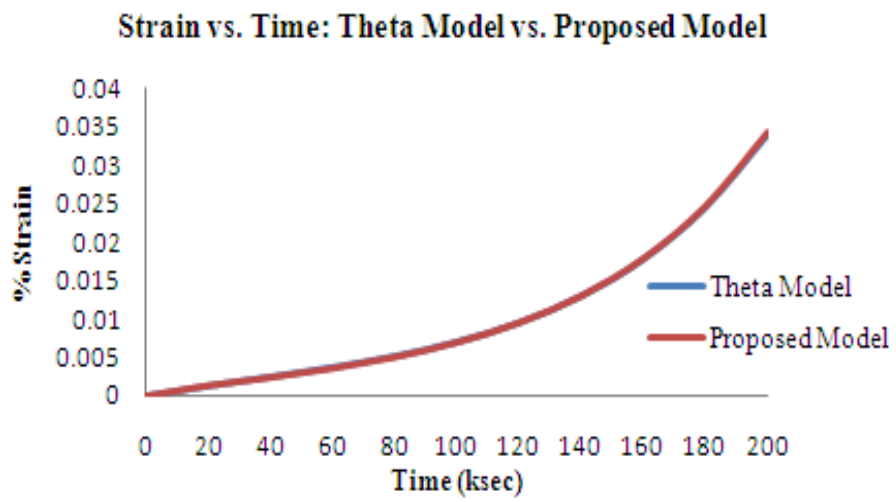


**Figure 2.6: Strain vs. time comparison of the theta and proposed models**

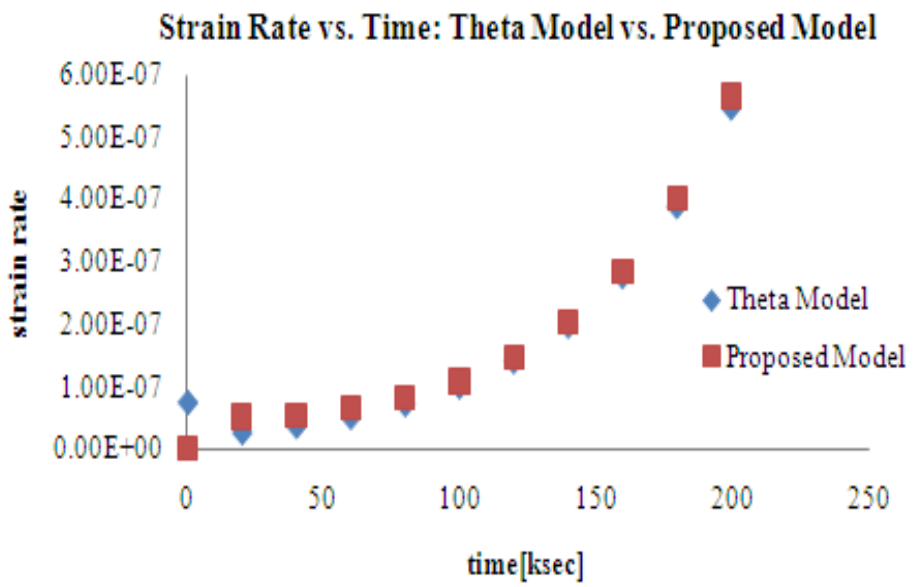


**Figure 2.7: Strain rate vs. time comparison of the theta and proposed models**

As it can be seen in Figure 2.6, the two models produce nearly identical strain vs. time curves. The difference of the corresponding values between the two curves is approximately $2.5 \times 10^{-5}$. The two models produce nearly identical strain rate vs. time curves, as well.

### 2.5.2. Comparison with Kachannov-Robotnov-Creep-Damage Model

In this part, the proposed empirical model is with one of the outstanding damage model of materials, called Kachanov damage model compared.

The phenomenological creep-damage equations were firstly proposed by Kachanov and (later by) Rabotnov [14]. Although, this model contains only one parameter, it can characterize a wide range of observed material. Besides, it is a relative robust model that can be quantified relatively easily.

Kachanov represents continuum damage as an effective loss in material cross section due to internal voids. The internal stress increases with time as a function of damage. Kachanov represents this damage by the ratio of the remaining effective area A, to the original area $A_0$. This area loss or damage is shown schematically in Figure 2.8.

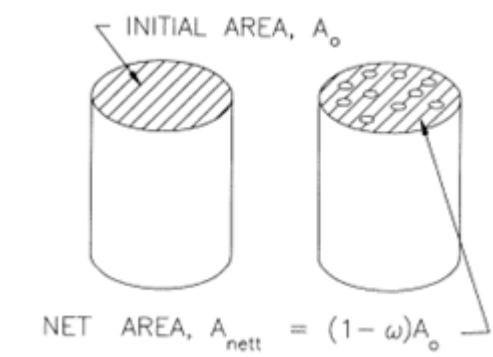


**Figure 2.8: Kachanov's damage model (area loss ~ damage) [13]**

As damages accumulates, the internal stress increases from $\sigma_0$ to $\sigma$ value:

$$\sigma = \sigma_0 \, A_0/A \tag{2.20}$$

Rabotnov replaced this relation with a damage parameter $\omega$ like:

$$\omega = (1 - A/A_0) \tag{2.21}$$

$$1 - \omega = A/A_0 \tag{2.22}$$

Kachanov then assumes that the material obeys a secondary creep law similar to the Norton relation [1]:

After some time t under the load (P= σ A), the original length $L_0$ increased to L, and area $A_0$ reduces to an area A. As a result the true stress at time t, for constant volume $A_0 L_0 = A L$ is:

$$\sigma = \sigma_0 \frac{A_0}{A} = \sigma_0 \frac{L}{L_0} \tag{2.23}$$

Substituting this stress in the creep rate gives:

$$\frac{\dot{\varepsilon}_c}{\dot{\varepsilon}_0} = \left(\frac{\sigma}{\sigma_0}\right)^m = \left(\frac{A_0}{A}\right)^m = \frac{1}{(1-\omega)^m} \tag{2.24}$$

$$\dot{\varepsilon}_c = \frac{\dot{\varepsilon}_m}{(1-\omega)^p} = \frac{k\sigma_0^m}{(1-\omega)^p} \tag{2.25}$$

where m and p are constants.

At time zero, ω =0 (no damage), but as damage increases, the creep rate increases. Finally, when ω reaches some critical value $\omega_f$ , the strain rate tends to infinity and damage occurs (for $\omega_f$ =1).

Kachanov made a simple assumption that the damage rate should be a function of the $\sigma_0$:

$$\frac{d\omega}{dt} = \dot{\omega} = \frac{k\sigma_0^k}{(1-\omega)^r} \tag{2.26}$$

Solving the two rate equations together, one can estimate the continuity relation:

$$\varepsilon_c = \lambda \dot{\varepsilon}_0 t_R \left[1 - \left(1 - \frac{t}{t_R}\right)^{1/\lambda}\right] = \lambda \varepsilon^* \left[1 - \left(1 - \frac{t}{t_R}\right)^{1/\lambda}\right] \tag{2.27}$$

$$\frac{\varepsilon}{\varepsilon_R} = \left[1 - \left(1 - \frac{t}{t_R}\right)^{1/\lambda}\right] \tag{2.28}$$

where $t_R$ is the rupture time and is given by:

The rupture time is given by the following relation:

$$t_R = \frac{1}{B(1+r)\sigma_0^k} \tag{2.29}$$

And the rupture strain

$$\varepsilon_R = \lambda \cdot \varepsilon^* \tag{2.30}$$

where

$$\varepsilon^* = \dot{\varepsilon}_0 \cdot t_R \tag{2.31}$$

And

$$\lambda = \frac{1+r}{1+r+p} \tag{2.32}$$

The shape of the strain-time curve is described by Equation (2.27) and is shown in Figure 2.9.

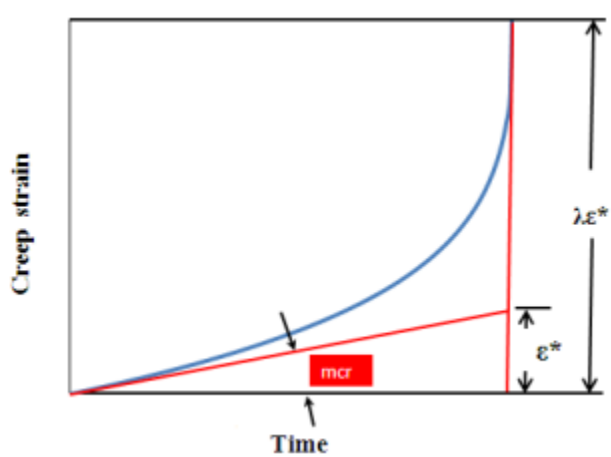


**Figure 2.9: Kachanov's strain-time relation, mcr=minimum creep rate [13]**

By applying Kachanov's equation for different λ values, one can apply it to almost all classes of material.

Its shape is given by quantities which can be easily measured and within some limits it can approximate 0.90 percent of the life fractions of most of the materials [13]. Figure 2.10 gives the strain fraction versus life fraction for different λ values. The damage character can be estimated using the $\lambda$ values: $\lambda$=6, for ductile damage mode, $\lambda$=2, for brittle damage mode, and ($2 \leq \lambda \leq 6$) describes the "mixed" damage mode of materials.

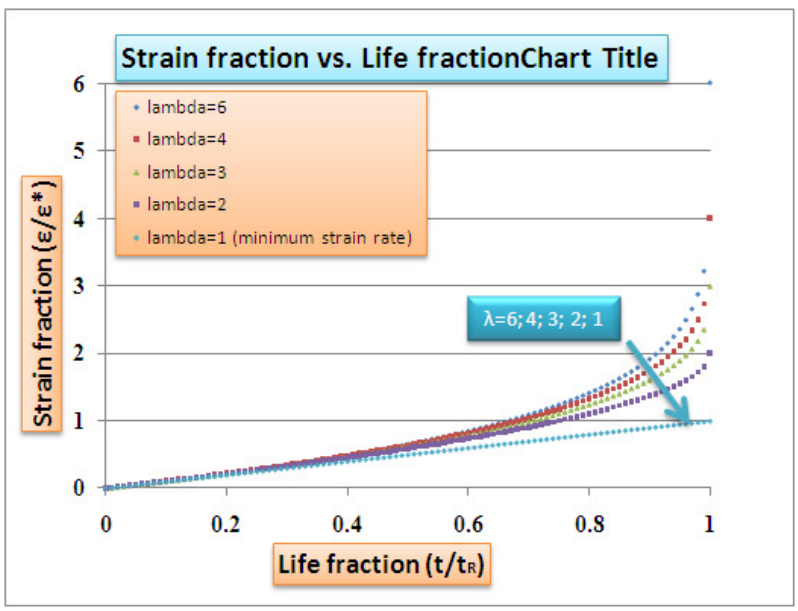


**Figure 2.10: Strain fraction versus life fraction for different λ values describing different damage modes of materials from ductile (λ=6) to brittle (λ=2) [13]**

The creep strain assessments can be regarded as robust measurements of damage. Kachanov model uses a simple physical explanation to describe the tertiary part of creep curve. Although it gives almost good approximation for some materials, it is a model which considers

more characteristics of the third stage. As it is shown in the Figure 2.10, the primary part of creep curve is ignored.

For damage evaluations, all three stages are important. Figure 2.11 gives a schematic creep curve that contains all three stages and we want to prove (check) our proposed empirical equation with it.

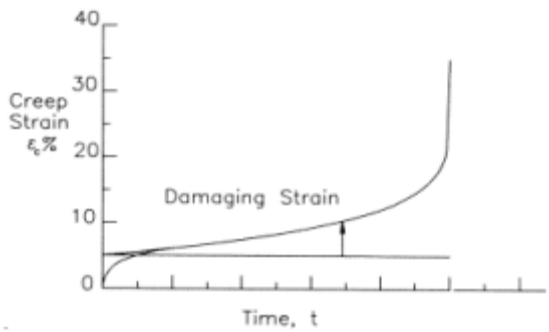


**Figure 2.11: Kachanov's strain -time relation with and without primary strain [13]**

Figure 2.12 represent comparison of our empirical model with the Kachnov damage model.

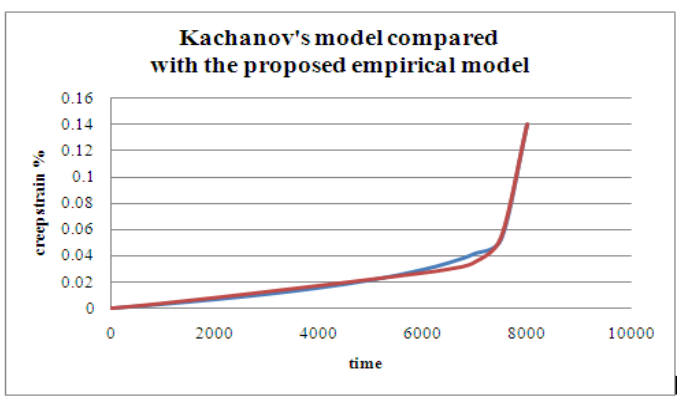


**Figures 2.12: Kachanov's strain-time model (blue) compared with the proposed empirical model (red)**

Kachanov's creep equation with numerical values looks like [13]:

$$\varepsilon_c = 0.14 * [1 - \left(1 - \frac{t}{8000}\right)^{0.17}] \tag{2.33}$$

Then the numerical values of the proposed empirical model were evaluated and were compared with Kachanov creep-damage equations:

$$\varepsilon_c = 2.025 \times 10^{-6}\, t^{1.091} + 3.6638 \times 10^{-84} t^{20.55} \exp\,(0.000645t) \tag{2.34}$$

As it is seen in Figure 2.12, the proposed empirical model fits the Kachanov's damage model very well, and thus it can be used as an abrupt damage model as well.

## 2.6. Statistical Consideration: Comparison of Our Empirical Model with Theta Model for Derivation of Residual Errors

Creep curves derived under the same test conditions usually exhibit a wide range of error and uncertainties. The error and uncertainties are not only arisen from the imperfection (and uncertainties) in the test methods, but also from the parameter estimations. To consider (and therefore control) the presence of errors in parameters estimations (which vitally affect the results of analyses); one should study the error propagation, the regression analyses and the parameter dependencies (autocorrelation).

One of the established empirical relations for describing the creep process is the theta-projection model. However, although it is a "good representation of the creep curves for materials of moderate and high ductility" (by using the exponential concepts in the primary and tertiary part of the creep curves), "it gives a poorer fit at low strains and times" [15]. One attempt to modify theta-projection model has been made by adding further parameters to achieve better agreement with given experimental data.

The modification has been performed by using nonlinear regression analysis to fit the data with theta (4)-projection and extended theta (6) models; then the residual is calculates as a measure of exactness for model comparison [15, 16].

Numbers (4) and (6) added to the titles of theta model indicates the number of parameters used in their relations. However, it should be mentioned that adding two extra parameters to theta (4) model makes the calculations and regression analysis more complicated.

The proposed empirical model that considers the variation of residual with time as a measure of fitting, gives satisfactory results. Besides, it captures the primary part of the creep curve much better than the other two theta-models for the Aluminum alloy tested at 100 $^0$C and 340 MPa stress. Figure 2.13 shows the creep curves for an Aluminum alloy tested at 100$^0$C and340 MPa with data of three models.

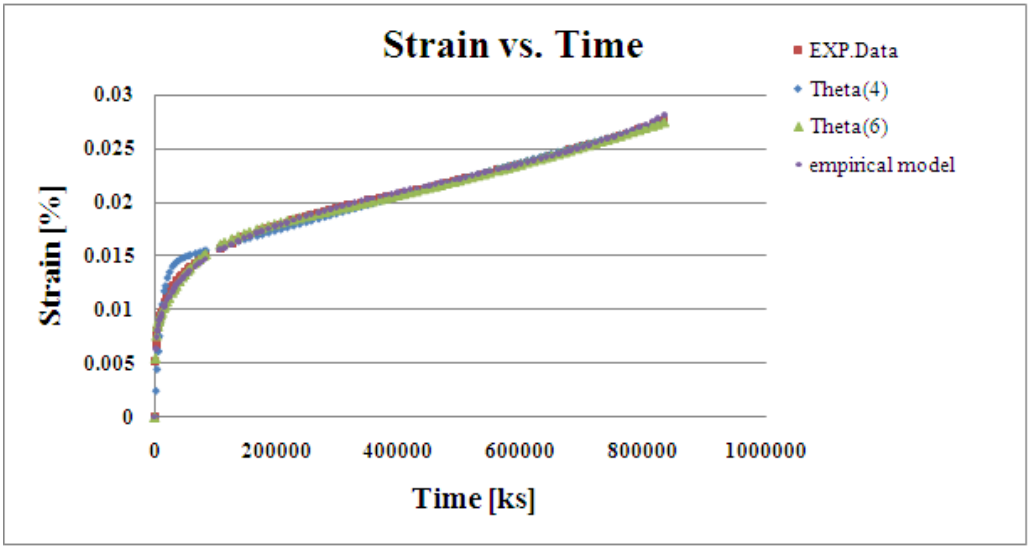


**Figure 2.13: Creep curves for an Aluminum alloy tested at 100$^0$C and340 MPa with the data of three models [15]**

Figure 2.14 compares the residual calculated for both theta (4) and theta (6) models.

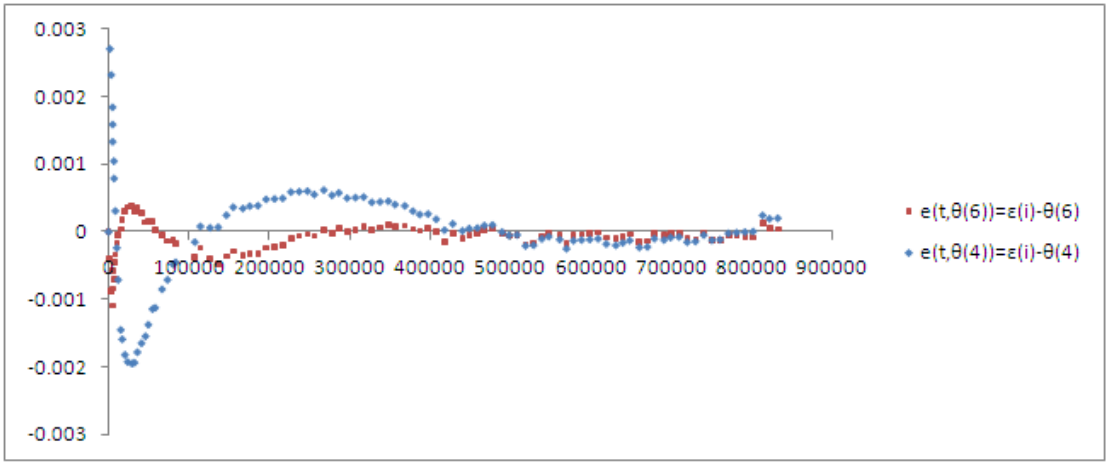


**Figure 2.14: Residual errors for theta (4) and theta (6) models**

Figure 2.15 shows the residual versus time for our empirical model; it also shows the superiority of our empirical power law model to capture the primary region of the creep curve.

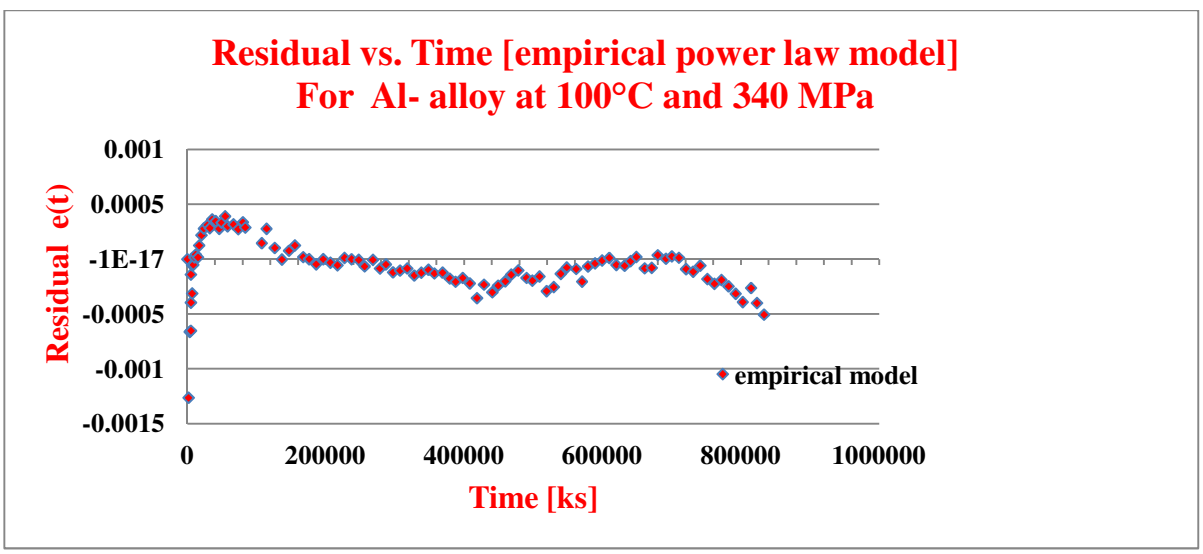


**Figure 2.15: Residual errors versus time**

As it is shown in the Figure 2.15, residuals of the proposed model is in the range of ± 0.0005, also closer to zero level compared with 6-θ model.

## 2.7. Model Comparison with Akaike Relation

Akaike, (1973-1974) [17] found a formal relationship for model comparison with the name of Akaike's Information Criterion (AIC). AIC is described by:

$$AIC = n\log(\hat{\sigma}) + 2K, \quad with\ \hat{\sigma}^2 = \frac{\sum \hat{e}_i^{\,2}}{n}, and\ \ \hat{e}_i = w_i(y(x_i) - \hat{y}(x_i)) \tag{2.35}$$

where $\hat{e}_i$ is the estimated residual from the fitted model, and K is the number of model parameters. *n:* Number of independent measurements , and $w_i$ = Weight applied to residual of acquisition i, $y(x_i)=f(x_i)$ =for experimental data, and $\hat{y}(x_i) =$ for fitted values.

It is easy to compute AIC from the results of least-square estimation or a likelihood-based analysis. Akaike's approach allows identifying the best model in a group of models and allows ranking the rest of the models easily [see more in Appendix G]. The best model has the smallest AIC value.

Long-term constant loading at elevated temperatures of materials leads to the development of creep behavior as a material damage process and to the failure of engineering structures or component [18]. Creep properties of materials form the basis to analyze the high-temperature structure strength and life of materials under constant applied stresses. There exist some creep-damage equations, such as Kachanov–Rabotnov (K–R) creep-damage formula [19-21], theta projection [22-28] model, and modified Theta-Omega model [21] that have been widely used to predict the creep damage and the residual strength of different materials. The proposed model is compared with these four models (using the Akaike information criterion).

Four different models are:

- Kachanov–Rabotnov (K–R) constitutive

$$\dot{\varepsilon}_e = B\frac{(\sigma_e)^n}{(1-\omega)^n} \qquad \dot{\omega} = D\frac{(\lambda\sigma_1+(1-\lambda)\sigma_e)^{\chi}}{(1-\omega)^{\phi}} \tag{2.36}$$

Integration of $\dot{\omega}$ and substitution in the relation for $\dot{\varepsilon}_e$ and further integration results to the following simplified strain time equation:

$$\varepsilon = \varepsilon_R\left[1-\left(1-\frac{t}{t_R}\right)^{1/\lambda}\right] \tag{2.37}$$

where $\varepsilon_e$ and $\sigma_e$ are, respectively equivalent creep strain and stress. $\sigma_1$ is the maximum principal stress, $\omega$ is the damage variable which can be ranges from 0 (no damage) to 1 (full damage), and $\varepsilon_R$ and $t_R$ are strain and time to rupture. The terms $D$, $B$, $n$, $\Phi$, $\chi$, and $\lambda$ are material parameters which can be obtained from uniaxial tensile creep curves and the optimum method.

- Theta-projection model

$$\varepsilon_C = \theta_1\{1-exp(-\theta_2 t)\} + \theta_3\{exp(\theta_4 t)-1\} \tag{2.38}$$

where t is the time, $\theta_1, \theta_2, \theta_3$ and $\theta_4$ are parameter constants determined by fitting the equation to experimental data.

- Theta-Omega model

$$\varepsilon_C = X(1)\{1-exp(-X(2)t)\} + \left(\frac{-1}{X(3)}\right) ln(1-X(4)t) \tag{2.39}$$

where $X(1), X(2), X(3)$ and $X(4)$ are parameter constants characterizing creep curve shapes

- Proposed empirical model

$$\varepsilon_C = a\,t^n + c\,t^m \exp\,(p\,t) \tag{2.40}$$

where a, n, c, m and p are parameter constants describing the creep curve.

The data from experimental and damage simulation of creep damage for duralumin alloy 2A12, given in the literature [29] was used and fitted to all above-mentioned models. Then Akaike Information Criterion (AIC) was calculated. The results are given in Figure 2.16.

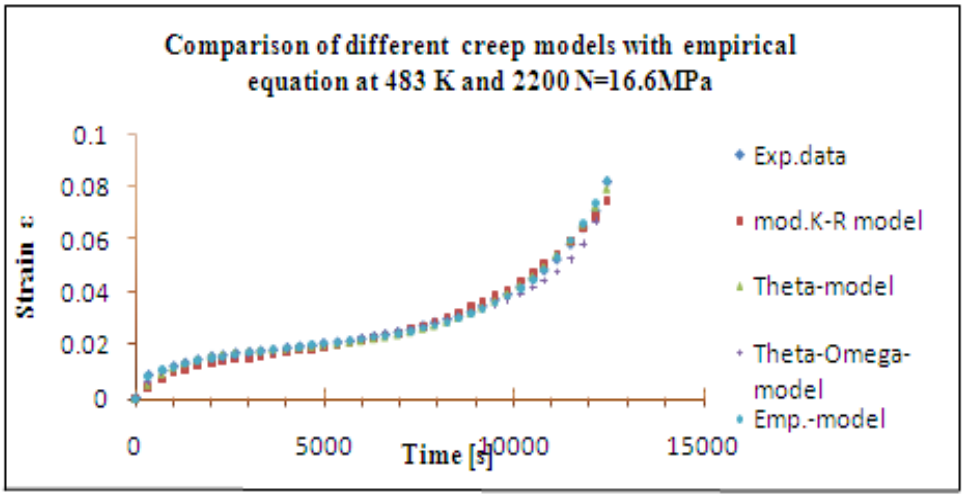


**Figure 2.16: Comparison of different creep models with the given experimental data**

Besides, the corresponding AIC values for different are given in the Table 2.1.

**Table 2.1: AIC-values from comparison of different creep models for the given experimental data**

| | **Empirical-model** | **Theta-model** | **Theta-Omega-model** | **K-R-model** |
|---|---|---|---|---|
| n | 39 | 39 | 39 | 39 |
| k | 5 | 4 | 4 | 6 |
| AIC | **-432.3 <** | **-422 <** | **-363 <** | **-357** |

where n is the number of observant (data), K is the number of parameters in the fitted model and AIC's are values calculated for different models.

As it can be seen in Table 2.1, the AIC-values can be ranked in ascending order as follows: Empirical Model, Theta Model, Theta-Omega Model and the K-R Model respectively, which indicates that the proposed empirical model is a superior model for describing the creep-damage process. It should be mentioned that K-R model which has the highest number of parameters (variables), has the worst ranking.

## 2.8. Model Uncertainty (Bayesian) Approach for Model Comparison

In order to compare the models from Bayesian inference [30] point of view, we use model uncertainty approach with the use of experimental strain data of duralumin alloy 2A12, extracted from literatures [29, 31]. For this comparison WinBUGS program (a Windows-based environment for Markov Chain Monte Carlo (MCMC) simulation) was used.

We estimated 2.5% and 97.5% boundary confidence intervals for all four models. As it can be seen in Figure 2.17, the confidence intervals of our empirical probabilistic model are closer to the experimental data. This indicates that our model can fit the experimental data better than the other models.

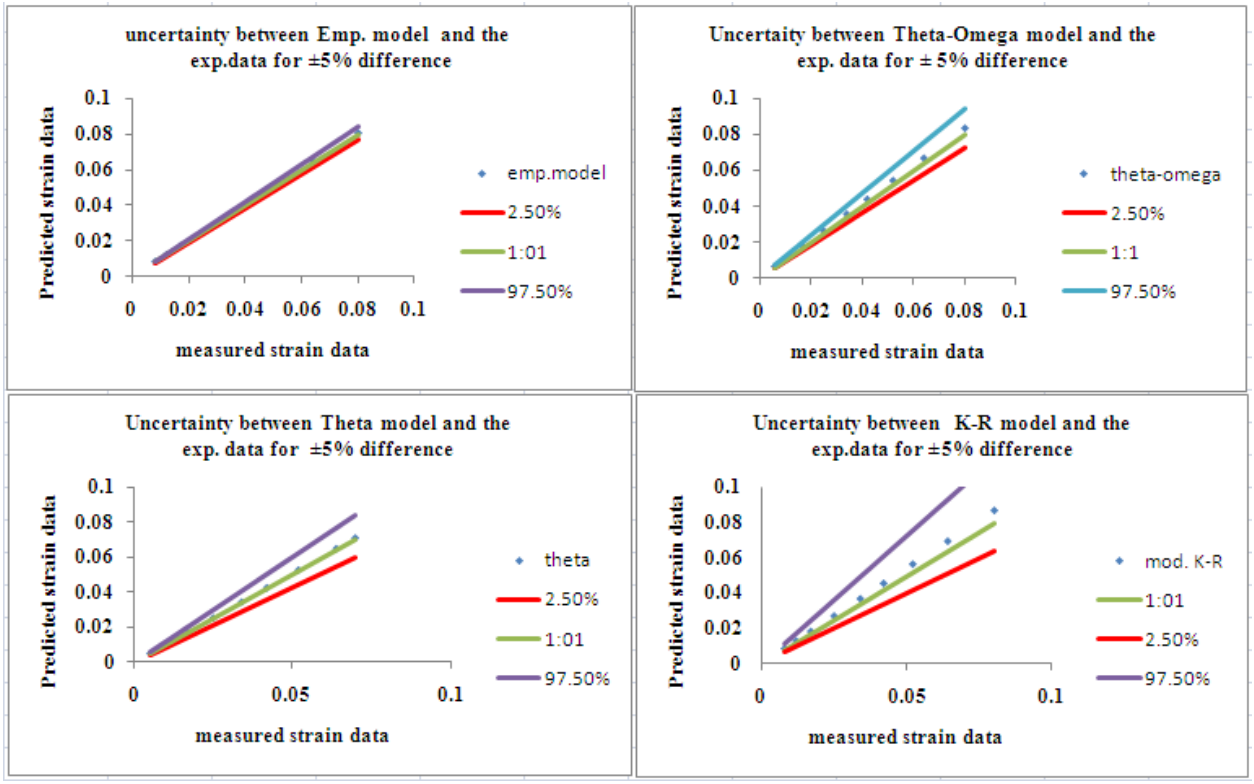


**Figure 2.17: Comparing different model data: predicted strain model data with the measured data**

# Chapter 3:

# Specifying Stress and Temperature Dependencies of Our Creep Curve Parameters

## 3.1. Specifying Stress Dependencies

According to American Standard for Testing Materials (ASTM), Creep deformation is defined as any strain that occurs when a material is subjected to a sustained stress [1-2]. During creep, tensile specimen under a constant load will continually deformed with time. This deformation depends on three major parameters: stress, time and temperature. Therefore, the most general form of creep equation is:

$$\varepsilon_c = f(\sigma, t, T) \tag{3.1}$$

Although different forms of stress dependencies have been reported for the creep strains [1-5], there are two forms that are widely used:

- Power law, given by Norton and Bailey (1929) [4], and , Johnson et.al. (1963) [5]:

  $$\varepsilon_c = A \cdot \sigma^n \cdot t^m \tag{3.2}$$

  where σ, is the stress, and A, n, and m are material dependent parameters.

- Exponential forms, given by Dorn (1955) [6], Soderberg (1936) [7], McVetty (1963) [8], Garofalo (1965) [9], and Evans and Wilshire (1985) [10,11], which gives the dependencies in an exponential form:

  $$\varepsilon_c \cong A \cdot \exp\,(\sigma/\sigma_0) \tag{3.3}$$

  where σ, is the applied stress, and $\sigma_0$ is the initial stress, (material constant)

like the yield strength, $\sigma_y$.

This research suggests the following form for the stress dependencies for the parameters of the proposed empirical model:

$$\varepsilon_c = A \cdot t^n + B \cdot t^m \exp(p \cdot t) \tag{3.4}$$

where $\varepsilon_c$ is the creep strain, t is the time and A, n, B, m, and p are material parameters (that depend on stress and temperature).

In doing so, Levi de Oliveira Buneo's [12] data used for 2-1/4Cr-1Mo high temperature pipeline steel (given for just one temperature (600°C), and one stress (138 MPa)) was extended to different stress conditions. Figure 3.1 shows Levi de Oliveira Bueno's experimental data versus the theta projection model [12].

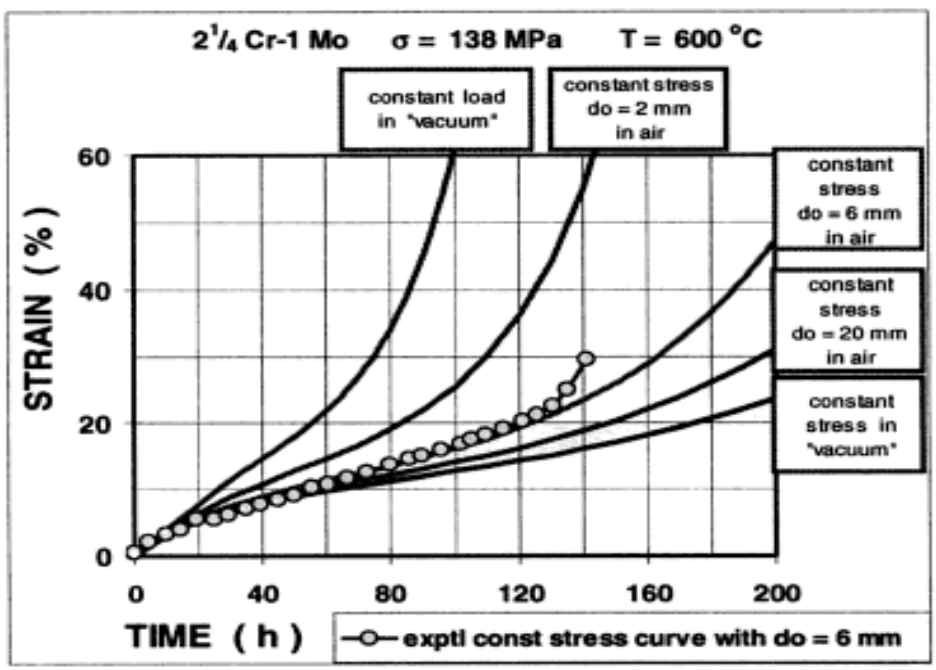


**Figure 3.1: Stain versus Time relation for 2-1/4Cr-1Mo pipeline alloy under an applied stresses of σ=138 MPa, and T=600 $^0$C in vacuum and air [12]**

### 3.2. Results and Discussion

Table 3.1 (a) and (b) show the extended-data for 2-1/4Cr-1Mo high temperature pipeline steel used for pressure vessels in power plants and oil refineries. We calculated the strain values versus time for different applied stress at $600^0$C.

**Table 3.1: Data calculated with our model at T=600°C, evaluated under different stress conditions (a), and (b) for (2-1/4)Cr-1 Mo pipeline steel material**

**(a)**

| **σ [MPa]** | **34.5** | **51.75** | **69** | **86.25** | **94.875** | **103.5** | **107.8** | **112.125** |
|---|---|---|---|---|---|---|---|---|
| **Time[hrs]** | **ε [%]** | **ε [%]** | **ε [%]** | **ε [%]** | **ε [%]** | **ε [%]** | **ε [%]** | **ε [%]** |
| **0** | 0 | 0 | 0 | 0 | 0 | 0 | 0 | 0 |
| **20** | 0.011 | 0.033 | 0.096 | 0.278 | 0.468 | 0.786 | 1.016 | 1.312 |
| **40** | 0.222 | 0.064 | 0.184 | 0.514 | 0.852 | 1.400 | 1.789 | 2.281 |
| **60** | 0.033 | 0.093 | 0.263 | 0.718 | 1.171 | 1.891 | 2.395 | 3.028 |
| **80** | 0.042 | 0.121 | 0.335 | 0.894 | 1.439 | 2.293 | 2.888 | 3.635 |
| **100** | 0.052 | 0.147 | 0.400 | 1.048 | 1.668 | 2.634 | 3.307 | 4.157 |
| **120** | 0.062 | 0.171 | 0.460 | 1.183 | 1.867 | 2.932 | 3.678 | 4.631 |
| **140** | 0.071 | 0.194 | 0.515 | 1.303 | 2.044 | 3.201 | 4.021 | 5.083 |
| **160** | 0.079 | 0.216 | 0.565 | 1.412 | 2.204 | 3.452 | 4.350 | 5.532 |
| **180** | 0.088 | 0.237 | 0.612 | 1.510 | 2.351 | 3.692 | 4.674 | 5.992 |
| **200** | 0.096 | 0.256 | 0.655 | 1.601 | 2.489 | 3.928 | 5.002 | 6.471 |

**(b)**

| **σ [MPa]** | **120.75** | **125** | **129.375** | **133.6** | **138** | **142** | **146.625** |
|---|---|---|---|---|---|---|---|
| **Time[hrs]** | **ε [%]** | **ε [%]** | **ε [%]** | **ε [%]** | **ε [%]** | **ε [%]** | **ε [%]** |
| **0** | 0 | 0 | 0 | 0 | **0** | 0 | 0 |
| **20** | 2.176 | 2.795 | 3.585 | 4.591 | **5.874** | 7.514 | 9.618 |
| **40** | 3.688 | 4.681 | 5.940 | 7.548 | **9.626** | 12.366 | 16.088 |
| **60** | 4.831 | 6.111 | 7.762 | 9.935 | **12.888** | 17.082 | 23.418 |
| **80** | 5.783 | 7.348 | 9.435 | 12.321 | **16.522** | 23.067 | 34.191 |
| **100** | 6.657 | 8.551 | 11.188 | 15.051 | **21.115** | 31.486 | 51.233 |
| **120** | 7.525 | 9.822 | 13.173 | 18.389 | **27.205** | 43.703 | 78.657 |
| **140** | 8.434 | 11.230 | 15.511 | 22.580 | **35.416** | 61.578 | 122.947 |
| **160** | 9.420 | 12.834 | 18.315 | 27.900 | **46.544** | 87.795 | 194.532 |
| **180** | 10.510 | 14.686 | 21.704 | 34.680 | **61.654** | 126.269 | 310.252 |
| **200** | 11.731 | 16.837 | 25.816 | 43.335 | **82.181** | 182.737 | 497.327 |

The stress dependencies of each parameter (A, n, B, m, and p) of our empirical model is given as follow:

$$A = \alpha_A \cdot \exp(\beta_A \cdot \sigma)\,, and\ n = \alpha_n \cdot \sigma + \beta_n \tag{3.5}$$

$$B = \alpha_B \cdot \exp(\beta_B \cdot \sigma)\,,\ m = \alpha_m \cdot \sigma + \beta_m,\ and\ p = \alpha_p \cdot \exp(\beta_p \cdot \sigma) \tag{3.6}$$

where parameters $\alpha_i$, and $\beta_i$ with (i=A, n, B, m, and p) are material constants.

The use of exponential stress dependencies for empirical parameters is justified by several literatures [10, 11, 13-17].

The creep curves were estimated from the data given in Table 4.1 and are shown in Figure 3.2.

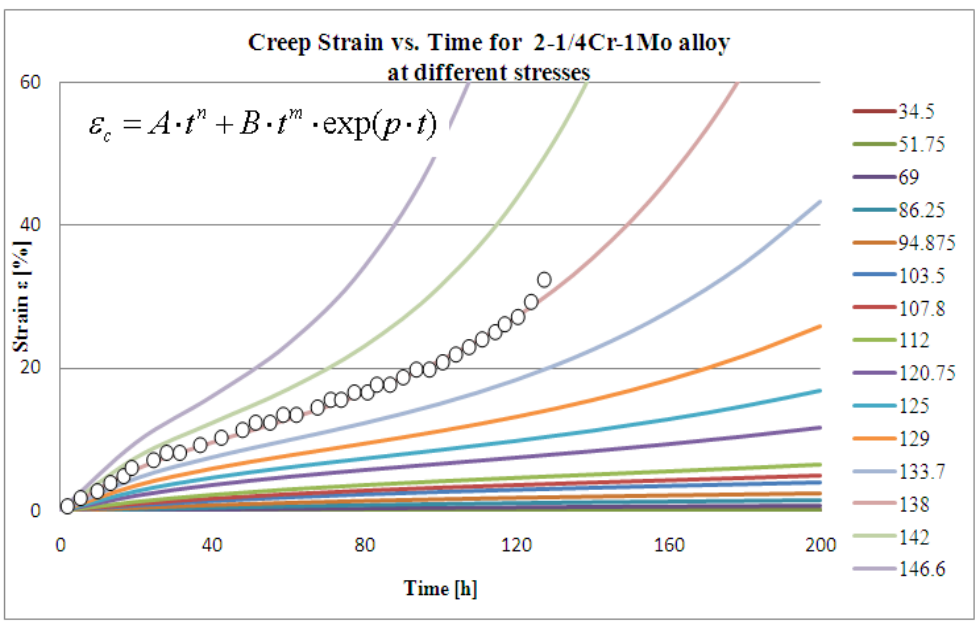


**Figure 3.2: Creep curves from data given in Table 4.1 to estimate stress dependency of the parameters of the empirical model; series 1 to 15 correspond to 15 different stress conditions**

### 3.3. Specifying Temperature Dependencies

Creep is generally associated with time dependent plasticity of materials under a fixed stress at an elevated temperature, often greater than approximately 0.4-0.5$T_m$, where $T_m$ is the absolute melting temperature. The process is also temperature-dependent since the creep or dimensional change that occurs under an applied stress increases considerably as temperature increases [18, 19].

Dorn [19] and Evans [20, 21] suggest that temperature dependency has the exponential form like:

$$\dot{\varepsilon} = \frac{d\varepsilon}{dt} = A \cdot \sigma^n \cdot \exp\left(-Q/RT\right) \tag{8.1}$$

where $\dot{\varepsilon}$ is the strain rate of the creep and Q is the activation energy of the corresponding creep process and A is a material constant.

To study the temperature dependencies of creep parameters, we suggest the following empirical model:

$$\varepsilon_c = A \cdot t^n + B \cdot t^m \exp\left(p \cdot t\right) \tag{8.2}$$

where, $\varepsilon_c$ is the creep strain, t is the time and A, n, B, m, and p are stress and temperature dependent material parameters.

To explain the temperature dependency of the parameters of our generic empirical model, we used the temperature dependency diagram given by R.W.Bailey [22]. Bailey's temperature dependency diagram is given in Figure 3.3.

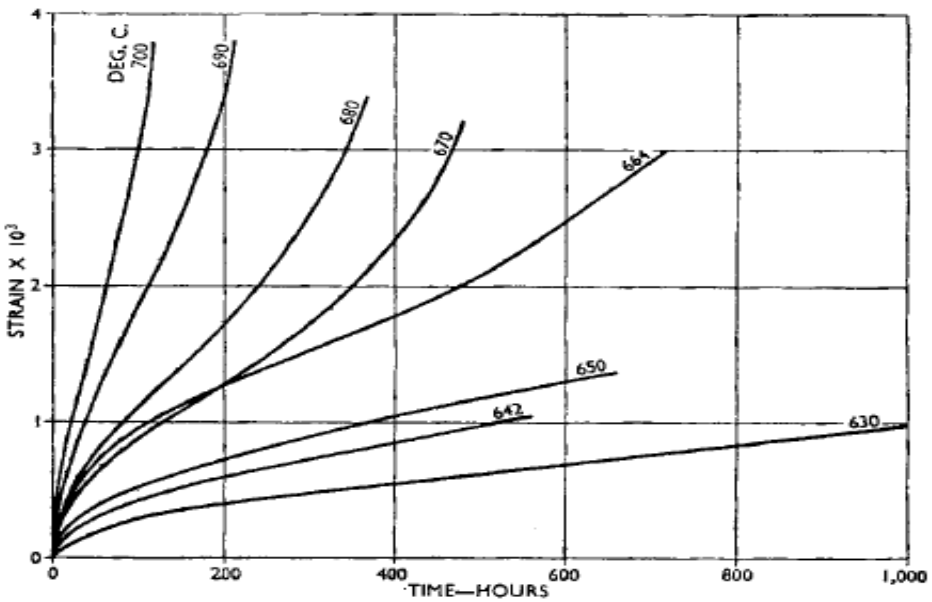


**Figure 3.3: Creep test results for Mo-V steel for a given stress [22]**

In this research the high temperature pipeline steel's data were used to evaluate the general temperature dependency of parameters a, n, c, m and p of the above mentioned empirical relation. Figure 3.4 shows the corresponding simulated data, evaluated by Digitalizer, and Excel and WinBUGS program.

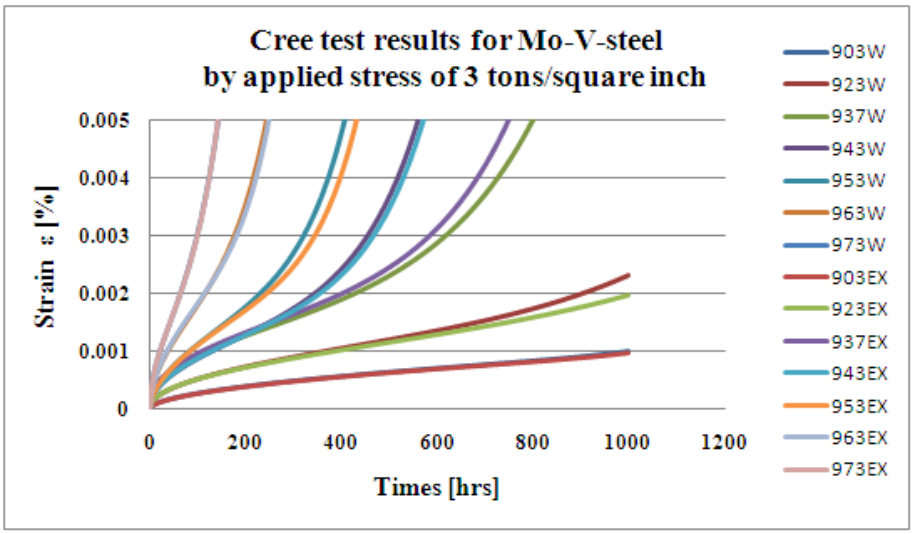


**Figure 3.4: Simulated creep test result for Mo-V steel by Excel (EX), and WinBUGS (W)**

To do the regression analysis with WinBUGS, one needs to guess prior values for the parameters; In fact, one of the major challenges in WinBUGS is to choose the most appropriate values for the prior distribution of the parameters.

### 3.4. Results and Discussion

Table 3.2 (a and b) shows the estimated parameters data for high temperature pipeline Mo-V steel used for pressure vessels in power plants and oil refineries. The values of strains versus times are calculated for different temperatures by a given applied stress, using Excel and WinBUGS Bayesian regression analysis. The uncertainty between experimental values (Excel) and values estimated by WinBUGS program is approximately $6.5 \times 10^{-4}$.

**Table 3.2: Data calculated by Regression Analysis in Excel (a) and by WinBUGS (b) to develop the proposed model, evaluated under seven different temperature conditions for Mo-V pipeline steel at a given definite applied stress of 3 tons/ square inch**

**(a)**

| T[K] | A | *n* | B | *m* | *p* |
|---|---|---|---|---|---|
| **903K** | 2.33E-05 | 0.531649 | 8.60E-09 | 0.06101 | 0.00852 |
| **923K** | 5.78E-05 | 0.4665 | 5.32E-06 | 0.2462 | 0.00288 |
| **937K** | 1.33E-04 | 0.421 | 5.40E-06 | 0.324 | 0.0055 |
| **943K** | 9.25E-05 | 0.48406 | 8.90E-08 | 1.019 | 0.00692 |
| **953K** | 8.20E-05 | 0.563 | 2.18E-09 | 1.68 | 0.0087 |
| **963K** | 1.44E-04 | 0.5398 | 3.08E-08 | 1.501 | 0.0116 |
| **973K** | 2.10E-04 | 0.503 | 1.54E-07 | 1.67 | 0.0098 |

**(b)**

| T[K] | A | *n* | B | *m* | *p* |
|---|---|---|---|---|---|
| **903** | 2.37E-05 | 0.5282 | 2.95E-08 | 0.03948 | 0.007653 |
| **923** | 5.55E-05 | 0.4779 | 3.70E-06 | 0.2812 | 0.003444 |
| **937** | 1.38E-04 | 0.3997 | 8.93E-06 | 0.324 | 0.004569 |
| **943** | 8.63E-05 | 0.4875 | 9.26E-06 | 0.2234 | 0.007852 |
| **953** | 8.68E-05 | 0.5496 | 1.86E-08 | 1.412 | 0.008295 |
| **963** | 1.50E-04 | 0.5174 | 1.41E-07 | 1.342 | 0.009736 |
| **973** | 2.11E-04 | 0.502 | 7.77E-08 | 1.875 | 0.007409 |

According to our calculations, parameters n, B and p are temperature independent.

The temperature dependency of A and m parameters are given as:

$$\varepsilon(t) = A \cdot t^n + B \cdot t^m \exp\,(p \cdot t) \tag{8.3}$$

$$A = \alpha'_A \cdot \exp(-E_A/RT)\,, and\ n = \alpha'_n \cdot T + \beta'_n \tag{8.4}$$

$$m = \alpha'_m \cdot T + \beta'_m, or\ \ m = \alpha'_m \cdot \exp\,(\beta'_m \cdot T)\,, and\ \ \ p = \alpha'_p \cdot \exp\left(\beta'_p \cdot T\right) \tag{8.5}$$

where $E_A$ is the creep's activation energy

The use of exponential Arrhenius and linear temperature dependencies for empirical parameters is justified by several literatures [23-25].

It should be mentioned that the temperature and stress dependencies of similar parameters were justified by corrosion experiments on X-70 carbon steel in the physics of failure laboratory of the reliability department of the University of Maryland.

# Chapter 4:

# Experimental Efforts for Al-7075-T6 and X-70 Carbon Steel

## 4.1. Experimental Efforts for creep tests

## 4.2. Introduction

Creep experiments take time, usually from days to months. To perform an accurate creep experiment it is necessary to have an especial creep machine, equipped with a high temperature furnace and high temperature extensometers for estimation the amount of strain. This thesis began its work by a fundamental research in creep literature and we tried to gather all different possibilities to make our homemade equipments. To perform creep experiments on Al-7075 and X-70 carbon steel a MTS machine available at the University of Maryland is used. K-type thermometer is used to adjust the sample temperature in the redesigned furnace during the creep experiment.

In this chapter, we described the equipments that we made for performing the creep experiments. We also explain how we prepared our samples and the problems we faced in this regard. Finally, we give the results of our preliminary and final experiments together with data evaluation for the final experiments.

## 4.3. Experimental Equipments Developed

To perform corrosion, corrosion fatigue, stress corrosion cracking (SCC), and corrosion creep (at low temperature), different chambers were designed and their workability in a MTS machine were checked. These chambers are capable to perform the experiments in different liquid environments from tap water to crude oils.

Also designed was a high temperature furnace (up to 1200°C) especially for creep experiments. This furnace has accuracy for setting temperature of ±5°C.

Special grips for holding different types of specimens from CT to dog boned samples were designed. These grips can be cooled with especially designed copper coils to prevent the heat transfer to the MTS grips.

Figure 4.1 shows the small and large scaled corrosion-fatigue chamber designed and tested for dog-bone specimens; its workability is checked in a corrosion-fatigue experiment for an Aluminum prototype sample. Figure 4.1 also shows the chamber with the prototype Dog-bone specimen in MTS machine.

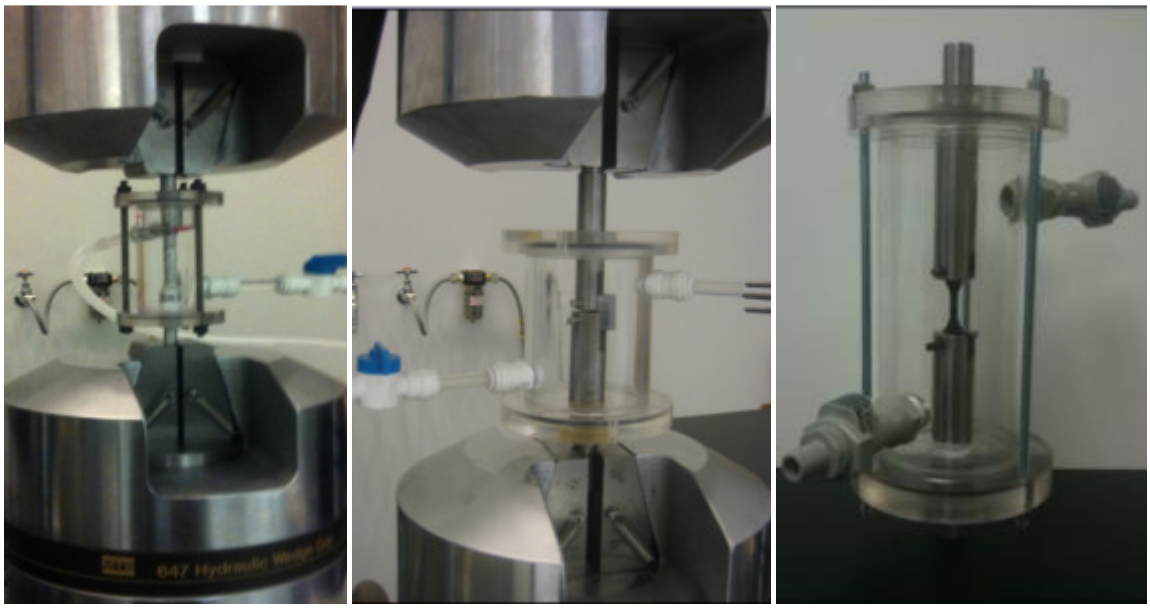

**Figure 4.1: The corrosion-fatigue chamber with the prototype dog-bone, and CT specimens in MTS machine.**

Figure 4.2 shows a complicated test chamber for CT-specimens (installed in the MTS equipment), which we designed, made and tested. The chamber is used for stress corrosion cracking tests of Aluminium and X-70carbon steel CT-samples.

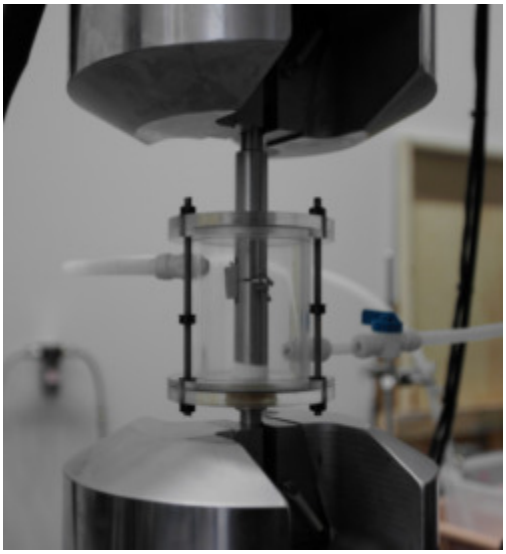

**Figure 4.2: The corrosion fatigue and SCC chamber installed in the MTS equipment. The top left and right bottom pipes are the inlet and outlet of corrosive liquid.**

Due to high price of the heating chamber (for creep experiment) in the market, a laboratory chamber has been designed, made and tested. Figure 4.3 shows this furnace during the temperature test. The grips that are holding the sample inside the chamber are connected to the MTS machine for applying (variable or constant) stress. The two ends of the holding grips (at the top and bottom of the chamber) are cooled to prevent heat transfer to the MTS grips. This chamber provides the facility to do the creep experiment for almost all the metallic samples up to $800^{\circ}C$ .

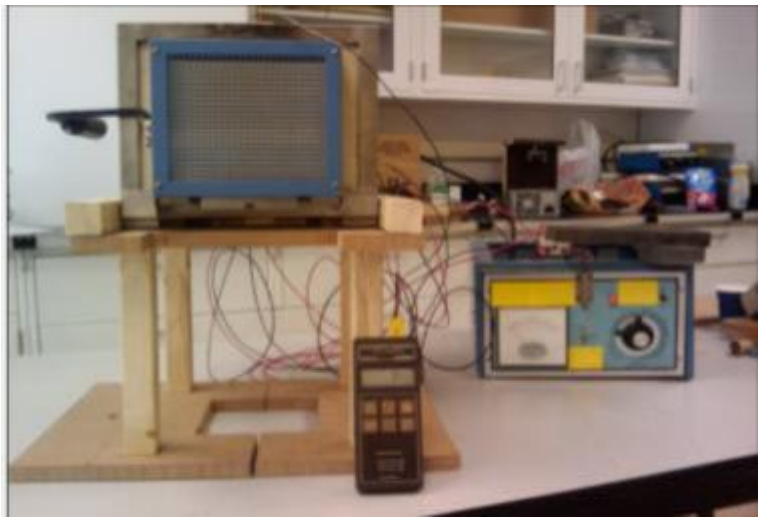

**Figure 4.3: The heating chamber for creep experiment during the temperature test before installing in the MTS machine.**

## 4.4. Sample Preparations and Accompanied Problems

Two types of samples for performing the experiments on: Aluminum 7075-T6 and X-70 carbon steel were prepared as follow:

### 4.4.1. Al-7075-T6-Samples

In order to do the creep experiment, Aluminum 7075 dog-bone (ASTM-standardized) samples were prepared. Figure 4.4 shows these specimens with their appropriate stainless holders for fixing them in the furnace; the holders are installed in the grips of the MTS machine.

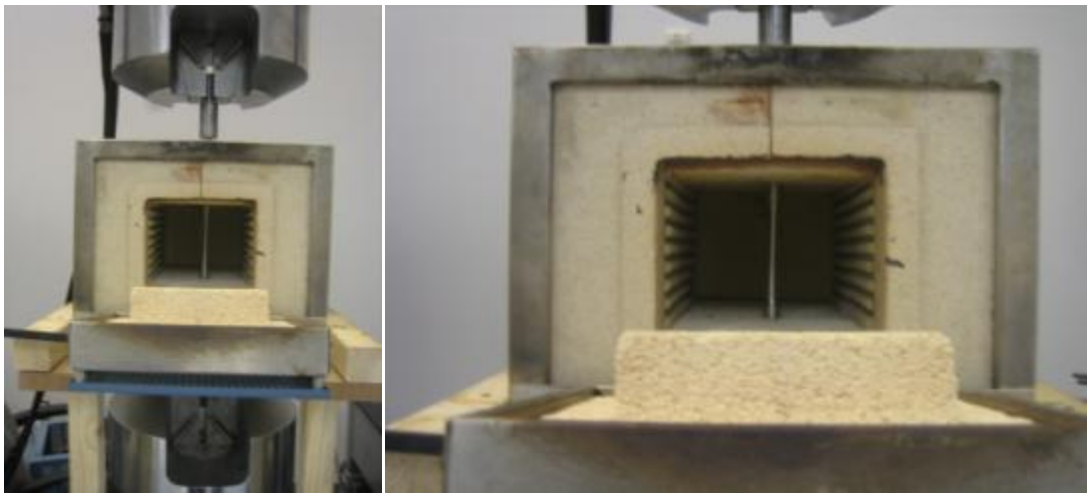

**Figure 4.4: Al-sample fixed in the threaded holders (left) and into the grips of MTS machine (right)**

Figure 4.5 shows the Al sample with the top and bottom holders.

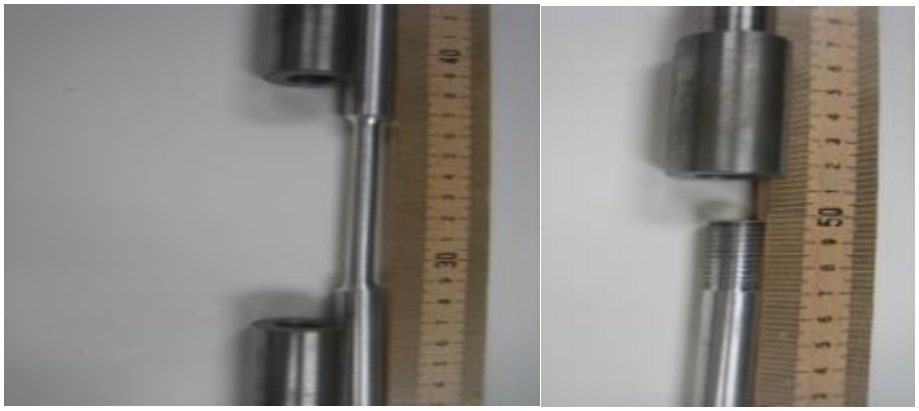

**Figure 4.5: Al-sample with two threaded holders (left), in top or bottom view (right)**

### 4.4.2. X-70 Carbon Steel Samples

X70 carbon steel specimens need special long stainless steel holders that are specially threaded at the top and can be fixed to the CT specimens. Figure 4.6 shows these special grips, CT specimen and the form that they are fixed in MTS machine.

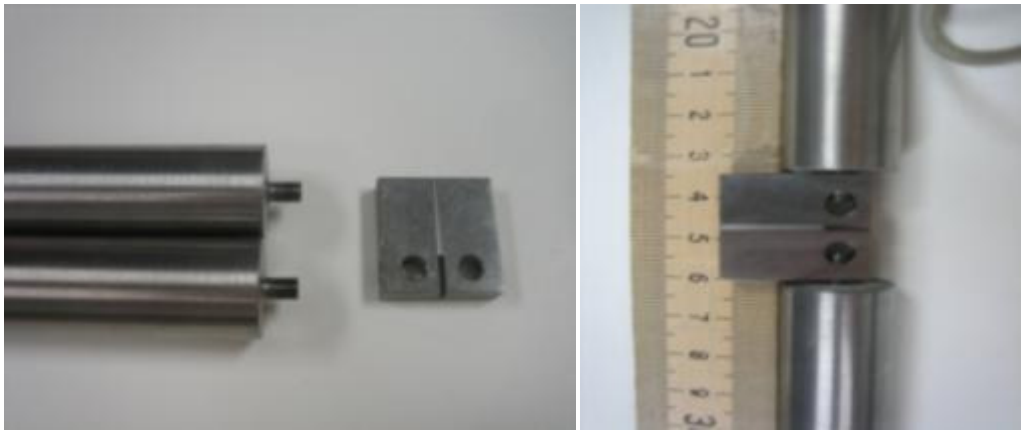

**Figure 4.6: X70 carbon steel  with top and bottom threaded grips**

**Figure 4.7: X70 carbon steel fixed in the furnace (left)  and connected to the MTS macine (right)**

Preparation of long Al-7075-T6 samples was easier than the ones for X-70 CT samples. First of all they are cheaper but they need appropriate cooling with tap water because of their length and heat conduction to the MTS grips. It was not so easy to keep the temperature of the samples constant during the whole creep experiments.

To conduct creep experiments on X-70 carbon steel, the top and bottom threaded CT samples were made. To apply constant force, two long pin threaded grips were made and

connected to the samples. All the creep experiments were performed in a house made high temperature furnace. Figure 4.8 shows the installed sample in MTS equipment.

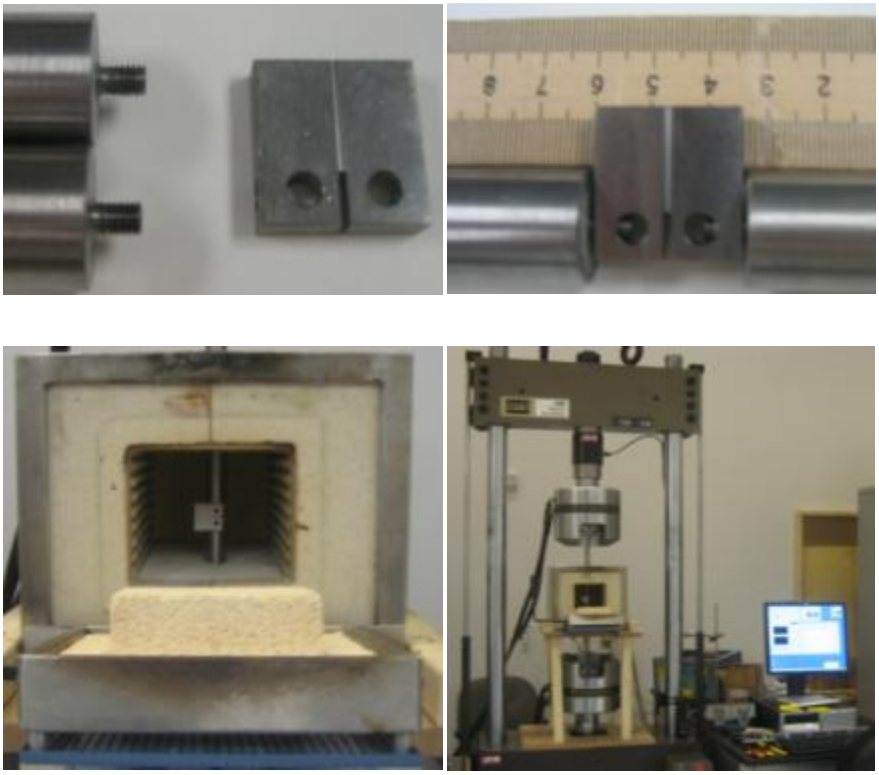

**Figure 4.8: X-70 samples with two long grips (top left), sample connected to the grips, real dimensions (top right), sample connected to grips in furnace (bottom left), and in MTS machine (bottom right)**

Since CT samples are very hard (with Vickers hardness of 295 HV at 10 kg [5]) while the grips are made from soft steel material, the following problems arise:

a) Grips could not apply the right stresses to the CT samples and therefore were deformed at the threaded top part and slide out from the threaded CT sample part;

b) Filling the threaded part of CT samples with hardened materials, using horizontal pins, and changing the grips didn't work due to hardness of CT samples;

c) Although, extension of the groove part of CT samples with some additional crack (similar to pre-crack) seems to work at first, it fails finally because of the soft grips connected to hard samples.

Figure 4.9 shows the deformed CT samples after the experiment together with the pin before and after the experiments.

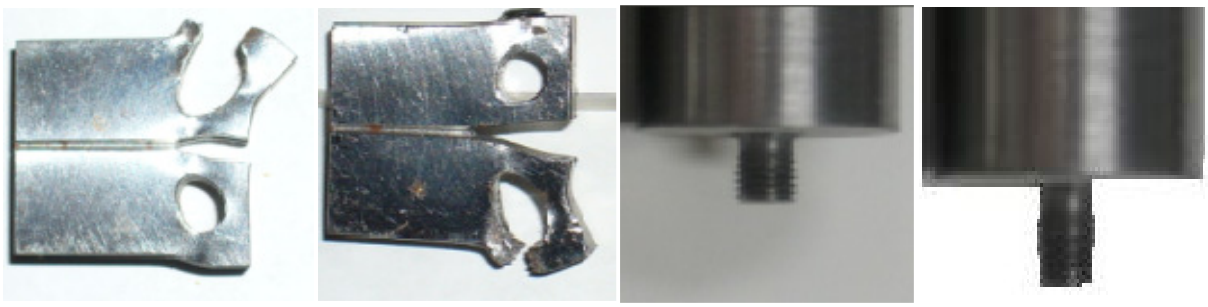

**Figure 4.9: deformed CT samples and the threaded grip part before and after deformation**

After the unsatisfactory experiments on CT samples, the morphology of the samples were changed and new threaded dog bone samples with appropriate grips were made. To estimate the applied stresses during the creep experiments, stress-strain curve for the X-70 carbon steel was performed.

The prepared dog bone X-70 carbon steel samples and threaded grips together with its installation in the furnace are shown in figure 4.10.

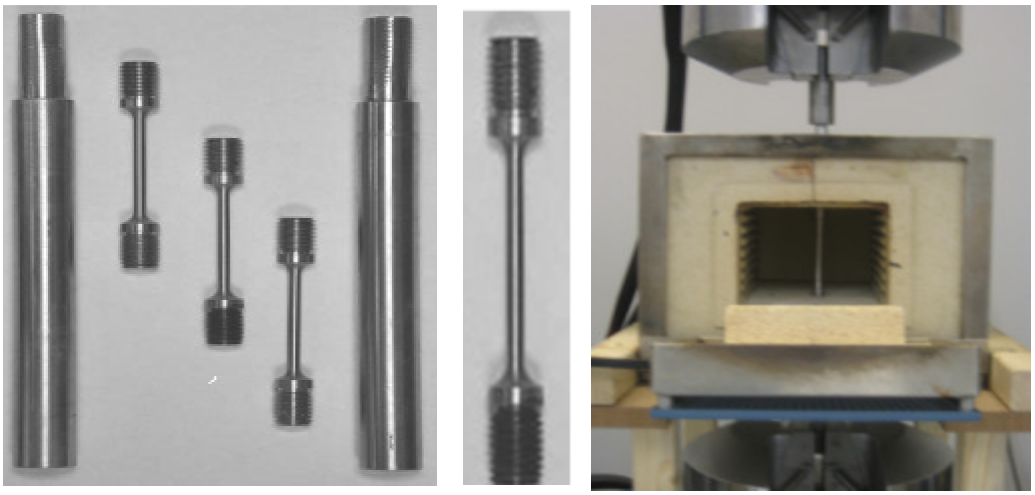

**Figure 4.10: X-70 threaded dog bone samples, 4mm cross section diameter, and gauge length of 45mm with grips for installation in the creep furnace**

### 4.5. Preliminary Creep Experiments with Al-7075-T6 Alloys

Creep of materials is generally associated with time dependent plasticity of materials under a constant stress (below the yield stress of the material) at an elevated temperature, often greater than approximately (0.4 to 0.5) $T_m$, where $T_m$ is the absolute melting temperature. To perform the creep experiments two different materials were considered: Al 7075-T6 and X-70 carbon steel (both are used in oil refinery industry).

First creep experiments were performed on Al-7075 samples because of its lower creep temperature requirement. Equipment reliability properties were checked under different load and displacement conditions at different temperatures. To estimate the amount of constant stress applied to the sample (for remaining in the elastic regime below the yield strength of the material), stress strain curve of these materials was used.

The stress-strain curve for Al 7075 and its counterpart from the literature are given in Figure 4.11. In order to determine the appropriate displacement required for testing, stress vs. displacement curve was created as shown in Figures 4.12.

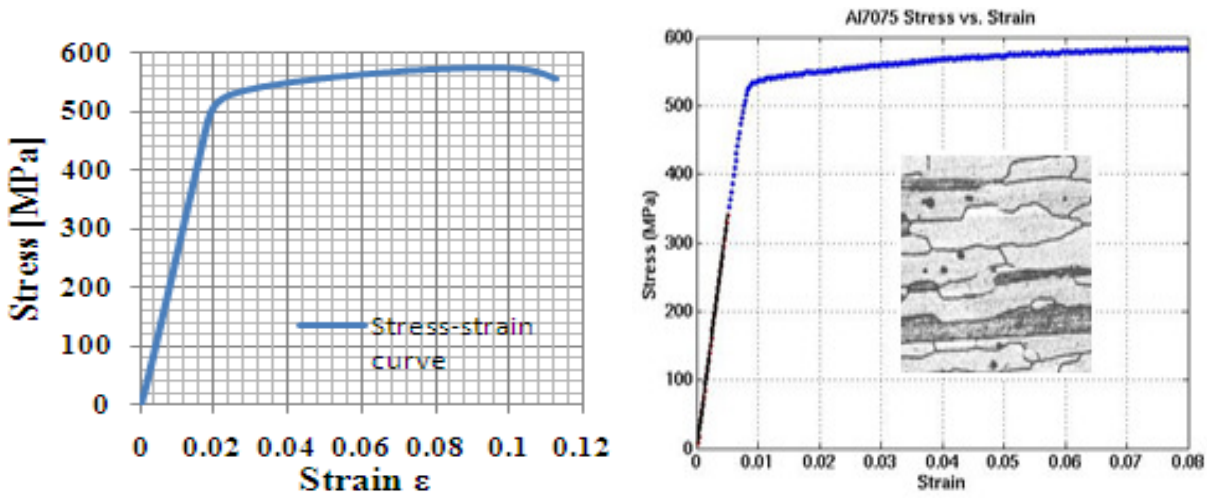


**Figure 4.11: Stress-strain curve of Al-7075-T6 alloy left , and stress-strain curve of the same alloy from the literature with elongated grains (etched with 10% phosphoric acid)[1]**

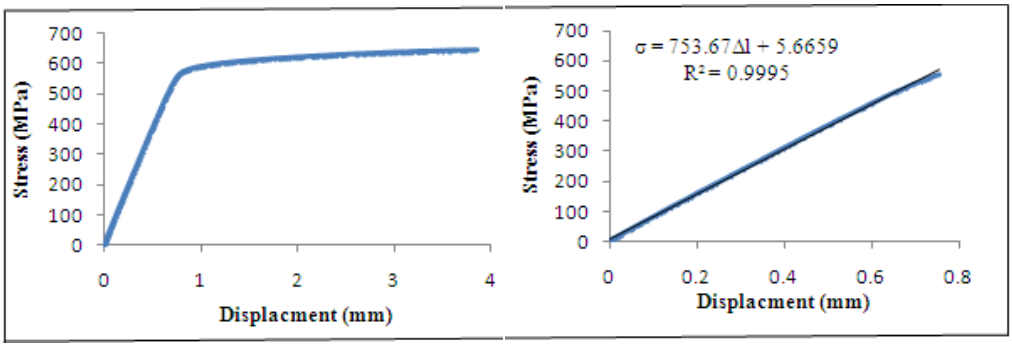


**Figure 4.12: Stress-displacement curve for Al 7075-T6 (left), and stress-displacement curve for Al 7075-T6 (elastic region) (right)**

Three different Al-7075-T6 samples were tested at different applied stresses of 100, 250, and 400 MPa, at 573 °K. The resulting displacement versus time of these samples is given in Figure 4.13.

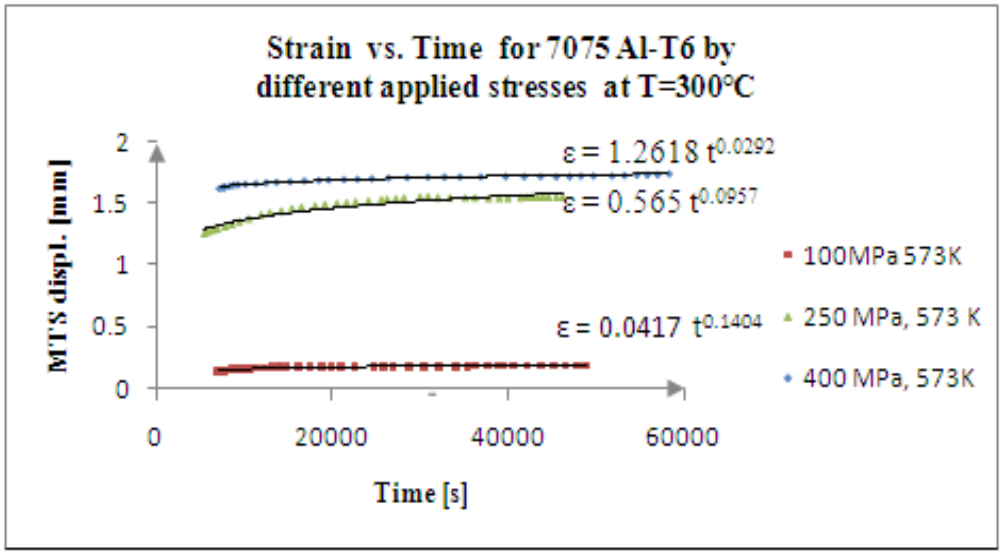


**Figure 4.13: MTS Displacement vs. Time for Different Al-7075-T5 Alloys at Different Stresses**

The stress, σ, dependency of the coefficient A, and exponent n, of the empirical equation for the primary part found, are given by the following relations:

$$A = \alpha\, \sigma^{m} \quad and \quad n = \beta\, \sigma + \gamma \tag{4.1}$$

with:

$$A = 4 \times 10^{-7} \sigma^{2.5123} and\ n = -0.0004 \times \sigma + 0.1811 \tag{4.2}$$

where α, m, β, and γ are material parameters that might depends on temperature and other material parameters.

The final stress dependent creep equation looks now like:

$$\varepsilon = 4 \times 10^{-7} \cdot \sigma^{2.5123} \cdot t^{-0.0004\times\sigma+0.1811} + [B t^{m} \exp(pt)] \tag{4.3}$$

Additional experiment was done on an Aluminum sample. This experiment allows the study of secondary and tertiary creep. The results of this creep experiment are shown in Figure 4.14.

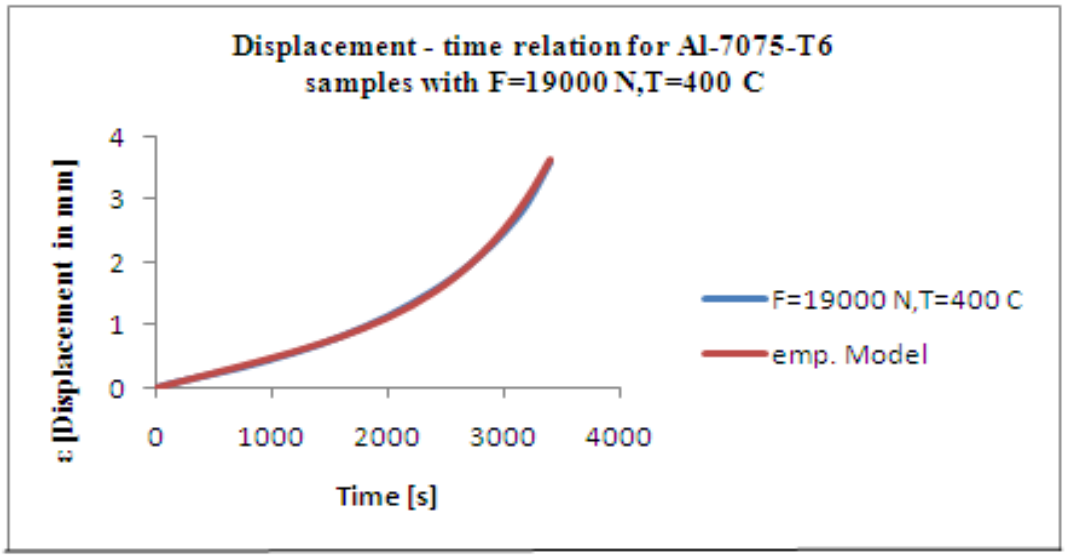


**Figure 4.14: Displacement-Time (creep curve) of Al-7075-T6 at 400°C**

The following relation was obtained for the creep behavior by an applied force of 19000 N, at 673K:

$$\varepsilon = 0.000685\, t^{0.939} + (1.695 \times 10^{-8})\, t^{1.965} \exp\,(0.000795\, t) \qquad (4.4)$$

Further experiments should be done to estimate the temperature and stress dependencies of the given parameters.

Since creep experiment takes a long time, and MTS machine was not always available, accelerated life tests (under high stress and high temperature conditions) have been performed to reduce the time of the creep test.

The broken Aluminum dog bone samples with the ductile transgranular mode and heat affected re-crytallisation (grain growth) form is shown in Figure 4.15.

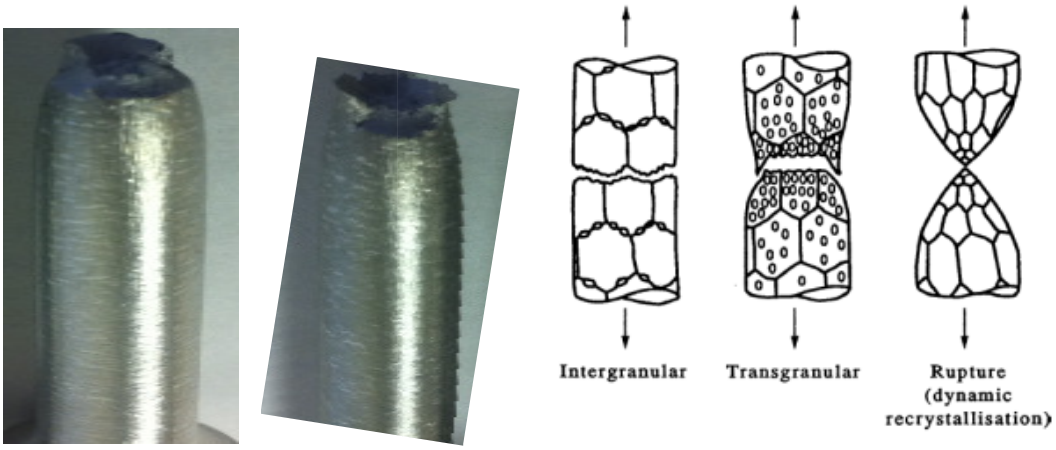


**Figure 4.15: Ductile transgranular mode of rupture form of Al-creep sample at 400°C, with recrystallized grain growth form and compared picture given in the literature**

After our unsatisfactory experiments on CT samples, new threaded dog bone samples with appropriate grips were prepared. For estimation the applied stresses during the creep experiments we made our own stress-strain curve for the X-70 carbon steel. For doing our creep test we choose the 60-80% of the yield point of the material and will prepare the experiment with our home made furnace at 500-700°C.

The prepared dog bone X-70 carbon steel samples and threaded grips together with its installation in the furnace are shown in Figure 4.16.

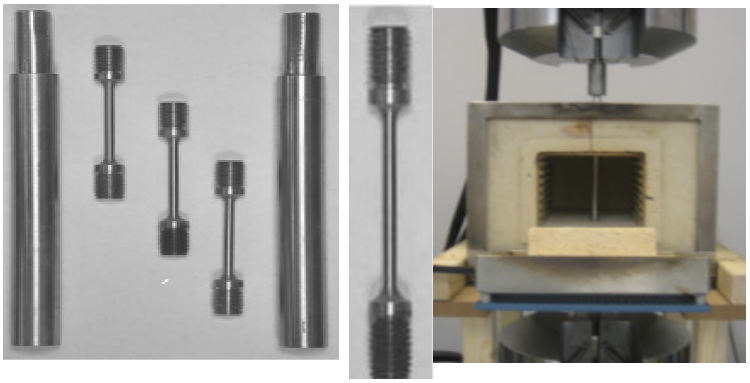

**Figure 4.16: X-70 threaded dog bone samples, 4mm cross section diameter, and gauge length of 45mm with grips for installation in the creep furnace]**

### 4.6. Preliminary Creep Experiments with X-70 Carbon Steel Samples

Stress–strain curve of X-70 carbon steel sample was estimated with an extension rate of 1mm/hr. X-70 carbon steel sample shows ductile cup and cone form after breakage with elongated grains toward the rupture cross section. Figure 4.17 shows the stress-strain curve of X-70 carbon steel and Figure 4.18 shows the same sample in its necking and broken forms. The cup and cone mode of the broken parts shows a trans-granular mode of rupture form.

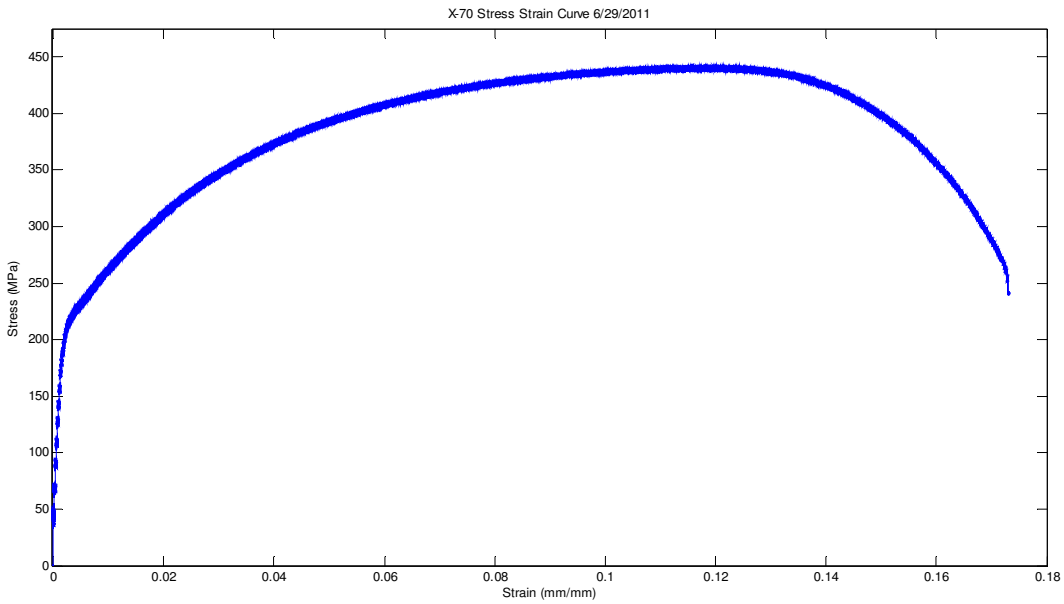


**Figure 4.17: Stress-strain curve of X-70 carbon steel**

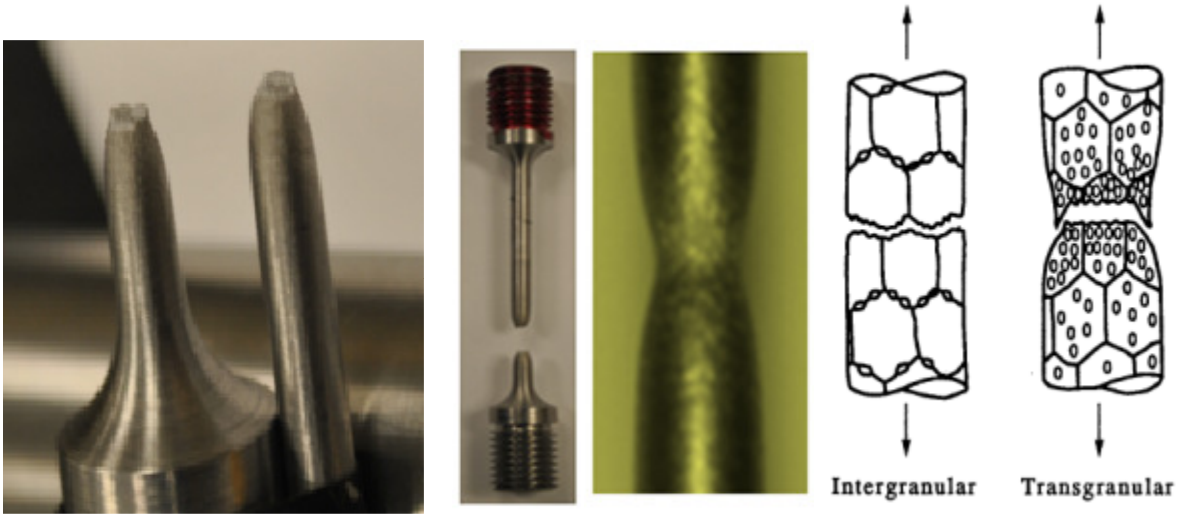


**Figure 4.18: Ductile cup and cone form of rupture cross section of X-70 carbon steel, broken sample parts, and grain elongation toward the necking region**

It should be mentioned that exact estimation of temperature and stress dependencies of parameters need more time and samples and is costly. Besides creep experiment needs its own creep equipment and specific high temperature extensometers, instead of a MTS machine that is more specified for estimation of stress-strain behaviors of metallic materials.

### 4.7. Final Experiments on Al-7075-T6 Alloys

Creep experiments of Al-7075T6 samples were performed in a MTS tensile (810)-machine and in a homemade furnace extra prepared and equipped with a tap water circulation (for cooling the grips connected to the samples). Grips were cooled additionally with two small fans to prevent the heat extension to MTS gripes and to provide a constant temperature for the samples during the creep experiments. MTS-machine equipped with furnace and computer connected for data acquisition is given in Figure 4.19.

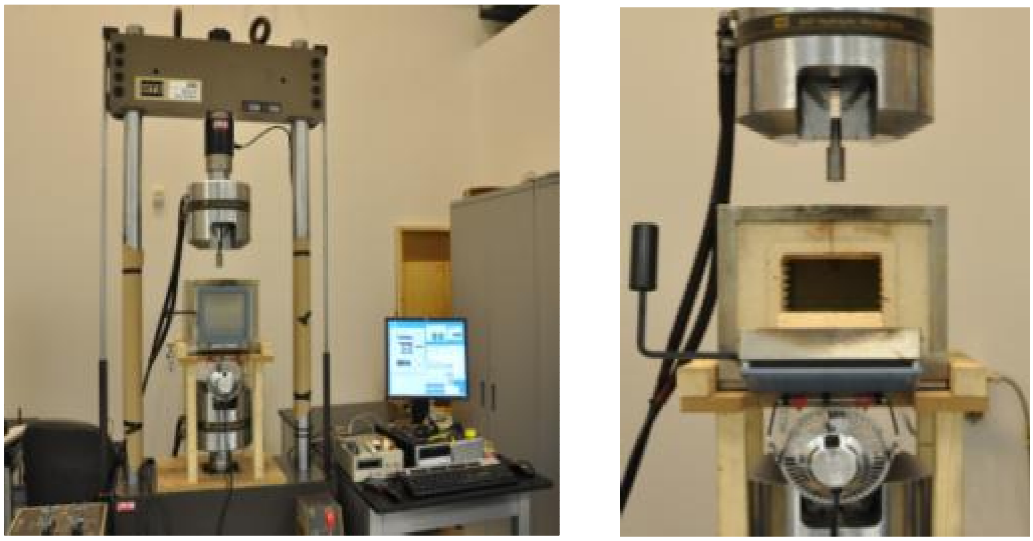

**Figure 4.19: MTS-810 Material Test System equipped with creep furnace and data acquisition.**

It should be mentioned that cooling with ice cooled water causes a negative creep rate in the samples during the creep experiment.

Al-samples used in the creep experiment are shown in the Figure 4.20. Ductile cup and cone fracture cross section after the creep experiments are clearly visible in the figure.

**Figure 4.20: Al-7075-T6 used in creep experiments with hardened grip holders**

Stress strain diagram is an important part of a creep experiment. The amount of stress applied during a creep experiment can be taken from the stress strain diagram. Applied stress is chosen usually 60 to 80 percent of the yield point (or of the ultimate strength) of materials. Estimated stress strain curve of Al-7075 material at different temperatures and its counterpart at room temperature [9] are given in Figure 4.21.

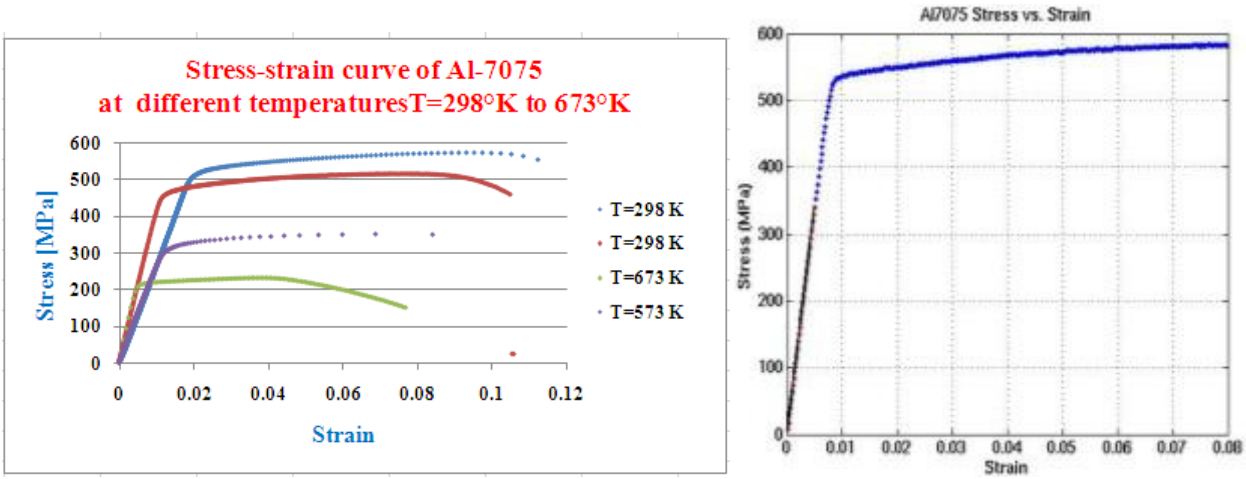


**Figure 4.21: Stress strain curve of Al-7075 at different temperature compared with the given stress strain curve at room temperature from the literature [1]**

A complete creep experiments takes usually months or years and because of unavailability of the MTS machine to perform a long time experiment we tried to accelerate our creep experiments. To get some acceptable data, we reduced the breaking times to hours or days. Figure 4.22 shows the creep curves experimentally taken and theoretically modeled and fitted with our proposed empirical model.

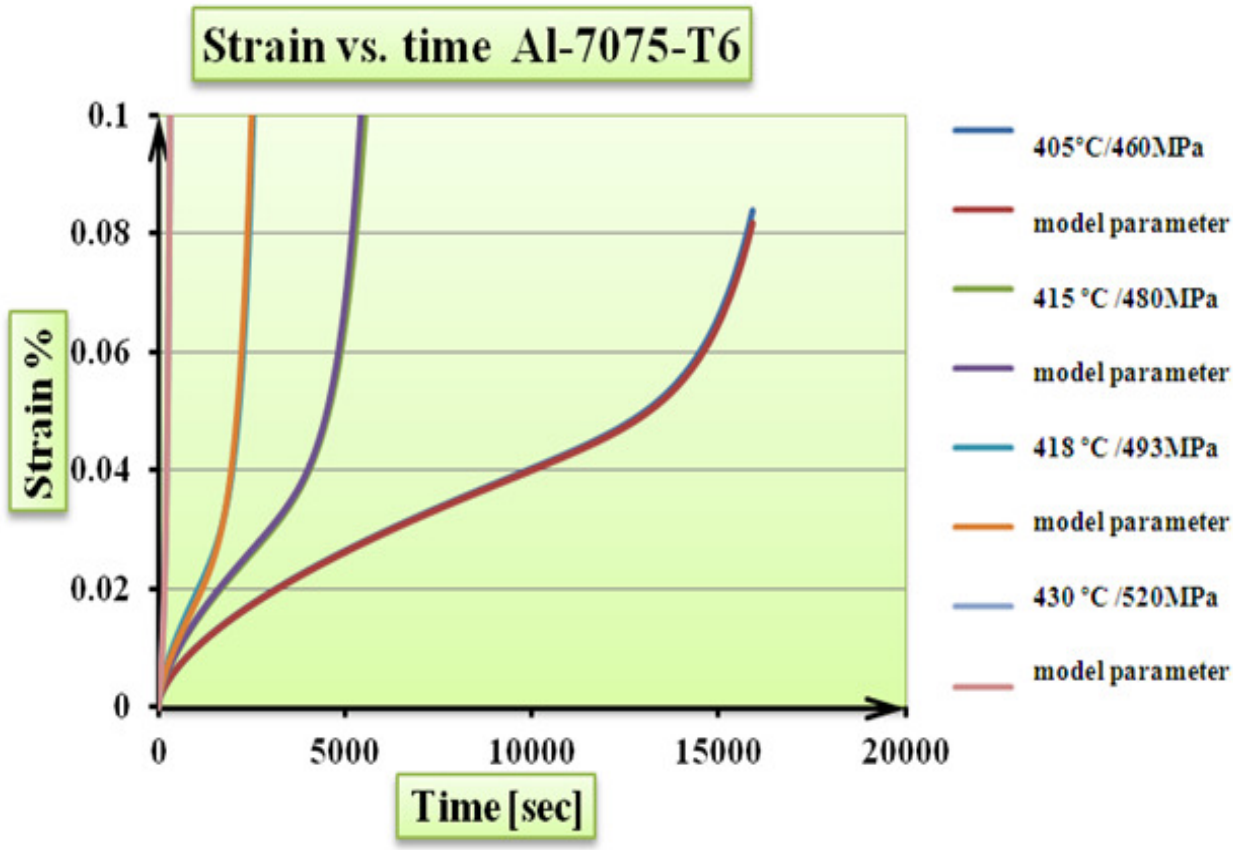


**Figure 4.22: Creep curves of Al-7075 from experiment and fitted with the proposed empirical model by Excel**

Proposed empirical model had the following form and the corresponding parameter values are given in the table 1.

$$\varepsilon = A \cdot t^n + C \cdot t^m \cdot \exp(p \cdot t) \tag{4.5}$$

where A, n, B, m, and p are material parameters and depend on temperature and applied stresses.

**Table 4.1: Numerical values for corresponding parameters of the proposed empirical model**

| T [°C] | T [°K] | σ [MPa] | A | n | B | m | p |
|---|---|---|---|---|---|---|---|
| 405 | 678 | 460 | 0.000157 | 0.601998 | 1.78698E-12 | 1.2309739 | 0.00073 |
| 415 | 688 | 480 | 0.000196 | 0.634809 | 1.67424E-10 | 1.3563949 | 0.001474 |
| 418 | 691 | 493 | 0.000198 | 0.649756 | 3.20199E-09 | 1.4138459 | 0.002327 |
| 430 | 703 | 520 | 0.00248 | 0.691316 | 1.46964E-06 | 1.5728474 | 0.006008 |

So it was possible to estimate the temperature and stress dependency of parameters.

Parameters A, B, and p have exponential dependencies on Temperature and stress. Parameters n, and m have a linear dependency on temperature and stress.

Exponential dependency on temperature for parameter A is known in the creep literature but important linear dependencies of n, and m parameters on temperature and stress are shown for the first time.

Parameter values were estimated by Excel and the distributions for A and C parameters by MATLAB program. Following figures show the creep curves by MATLAB program. General empirical creep relation and parameters have the following forms:

$$\boldsymbol{\varepsilon = A \cdot t^n + B \cdot t^m \cdot \exp(p \cdot t)} \tag{4.6}$$

With:

$$\boldsymbol{A = (3.9266E8) \cdot exp(-0.0073 \cdot \sigma_i) \cdot exp(-142000/RT_i)} \tag{4.7}$$

$$\boldsymbol{A' = 3.9266E8} \tag{4.8}$$

$$\boldsymbol{n = 0.0018228T_i + 0.00072913\sigma_i - 0.96926)} \tag{4.9}$$

$$\boldsymbol{B = (8.0E - 58) \cdot exp(0.227 \cdot \sigma_i)} \tag{4.10}$$

$$\boldsymbol{B' = 8.0E - 58} \tag{4.11}$$

$$\boldsymbol{m = 0.0068779T_i + 0.0028321\sigma_i - 4.7350083} \tag{4.12}$$

$$\boldsymbol{p = [(7.00182E - 11) \cdot exp(0.03513 \cdot \sigma_i)} \tag{4.13}$$

The final equation for the empirical model changes to the following complex form.

$$\varepsilon = A' \cdot [\exp(\alpha \cdot \boldsymbol{\sigma}) \cdot \exp(Q_A/R\boldsymbol{T})] \cdot \boldsymbol{t}^{\beta \boldsymbol{T} + \gamma \boldsymbol{\sigma} + \delta} + B' \cdot \boldsymbol{exp}(\beta \cdot \boldsymbol{\sigma_i}) \cdot \boldsymbol{t}^{\beta' \boldsymbol{T} + \gamma' \boldsymbol{\sigma} + \delta'} \cdot \exp(p \cdot \boldsymbol{t}) \tag{4.14}$$

where α, β, β', γ, γ', δ, and δ' are now material parameters and their dependency on other material structural properties like (grain diameters, hardness etc.) is possible.

or,

$$\begin{aligned}
&\boldsymbol{\varepsilon(t_i)} \\
&\boldsymbol{= (3.9266E8) \cdot exp(-0.0073 \cdot \sigma_i)} \\
&\boldsymbol{\cdot exp(-142000/RT_i) \cdot t_i^{(0.0018228T_i + 0.00072913\sigma_i - 0.96926)} + (8.0E - 58) \cdot exp(0.227 \cdot \sigma_i)} \\
&\boldsymbol{\cdot t_i^{(0.0068779T_i + 0.0028321\sigma_i - 4.7350083)} \cdot exp[(7.00182E - 11) \cdot exp(0.03513 \cdot \sigma_i) \cdot t_i]}
\end{aligned} \tag{4.15}$$

Creep curves evaluated for Al-7075-T6, together with PDF and cumulative distributions for parameters A and C by MATLAB program are given in Figure 4.23.

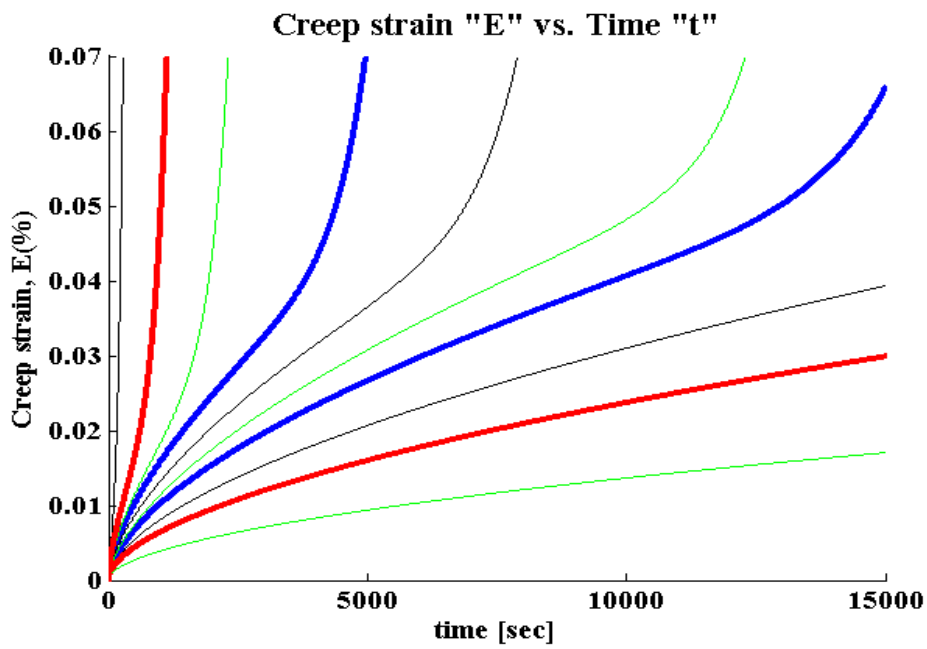


**Figure 4.23: Creep curves of Al-7075-T6 at different temperature and stresses from data given in the above table (bulk) and additional predicted creep curves at proposed temperature and stresses (thin lines)**

Parameters A, and B are lognormally distributed. Their PDF and cumulative are given in the following Figures 4.24, and 4.25.

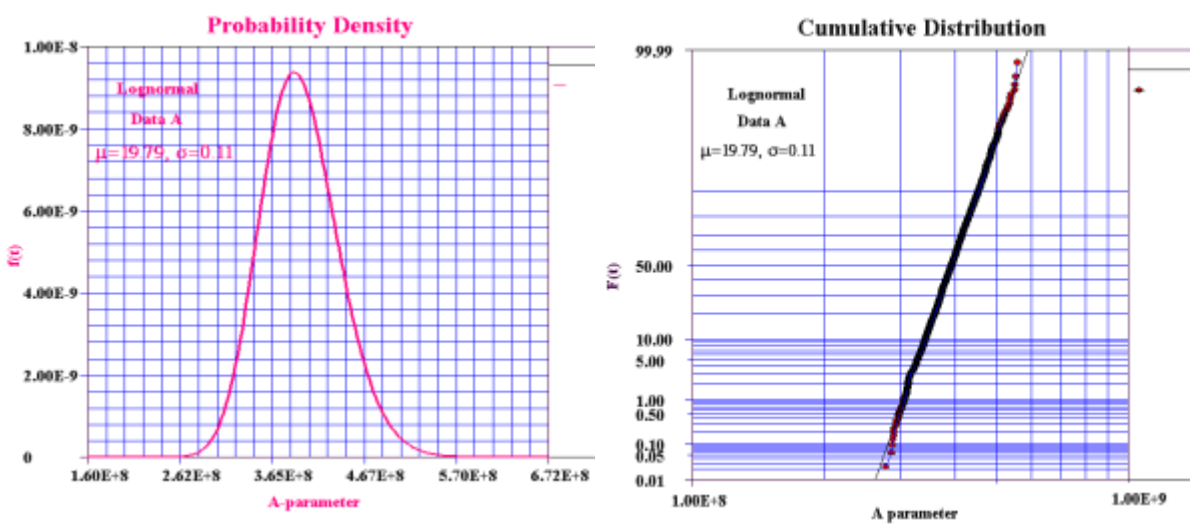


**Figure 4.24: PDF and CDF of parameter A = $\mathcal{LN}$ (μ=19.79, σ=0.11)**

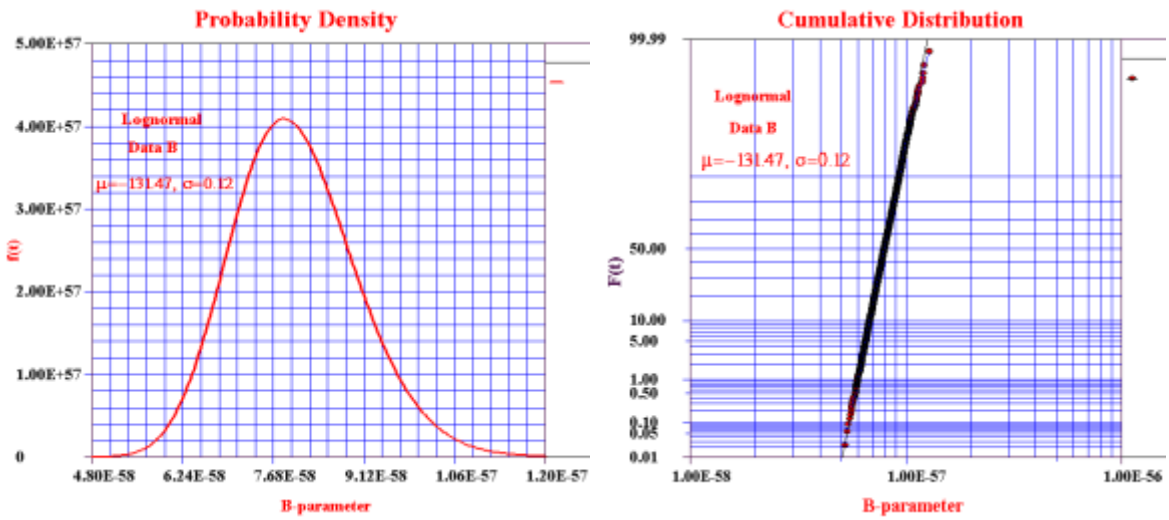


**Figure 4.25: PDF and CDF of parameter B= $\mathcal{LN}$ (μ=-131-47, σ=0.12)**

## 4.8. Final Experiments on X-70 Carbon Steel Alloys

As shown in Figure 4.26, three dog bone X-70 carbon steel samples with threaded parts at two ends were made from a part of X-70 carbon steel pipe. Threaded dog bone samples have 4mm cross-section diameter, and a gauge length of 45mm.

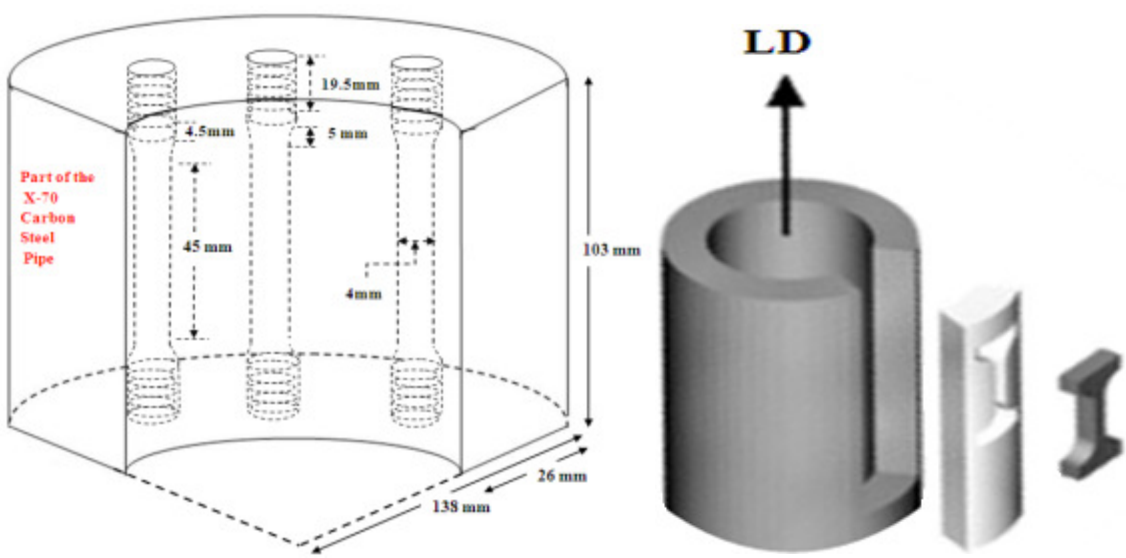


**Figure 4.26: Three dog bone X-70 carbon steel samples with threaded parts at two ends made from a part of X-70 carbon steel pipe**

Two threaded long grips for installation the samples in furnace were made.

Because of softness of the grip materials (compared with the X70 carbon steel samples) two threaded long grips were tempered at 900°C for approximately 3 hours and quenched in oil (Surface hardening).

Threaded samples and the corresponding hardened grips are given in Figure 4.27.

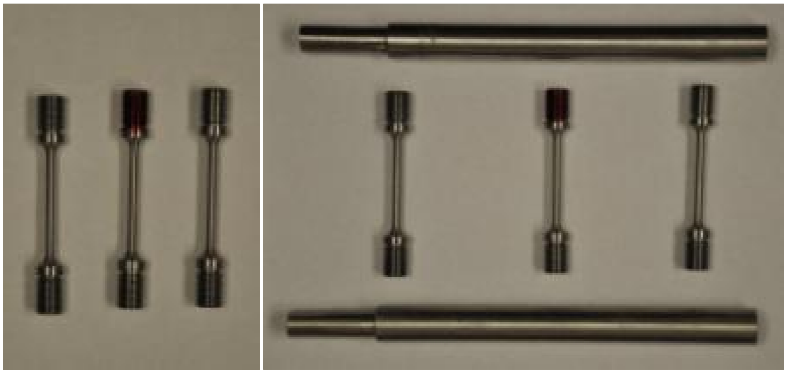

**Figure 4.27: Dog boned X70 carbon steel samples used for the creep experiment**

Broken sample for estimation the stress strain curve at room temperature has a cup and cone ductile form while the broken samples after the creep experiments show brittle fracture. These characteristics are shown in Figure 4.28.

**Figure 4.28: Broken sample at room temperature with cup and cone ductile breakage (left) and two X70 carbon steel samples after creep experiment with brittle fracture types (right)**

Creep curve estimated from one of the sample is shown in Figure 4.29. The first part of the curve shows some fluctuation (because of temperature variation from 418ºC to stabilized temperature of 450C).

Creep curve with completed secondary and tertiary parts is completely coverable with the proposed model.

The primary part up to 5000 second is then fitted with the proposed empirical equation after readjustment with a fracture life times estimated from the Monkman and Grant relation. Both experimentally find creep curves and two fitted parts with our proposed model are given in Figure 4.29.

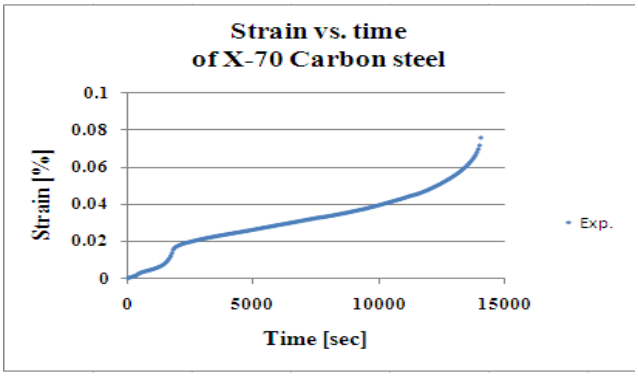


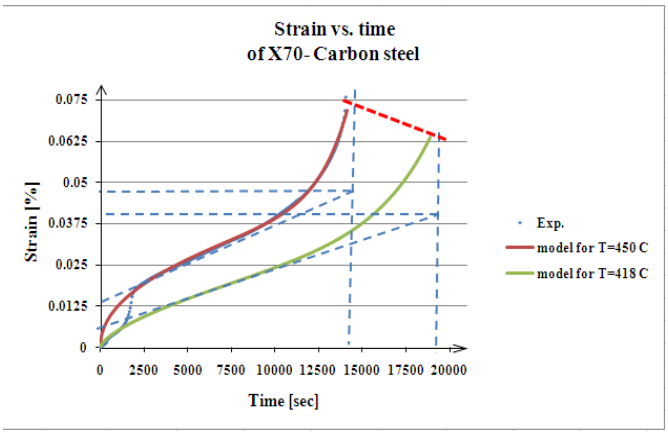


**Figure4.29: creep curve of X70 carbon steel at T=450°C and σ= 348MPa,(top) and predicted creep curve at 418°C both fitted with proposed empirical equation (bottom)**

Empirical equations for both of the creep curves are given below:

$$\varepsilon_{450} = (0.000488) \cdot \boldsymbol{t}^{0.4695} + (1.383 \times 10^{-10}) \cdot \boldsymbol{t}^{1.2362} \cdot \exp(0.0005198 \cdot \boldsymbol{t}) \quad (4.16)$$

$$\varepsilon_{418} = (0.000056) \cdot \boldsymbol{t}^{0.653} + (9.983 \times 10^{-10}) \cdot \boldsymbol{t}^{1.2362} \cdot \exp(0.000265 \cdot \boldsymbol{t}) \quad (4.17)$$

It should be mentioned that exact estimation of temperature and stress dependencies of parameters need more time and samples (and therefore additional cost). Besides creep experiments need their own creep equipment and specific high temperature extensometers

Figure 4.30 shows the creep curves experimentally taken and theoretically modeled and fitted with the proposed empirical model.

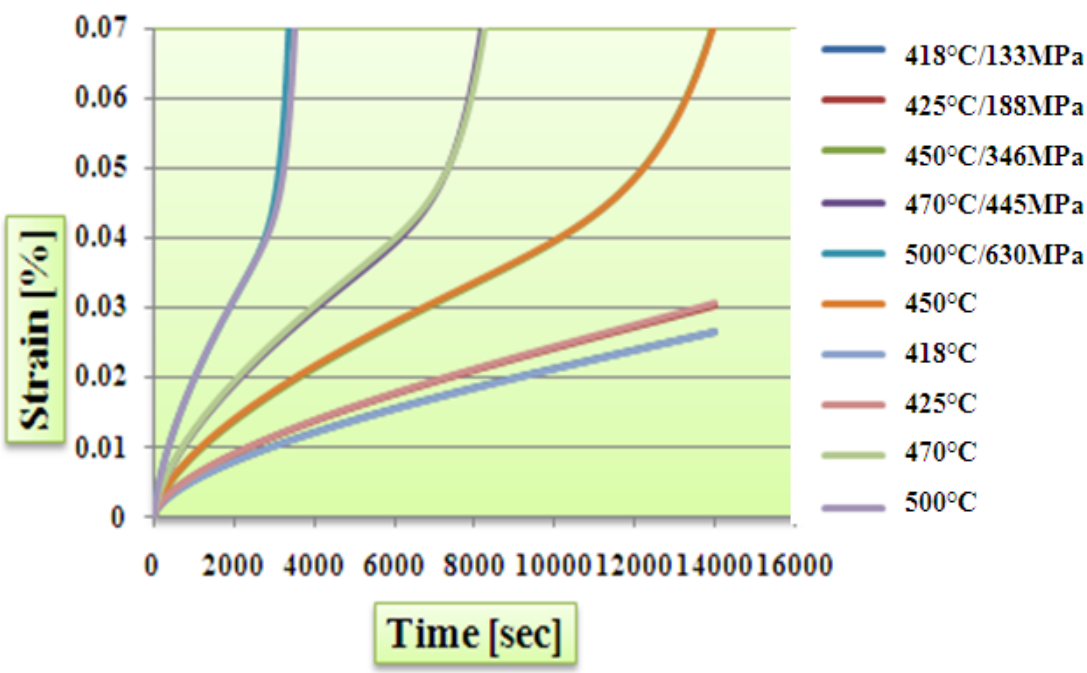


**Figure 4.30: Creep curves of X-70 carbon steel from experiment and fitted with the proposed empirical model by Excel**

Proposed empirical model had the following form and the corresponding parameter values are given in the Table 4.2.

$$\varepsilon = A \cdot t^n + C \cdot t^m \cdot \exp(p \cdot t) \tag{4.18}$$

where A, n, B, m, and p are material parameters and depend on temperature and applied stresses.

**Table 4.2: Numerical values for corresponding parameters of the proposed model**

| T [ C ] | T[K] | σ [MPa] | A | n | B | m | p |
|---|---|---|---|---|---|---|---|
| 418 | 691 | 133 | 8.1E-5 | 6.04E-01 | 2.87E-9 | 1.0488 | 0.000182 |
| 425 | 698 | 185 | 8.8E-5 | 0.6087 | 1.46E-9 | 1.03975 | 0.000239 |
| 450 | 723 | 346 | 1.2E-4 | 0.6255 | 1.7999E-10 | 1.0099 | 0.000639 |
| 470 | 743 | 445 | 1.5E-5 | 0.63745 | 4.9695E-11 | 0.989 | 0.001401 |
| 500 | 773 | 620 | 2.12E-4 | 0.6567 | 5.1085E-12 | 0.955 | 0.004551 |

Parameter values were estimated by Excel and the distributions for A and C parameters by MATLAB and Bayesian regression by WinBUGS program. Following figures show the creep curves by MATLAB program. General empirical creep relation and parameters have the following forms:

$$\boldsymbol{\varepsilon = A \cdot t^n + B \cdot t^m \cdot \exp(p \cdot \cdot t)} \tag{4.19}$$

with

$$\boldsymbol{A = (5.1E16) \cdot exp(-0.008 \cdot \sigma_i) \cdot exp(-269000/RT_i)} \tag{4.20}$$

$$\boldsymbol{A' = 5.1E16} \tag{4.21}$$

$$\boldsymbol{n = 0.0003T_i + 0.000045\sigma_i + 0.39303)} \tag{4.22}$$

$$\boldsymbol{B = (1.617.0E - 8) \cdot exp(-0.013 \cdot \sigma_i)} \tag{4.23}$$

$$\boldsymbol{B' = 1.617.0E - 8} \tag{4.24}$$

$$\boldsymbol{m = -0.0006T_i + 0.0001\sigma_i + 1.4784} \tag{4.25}$$

$$\boldsymbol{p} = [(\mathbf{0.00008015}) \cdot \boldsymbol{exp}(\mathbf{0.006} \cdot \boldsymbol{\sigma_i}) \tag{4.26}$$

The final equation for the empirical model changes to the following complex form.

$$\varepsilon = A' \cdot [\exp(\alpha \cdot \boldsymbol{\sigma}) \cdot \exp(-Q_A/R\boldsymbol{T})] \cdot \boldsymbol{t}^{\beta \boldsymbol{T} + \gamma \boldsymbol{\sigma} + \delta} + B' \cdot \boldsymbol{exp}(\beta \cdot \boldsymbol{\sigma_i})\, \boldsymbol{t}^{\beta' \boldsymbol{T} + \gamma' \boldsymbol{\sigma} + \delta'} \cdot \exp(p \cdot \boldsymbol{t}) \tag{4.27}$$

where α, β, β', γ, γ', δ, and δ' are now material parameters and their dependency on other material structural properties like (grain diameters, hardness etc.) is possible.

$$\begin{aligned}
&\boldsymbol{\varepsilon}(\boldsymbol{t_i}) \\
&= (\mathbf{5.1}\boldsymbol{E}\mathbf{16}) \cdot \boldsymbol{exp}(-\mathbf{0.008} \cdot \boldsymbol{\sigma_i}) \\
&\cdot \boldsymbol{exp}(-\mathbf{269000}/\boldsymbol{RT_i}) \cdot \boldsymbol{t_i}^{(\mathbf{0.0003}\boldsymbol{T_i} + \mathbf{0.000045}\boldsymbol{\sigma_i} + \mathbf{0.39303})} + (\mathbf{1.617}\boldsymbol{E} - \mathbf{8}) \cdot \boldsymbol{exp}(-\mathbf{0.013} \cdot \boldsymbol{\sigma_i}) \\
&\cdot \boldsymbol{t_i}^{(-\mathbf{0.0006}\boldsymbol{T_i} + \mathbf{0.0001}\boldsymbol{\sigma_i} + \mathbf{1.4784})} \cdot \boldsymbol{exp}[(\mathbf{0.00008015}) \cdot \boldsymbol{exp}(\mathbf{0.006} \cdot \boldsymbol{\sigma_i}) \cdot \boldsymbol{t_i}]
\end{aligned} \tag{4.28}$$

Creep curves evaluated for X-70carbon steel, together with PDF and cumulative distributions for parameters A and C by MATLAB program are given in the following Figures 4.31 to 4.33.

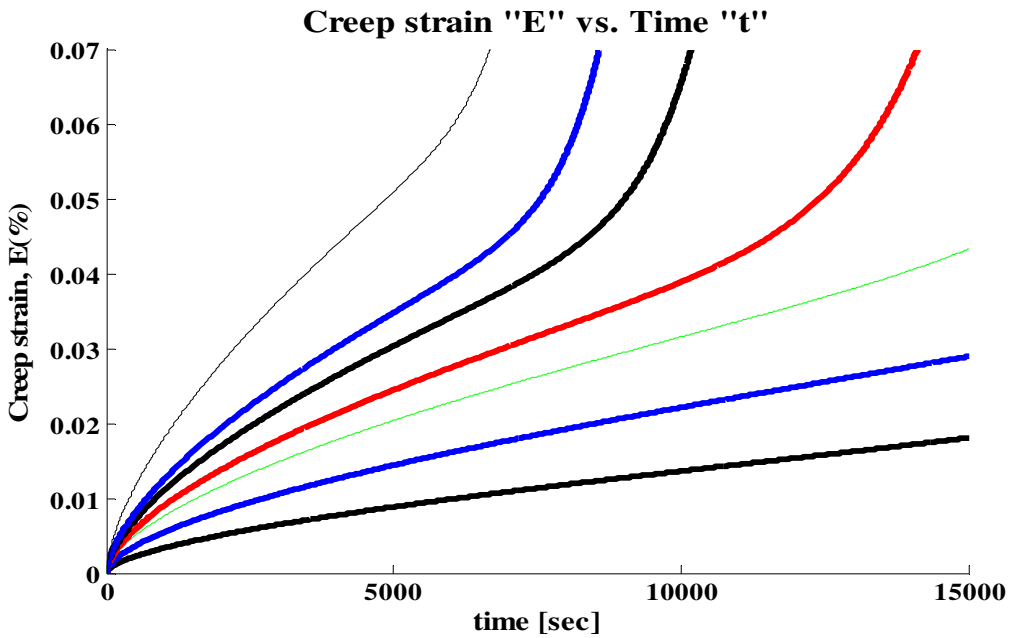


**Figure 4.31: Creep curves of X-70 carbon steel at different T and σ from data in the above table (bulk) and predicted creep curves at proposed temperature and stresses (thin lines)**

A, and B parameters are lognormal distributed. Their PDF and cumulative are given in the following figures.

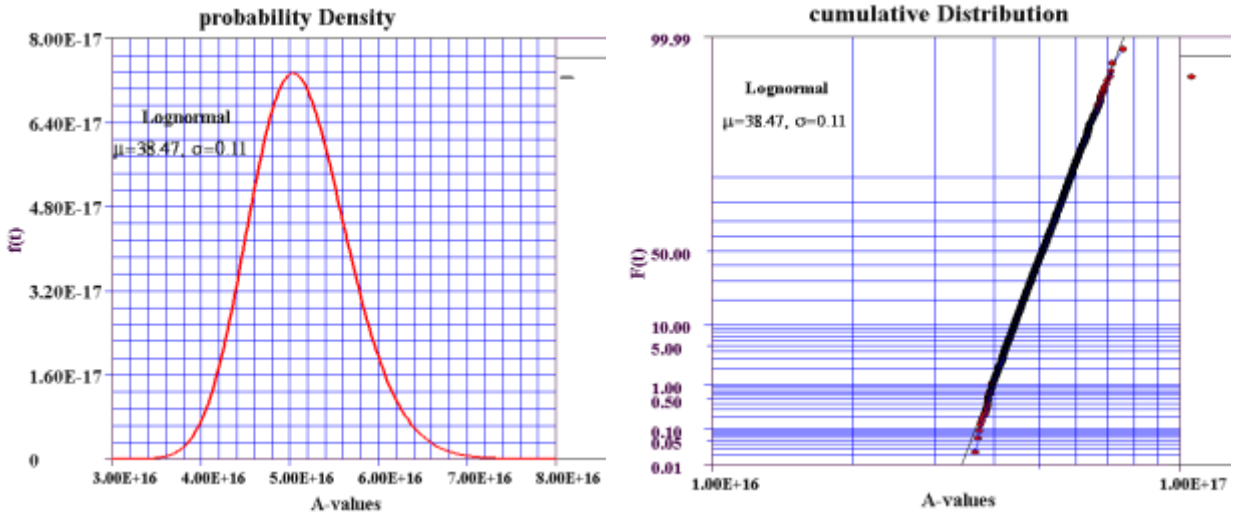


**Figure 4.32: PDF and CDF of parameter A = $\mathcal{LN}$ (μ=38.47, σ=0.11)**

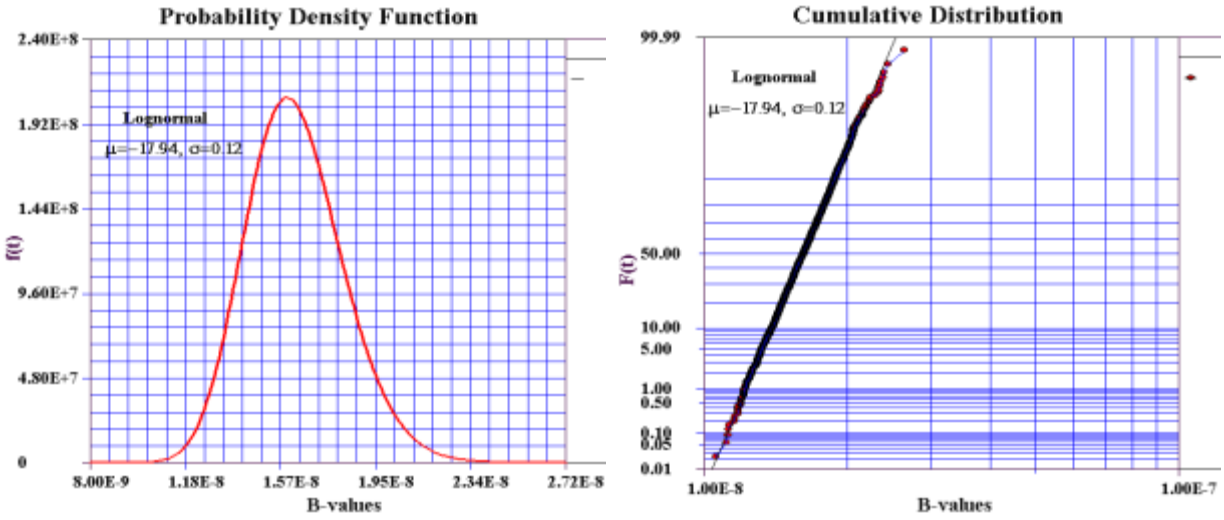


**Figure 4.33: PDF and CDF of parameter B= $\mathcal{LN}$ (μ= -17.94, σ=0.12)**

# Chapter 5:

# Estimation of the Proposed Empirical Model Parameters Using Bayesian Inference

## 5.1. Introduction

Initially, we estimated parameters A and B of our empirical model, using the generic data from the creep literature as benchmark model. This estimation may be used as prior estimates of the empirical model parameters in a Bayesian updating frame-work. In this section, the Bayesian inference of the model parameters represented as joint distribution of A and B. Assuming a lognormal distribution to represent the variability of creep strain, the likelihood function of the creep strain [%] and the corresponding different percentiles of this distribution is expressed as:

$$f(\varepsilon_i) = LN(\mu_i, s_i) \tag{5.1}$$

$$\mu_i = LN[\boldsymbol{A} \cdot \boldsymbol{t^n} + \boldsymbol{B} \cdot \boldsymbol{t^m} \cdot \mathbf{exp}(\boldsymbol{p} \cdot \cdot \boldsymbol{t})] \tag{5.2}$$

with corresponding parameter dependencies on T and σ.

where $\mu_i$ and $s_i$ are the log-mean and log-standard deviation of the strain distribution.

By using Equation

$$\boldsymbol{\varepsilon} = \boldsymbol{A} \cdot \boldsymbol{t^n} + \boldsymbol{B} \cdot \boldsymbol{t^m} \cdot \mathbf{exp}\ (\boldsymbol{p} \cdot \cdot \boldsymbol{t}) \tag{5.3}$$

one may replace the log-mean of the strain[%] distribution with Equation

$$\mu_i = Ln[f(T_i, \sigma_i, t)] \tag{5.4}$$

This equation is the proposed empirical Equation.

Substitution of equation

$$\mu_i = LN[\boldsymbol{A} \cdot \boldsymbol{t^n} + \boldsymbol{B} \cdot \boldsymbol{t^m} \cdot \mathbf{exp}(\boldsymbol{p} \cdot \cdot \boldsymbol{t})] \tag{5.5}$$

in the following relation,

$$\boldsymbol{f}(\boldsymbol{\varepsilon_i}) = \boldsymbol{LN}(\boldsymbol{\mu_i}, \boldsymbol{s_i}) \tag{5.6}$$

yields the conditional distribution function of the strain "ε" given stress conditions (temperature and applied stress and creep time):

$$f(\varepsilon_i|T, \sigma, t) = \frac{1}{s \cdot \varepsilon_i \cdot \sqrt{2\pi}} \cdot \exp\{\frac{-1}{2s^2}[Ln(\varepsilon_i) - Ln(\boldsymbol{A} \cdot \boldsymbol{t^n} + \boldsymbol{B} \cdot \boldsymbol{t^m} \cdot \mathbf{exp}(\boldsymbol{p} \cdot \cdot \boldsymbol{t}))]^2\} \tag{5.7}$$

Accordingly the likelihood function is given by:

$$L(\varepsilon_i) = \prod_{i=1}^{N} f(\varepsilon_i|T_i, \sigma_i, t) \tag{5.8}$$

Having the likelihood of the test data, one can derive the posterior distribution of parameters A and B and s utilizing Bayes' estimation according to:

$$f(A, B, s|\varepsilon_i) = \frac{f_0(A,B,s) \cdot L(A,B,s|\varepsilon_i)}{\int f_0(A,B,s) \cdot L(A,B,s|\varepsilon_i) dA dB ds} \tag{5.9}$$

where $f_o(A, B, s)$ is the subjective prior distribution (e.g. non-informative uniform distribution). This prior distribution was later updated using the experimental data from experiments. The likelihood $L(A, B, s|\varepsilon_i)$ is representing each data point *i*.

In the general form, there is no analytical solution available for posteriors like the equation (5.9), and Bayesian posteriors are usually estimated using sophisticated sampling approach, such as the Markov Chain Monte Carlo (MCMC) [1]. In this method the posterior function is recreated by generating enough samples rather than by direct integration. Then, a sample drawn from a generating distribution is modified through a series of conditional probability calculations until becomes a sample of the target posterior.

## 5.2. Estimation of Our Empirical Model Parameters for Al-7075-T6 Using Bayesian Inference

The WinBUGS program [2] is a windows-based environment for MCMC simulation. This program has been previously used in uncertainty management [3] as well as accelerated life testing data analysis [4] and has proved to be a reliable tool for such calculations. In this research the WinBUGs platform was used for solving posterior Equation. The general steps in the coded routine program in WinBUGS resembled that in Figure 5.1, which displays the calculated joint posteriors of A, B, and s with lognormal distributions for A and B as prior for up-dating the completed creep data from our experiments on Al-7075-T6 samples.

It should be mentioned that according to the WinBUGs program, parameter A and exponent n and parameter B and exponent m are strongly correlated. By considering this correlations in WinBUGs program the evaluated creep relation looks like:

$$\boldsymbol{\mu(i) = A \cdot exp(-0.0073 \cdot \sigma_i) \cdot exp(-142000/RT_i) \cdot t^{0.5945 \cdot exp(0.0001 \cdot \sigma_i)} +}$$

$$\boldsymbol{B \cdot exp(-0.227 \cdot \sigma_i) \cdot t^{1.0778 \cdot exp(-0.0002 \cdot \sigma_i)} \cdot exp[[(7.E - 11) \cdot exp(0.035 \cdot \sigma_i) \cdot t_i]} \quad (5.10)$$

where exponents n and m are both exponential functions dependent on stress:

$$\boldsymbol{n = 0.0018228T_i + 0.00072913\sigma_i - 0.96926 = f_1(\sigma_i)} \quad (5.11)$$

$$\boldsymbol{m = 0.0068779T_i + 0.0028321\sigma_i - 4.7350083 = f_2(\sigma_i)} \quad (5.12)$$

Where

$$\boldsymbol{f_1(\sigma_i) = (0.5945).exp(0.0001 \cdot \sigma_i)} \quad (5.13)$$

,and

$$\boldsymbol{f_2(\sigma_i) = (1.0778).exp(-0.0002 \cdot \sigma_i)} \quad (5.14)$$

In these equations, parameters n and m are given as the mere functions of applied stress. Only by considering these correlations, it was possible to get the uncertainties from the WinBUGS program.

Figure 5.1 shows the algorithm for the Bayesian approach and the corresponding posterior distributions of A, B parameters.

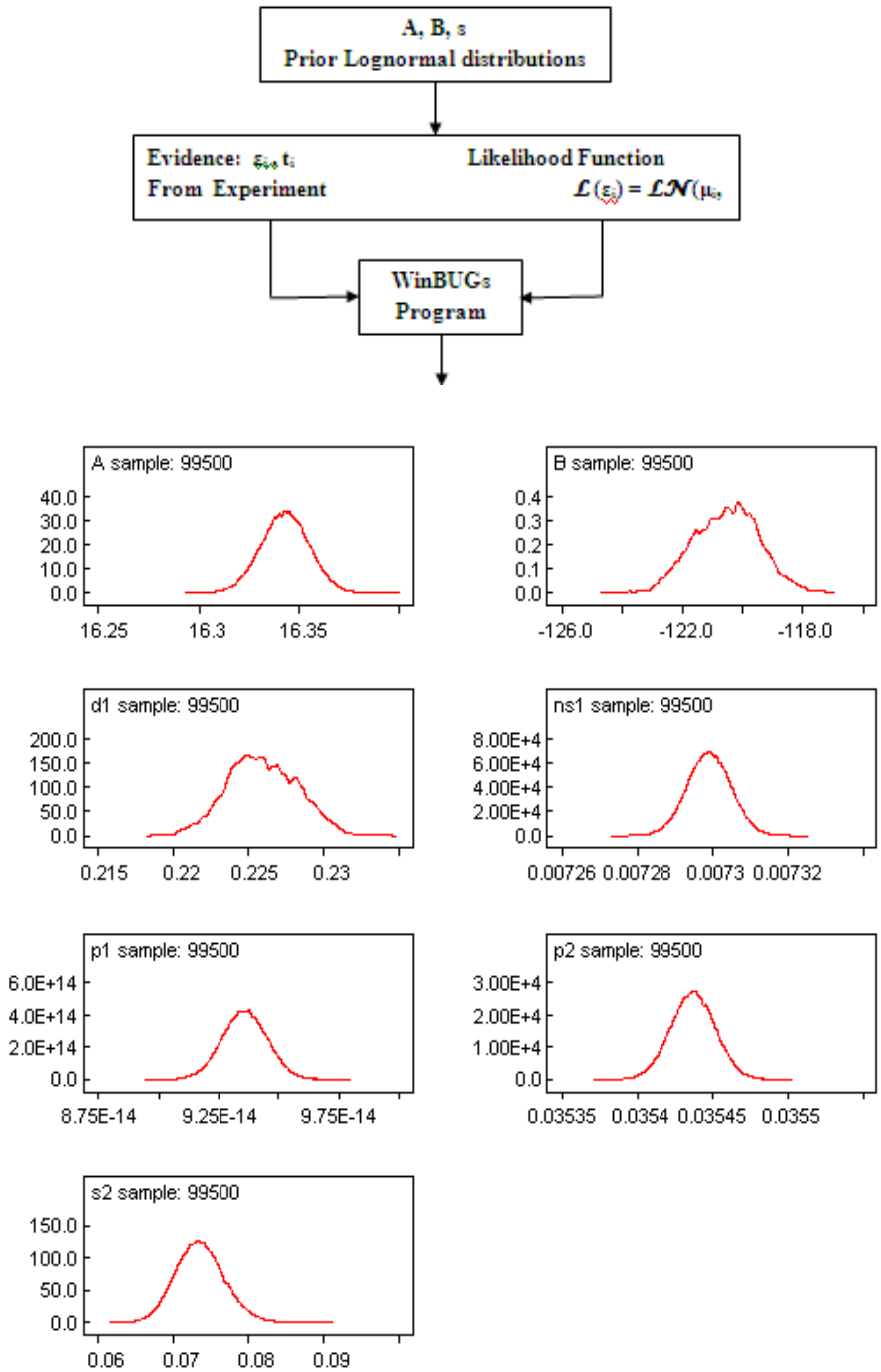


**Figure 5.1: Algorithm for the Bayesian approach (top) and the corresponding posterior distributions of A, B and s (bottom) for Al-7075-T6**

The posterior distributions for parameters A, and B for Al-7075-T6 samples are explained by the following probability density functions:

$$A = Ln(\mu = 16.34, \sigma = 0.012$$

$$B = Ln(\mu = -120.5, \sigma = 1.088)$$

$$s = Ln(\mu = 0.07352, \sigma = 0.003214)$$

The general node statistics of the parameters from WinBUGS program is given in Figure 5.2.

Node statistics

| node | mean | sd | MC error | 2.5% | median | 97.5% | start | sample |
|---|---|---|---|---|---|---|---|---|
| A | 16.34 | 0.012 | 1.223E-4 | 16.32 | 16.34 | 16.37 | 501 | 99500 |
| B | -120.5 | 1.088 | 0.05574 | -122.6 | -120.5 | -118.4 | 501 | 99500 |
| d1 | 0.2259 | 0.002351 | 1.203E-4 | 0.2214 | 0.2258 | 0.2305 | 501 | 99500 |
| ns1 | 0.007299 | 5.761E-6 | 1.831E-8 | 0.007288 | 0.007299 | 0.00731 | 501 | 99500 |
| p1 | 9.359E-14 | 1.0E-10 | 3.17E-13 | 9.176E-14 | 9.359E-14 | 9.542E-14 | 501 | 99500 |
| p2 | 0.03544 | 1.481E-5 | 4.654E-8 | 0.03541 | 0.03544 | 0.03547 | 501 | 99500 |
| s2 | 0.07352 | 0.003214 | 1.084E-5 | 0.06758 | 0.0734 | 0.08015 | 501 | 99500 |

**Figure 5.2: Values of node statistics for Al-7075-T6 model parameters taken from WinBUGS program**

Usually, to simplify the calculation for estimation the residual life of materials in service, the rupture time is given as a function of applied stresses.

In our case, rupture time of Al-7075-T6 material as a function of applied stress is given according to the following relation

$$\boldsymbol{log(t_r) = 74072 - 83204 \cdot log(\sigma) + 31165 \cdot (log(\sigma))^2 - 3892.2368 \cdot (log(\sigma))^3} \quad (5.14)$$

This relation allows us to estimate the residual lifetime of materials in service.

## 5.3. Estimation of Our Empirical Model Parameters for X-70 Carbon Steel Using Bayesian Inference

We apply the same updating procedure to estimate A and B distributions and other parameter uncertainties for X-70 carbon steel. Parameter A and n, and B and m correlated strongly together and we applied the same transformations in WinBUGS program (like Al-7075-T6 alloys- model parameter). So it is possible to estimate the posterior distributions for the strain by the WinBUGS program with an equation similar to (5.13).

Algorithms of the Bayesian inference and the corresponding posterior distributions of parameters A and B are shown in Figure 5.3.

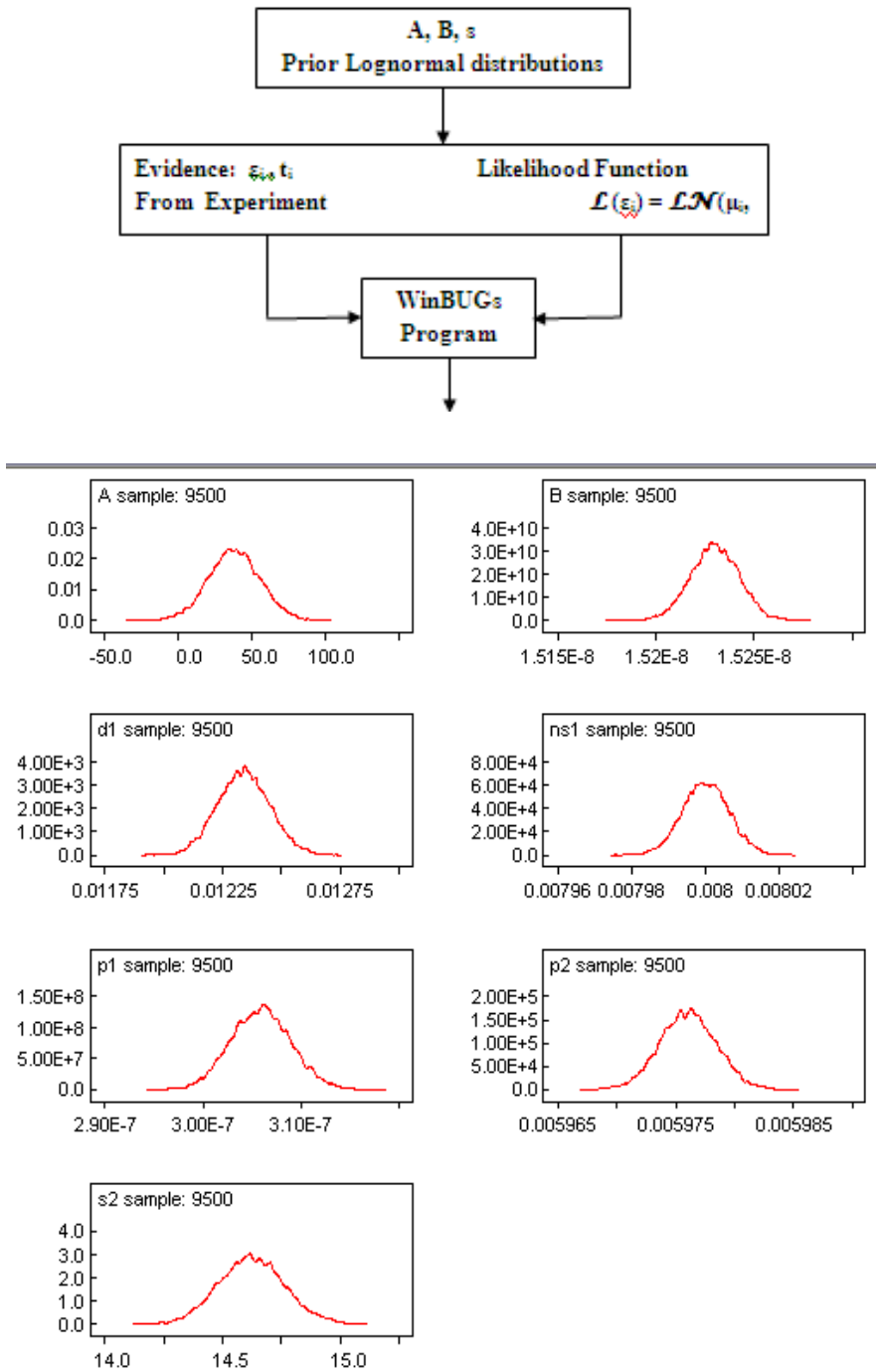


**Figure 5.3: Algorithm for the Bayesian approach (top) and the corresponding posterior distributions of A, B and s (bottom) for X-70 carbon steel**

The posterior distributions for parameters A, and B for X-70 carbon steel samples are explained by the following probability density functions:

$$A = Ln(\mu = 38.05, \sigma = 0.012$$

$$B = Ln(\mu = -17.999, \sigma = 0.11)$$

$$s = Ln(\mu = 2.68, \sigma = 0.1381)$$

The general node statistics of the parameters from WinBUGS program is given in Figure 5.4.

Node statistics

| node | mean | sd | MC error | 2.5% | median | 97.5% | start | sample |
|---|---|---|---|---|---|---|---|---|
| A | 38.05 | 17.6 | 0.194 | 3.133 | 37.96 | 72.74 | 501 | 9500 |
| B | 1.523E-8 | 1.008E-10 | 1.033E-12 | 1.521E-8 | 1.523E-8 | 1.525E-8 | 501 | 9500 |
| d1 | 0.01234 | 1.093E-4 | 1.031E-6 | 0.01213 | 0.01234 | 0.01255 | 501 | 9500 |
| ns1 | 0.008 | 6.293E-6 | 5.58E-8 | 0.007988 | 0.008 | 0.008013 | 501 | 9500 |
| p1 | 3.059E-7 | 3.041E-9 | 2.905E-11 | 3.0E-7 | 3.059E-7 | 3.12E-7 | 501 | 9500 |
| p2 | 0.005976 | 2.392E-6 | 2.45E-8 | 0.005971 | 0.005976 | 0.005981 | 501 | 9500 |
| s2 | 14.63 | 0.1381 | 0.001353 | 14.36 | 14.62 | 14.91 | 501 | 9500 |

**Figure 5.4: Values of node statistics for X-70 carbon steel model parameters taken from WinBUGS program**

Usually, to simplify the calculation for estimation the residual life of materials in service, the rupture time is given as a function of applied stresses.

In this case, rupture time of X-70 carbon steel material as a function of applied stress and temperature is given according to the following relation:

$$\boldsymbol{log(t_r) = 8.54145 - 2.7489 \cdot log(\sigma) + 1.2998 \cdot (log(\sigma))^2 - 0.25184 \cdot (log(\sigma))^3 + (9.1952E - 4) \cdot T \cdot log(\sigma)} \quad (5.15)$$

This relation allows us to estimate the residual lifetime of materials in service.

# Chapter 6:

# Calculation of Rupture Analysis, Creep Activation Energy, and Two Case Studies

## 6.1. Introduction

In this chapter, Monkman and Grant constant for Al-7075-T6 and X-70 carbon steel with the use of creep curves are calculated. Besides, Larson–Miller equation is derived and activation energies of Al-7075-T6 and X-70 carbon steel are estimated. Finally, two case studies are given. In the first case study the remaining life of a super-heater tube in service, knowing its creep rupture time, is calculated. In the second case study probability of excidance (PE) on 0.04% strain level of X-70 carbon steel sample is estimated.

## 6.2. Rupture Analysis for Al-7075-T6 and X-70 Carbon Steel

To estimate the lifetime in service, and residual life of heat exchanger tubes and turbine blade in oil refineries and power plants, the strain rate and time to rupture of the materials are used.

Rupture point of material represent the end point on the creep curve, and it is usually taken to characterize the other parameters of the curve.

Monkman and Grant [1] relation gives the proportionality between the rupture time and the minimum creep rate. Figure 6.1 is helpful to drive this relation which is given by Equation 6.1.

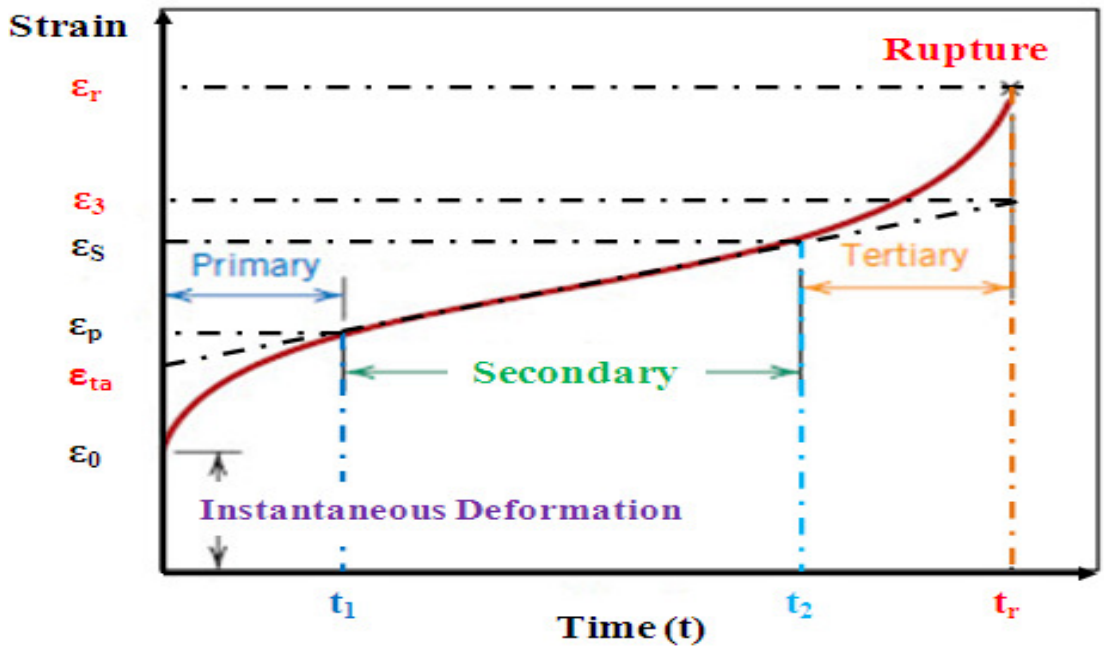


**Figure 6.1: Creep curve, prepared for estimation of Monkman-Grant relation**

$$\dot{\varepsilon}_S = \frac{\varepsilon_3 - \varepsilon_{ta}}{t_r} = \frac{\varepsilon_S - \varepsilon_p}{t_2 - t_1}, \quad or\ \dot{\varepsilon}_S \cdot t_r = constant \tag{6.1}$$

This relation is applied to our experimental data given in Figure 6.2, for Al-7075-T6 samples at 400°C and applied stress of 100Mpa (estimated after 44.3 hrs = 1.84 days).

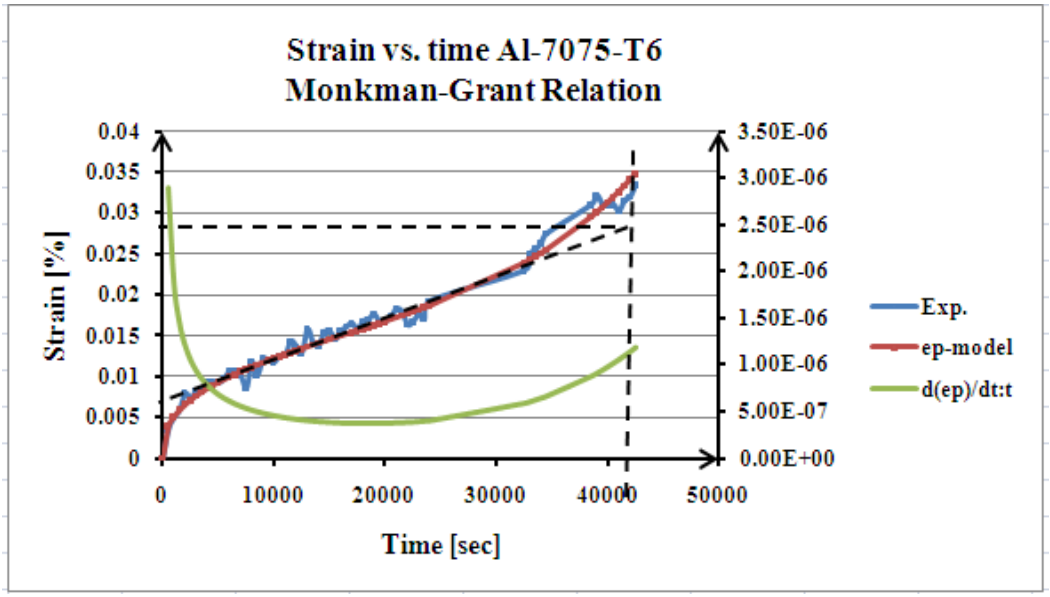


**Figure 6.2: Creep curve of Al-7075-T6 samples at T= 400°C and σ = 100Mpa, after 44.3 hrs = 1.84 days**

$$\dot{\varepsilon}_S = \frac{\varepsilon_3 - \varepsilon_{ta}}{t_r} = \frac{0.028 - 0.0065}{t_r[=11.7\ hrs]} = 0.00184 \ \ or\ \dot{\varepsilon}_S \cdot t_r = 0.0215 \tag{6.2}$$

Calculated value for Monkman and Grant constant is 0.0215 for Al-7075-T6, which is in good agreement with the published data [3, 4].

Monkman and Grant constant and (with C~20 for steels) were estimated for X70 carbon steel according to the creep experiments data given in Figure 6.3:

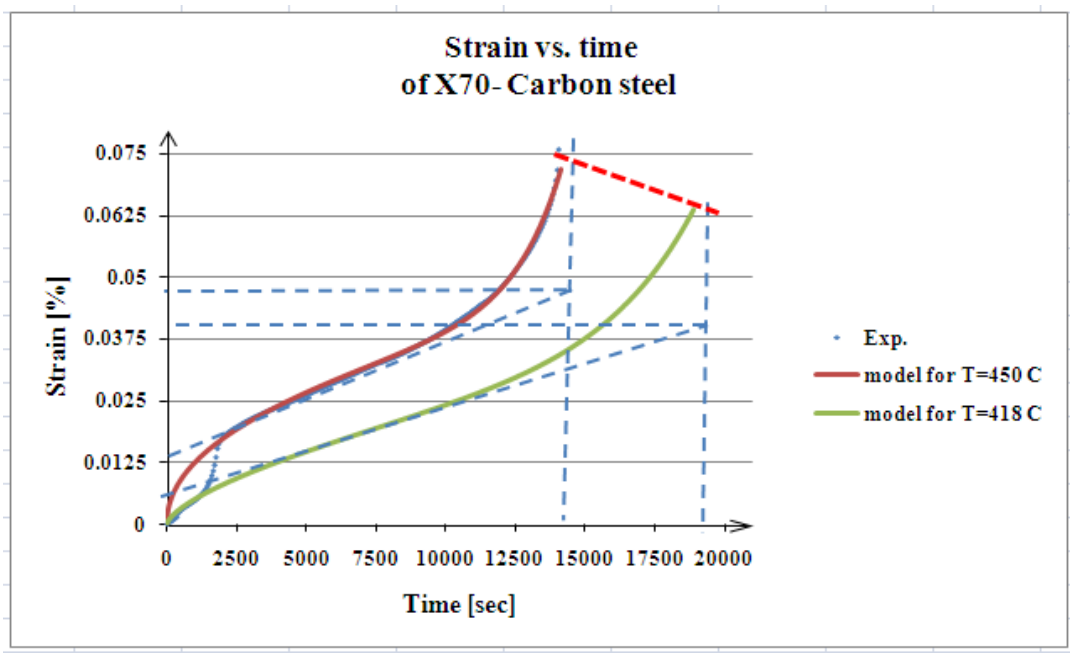


**Figure 6.3: Creep curve of X70carbon steel at T=450°C and predicted at T= 418°C and σ=348.8 MPa, fitted by our proposed model**

Then Monkman and Grant constant for X70 carbon steel at T=450°C and predicted at T= 418°C and σ=348.8 MPa is given by:

$$\dot{\varepsilon}_S = \frac{\varepsilon_3 - \varepsilon_{ta}}{t_r} = \frac{0.04 - 0.0125}{t_r[=3.82\ hrs]} = 0.0072 \quad or\ \dot{\varepsilon}_S \cdot t_r = 0.0275 \tag{6.3}$$

### 6.3. Creep Activation Energies for Al-7075-T6 and X-70 Carbon Steel

Larson–Miller parameter [6] is a useful parameter to estimate the creep activation energy of materials, Al-7075-T6 and X-70 carbon steel. Larson–Miller parameter can be derived from Dorn relation [Appendix number 22]:

$$\dot{\varepsilon}_s = A \cdot \sigma^n \cdot \exp\left(-\frac{\Delta H}{RT}\right) \tag{6.4}$$

where A, n, are constants, R is the gas constant, T is the absolute temperature in Kelvin, σ is the external applied stress, ΔH is the activation enthalpy of creep process, and $\dot{\varepsilon}_s$ is the secondary strain rate.

Then,

$$\boldsymbol{t_r = constant \cdot \sigma^{-n} \cdot \exp\left(\frac{\Delta H}{RT}\right)} \tag{6.5}$$

taking logarithms from both sides, results in:

$$\log(t_r) = \log(constant) - n \cdot \log(\sigma) + \frac{\Delta H}{2.3R} \cdot \frac{1}{T} \tag{6.6}$$

or

$$\mathrm{T} \cdot \log(t_r) = \mathrm{T} \cdot [\log(constant) - n \cdot \log(\sigma)] + \frac{\Delta H}{2.3R} = T \cdot [logC^*] + \frac{\Delta H}{2.3R} \tag{6.7}$$

Then by a given stress σ (constant value):

$$\mathrm{T} \cdot [\log(t_r) - logC^*] = \frac{\Delta H}{2.3R} \tag{6.8}$$

The Larson–Miller parameter is given by:

$$\mathbf{P_{LM}} = \boldsymbol{\frac{\Delta H}{2.3R}} = \mathbf{T} \cdot [\mathbf{log}(\boldsymbol{t_r}) + \boldsymbol{C}], \boldsymbol{with} \quad \mathbf{10} < \boldsymbol{C} < 20 \tag{6.10}$$

Parameter C for Al alloys in the 7xxx series (like 7075) is C=10 for cyclic and C=14 for static creep [3, 4]. Activation energy of Al-7075-T6 alloy is calculated by taking C=12 and $t_r$ = 11.7 hrs at T = 673K= (400°C):

$$\Delta H = Q_A = 168\,\mathrm{kJ/mol} \tag{6.9}$$

which is in good agreement with the published (142 - 145 kJ/mol) data [3].

Activation energy of X-70 carbon steel is calculated by considering C=20 as:

$$\Delta H = Q_A = 284.57\,\mathrm{kJ/mol}\,, \text{for } \mathrm{T} = 450°\mathrm{C} \text{ an } \mathrm{t_r} = 3.82 \text{ hrs} \tag{6.10}$$

$$\Delta H = Q_A = 271.97\ \mathrm{kJ/mol}\text{, for T} = 418°\mathrm{C}\text{ an } \mathrm{t_r} = 3.82\ \mathrm{hrs} \tag{6.11}$$

These values are in good agreement with the published values given for steel materials (245-300 kJ/mol) [8].

### 6.4. Practical Examples:

In this part, two case studies are represented. In the first case, the residual life of superheater (or reheater) tube after some operation time is calculated, assuming the final rupture time as a lognormal distributed. This example is a proof for the workability of our probabilistic approach with the final rupture time as a distribution.

In the second case study the probability of excidance for X-70 carbon steel pipe is calculated. The excidance is calculated based on a creep experiment at 450°C for a 0.04% strain level where the tertiary region begins.

#### 6.4.1. Case Study I: Estimation of Remaining Life of Super-heater/Re-heater Tubes

In this case study the remaining life of a superheater tube is calculated. Corrosion of the material due to fire-side, results in a decrease in wall thickness, and a consequent increase in stress. As a result of applied stress at high temperature creep rupture time of material decreases. Moles and Westwood [9, 10] derived a relation for estimation of remaining life under wall thinning condition by assuming a linear corrosion rate and under the application of a linear damage model:

$$t_{nr} = \frac{1}{K'} \cdot \left\{1 - [1 + K' \cdot (n-1) \cdot t_r]^{1/(1-n)}\right\} \tag{6.12}$$

where $t_{nr}$ is rupture life in service under wall-thinning conditions,

$K'$ is wall-thinning rate [$hr^{-1}$], and equal to:

$$K' = ((\frac{w_i - w_f}{w_i})/t_{op}) \quad (6.13)$$

- $w_i$, $w_f$ and $t_{op}$ as initial, final wall thickness and operational time [hr].
- n~4-8 for ferritic steel tube, is the stress sensitivity (Norton law exponent) and,
- $t_r$ is the time to rupture of a tube without wall thinning. $t_r$ can be estimated by Larson Miller Parameters or other related creep equations after creep experiments

The remaining lifetime is given by:

$$t_{res} = t_{nr} - t_{op} \quad (6.14)$$

Assuming uncertainty in estimation of wall thickness and consequent wall thinning under corrosion, the remaining life of the tube can be calculated.

If the mean value for wall thickness is taken as 3.81 mm, which is thinned by corrosion to the mean value of 2.49 mm, and if the time to rupture of the tube is given by $t_r$=1300000 hrs (with the stress sensitivity parameter n=4), then the calculated residual life after an operation time of 57000 hrs can be estimated.

The initial wall thickness and final wall thinned are assumed to be lognormal distributed with:

$$w(i) = Ln(\mu = 1.3376,\ \sigma = 0.07) \quad (6.18)$$

and,

$$w(f) = Ln(\mu = 0.9123,\ \sigma = 0.031) \quad (6.19)$$

And,

According to the proposed model, it is assumed that $t_r$ (the time to rupture of a tube without wall thinning) is lognormal distributed with:

$$t_r(i) = Ln(\mu = 14.0778,\ \sigma = 0.07) \tag{6.20}$$

then the remaining life calculated by MATLAB programs has a distribution given in Figure 6.4.

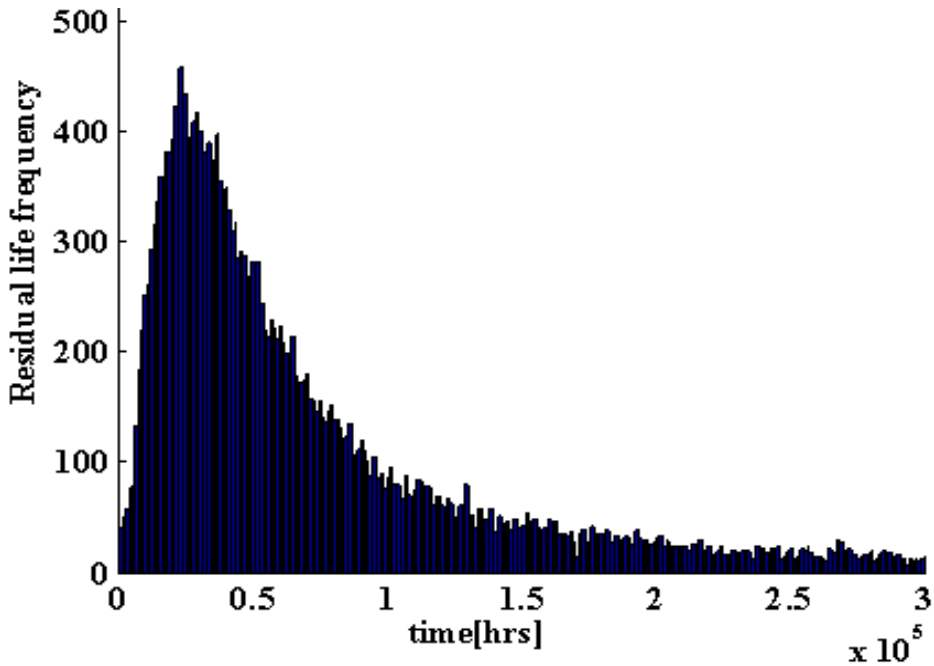


**Figure 6.4: The remaining life is lognormal distributed with a mean of 49600 hrs. calculated by MATLAB program**

Corresponding cumulative distribution of the residual life time calculated by Weibull++ program is shown in Figure 6.5.

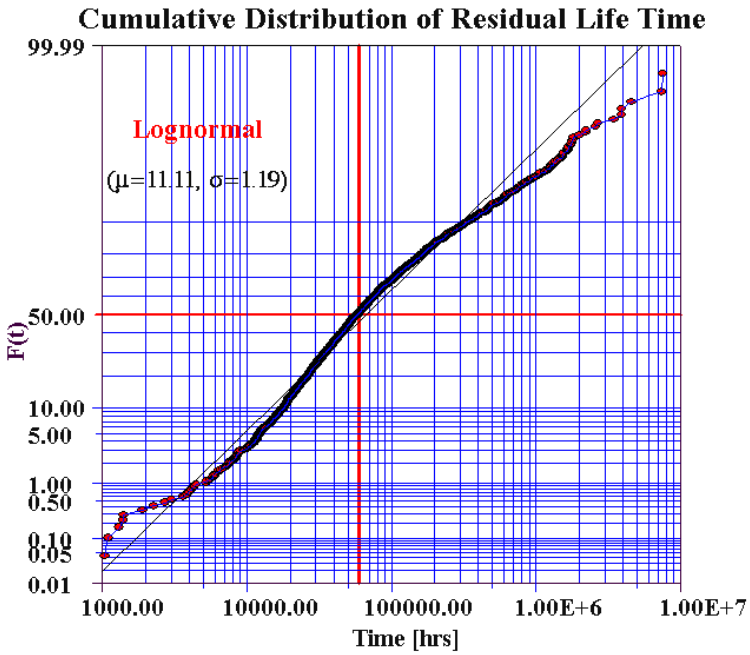


**Figure 6.5: The remaining life is lognormal distributed with a mean of 49600 hrs. calculated by Weibull++ program**

The result of this case study shows that remaining life is 49,600 hrs, which is in agreement with the published data [10, 11], and calculation by Omega creep relation for 2¼Cr-1Mo tube alloy at 450ºC [12].

### 6.4.2. Case Study II: Estimation of Probability of Exceedance (PE) on 0.04% Strain Level

The end point of the secondary region or the beginning point of the tertiary part of the creep curve is used to estimate the service and residual life of material. Severe structural deformation of material begins at this point, where most of the cavities begin to agglomerate and leads to a big crack. Figure 6.6 shows the creep curves of X-70 carbon steel samples at different temperatures and stresses. If 0.04 % strain line on the creep curve (for 723 °K and 346 MPa) is taken as the critical level of inspection, then it is possible to estimate the probability of exceedance above 0.04% strain level at different times. The

brown areas above 0.04 % strain (at t= 6000, 8000, 10000, and t=12500 sec) in Figure 6.6 show the amounts of failure accumulated (exceedance) on the creep curve at 450°C.

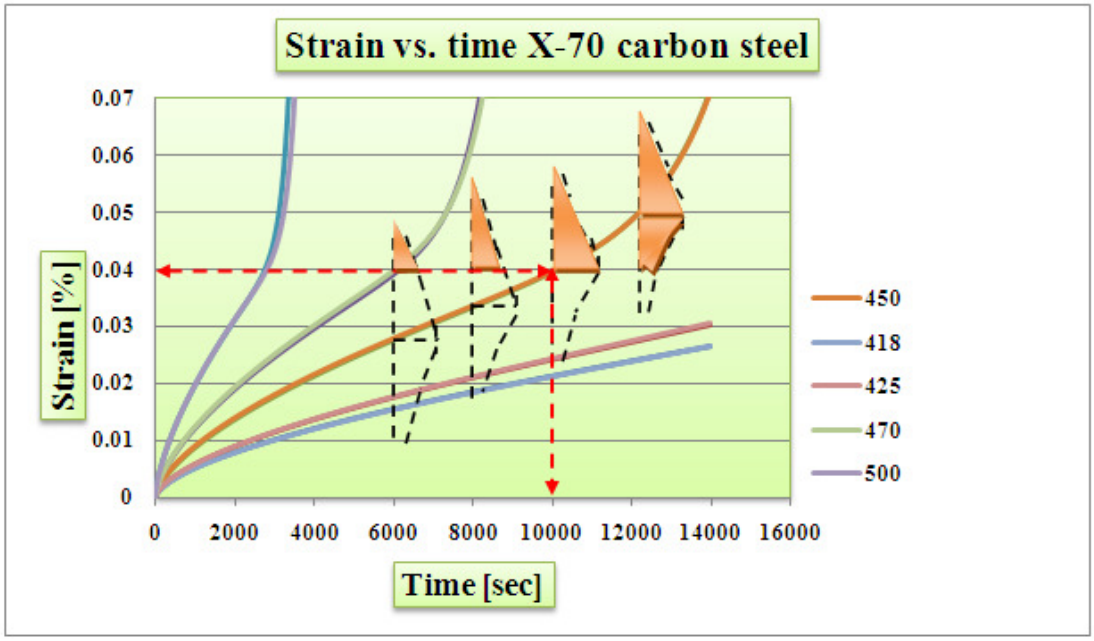


**Figure 6.6: Lognormal distributions estimated on 0.04 % strain with their corresponding probability of exceedance (filled brown areas)**

A MATLAB code is written to calculate the probability of exceedance ($P_E$) at different times based on the proposed empirical equation applied to the experimental data. The distributions in Figure 6.7 are the probability of exceedance above 0.04% strain level at different times for X-70 carbon steel, calculated by MATLAB code.

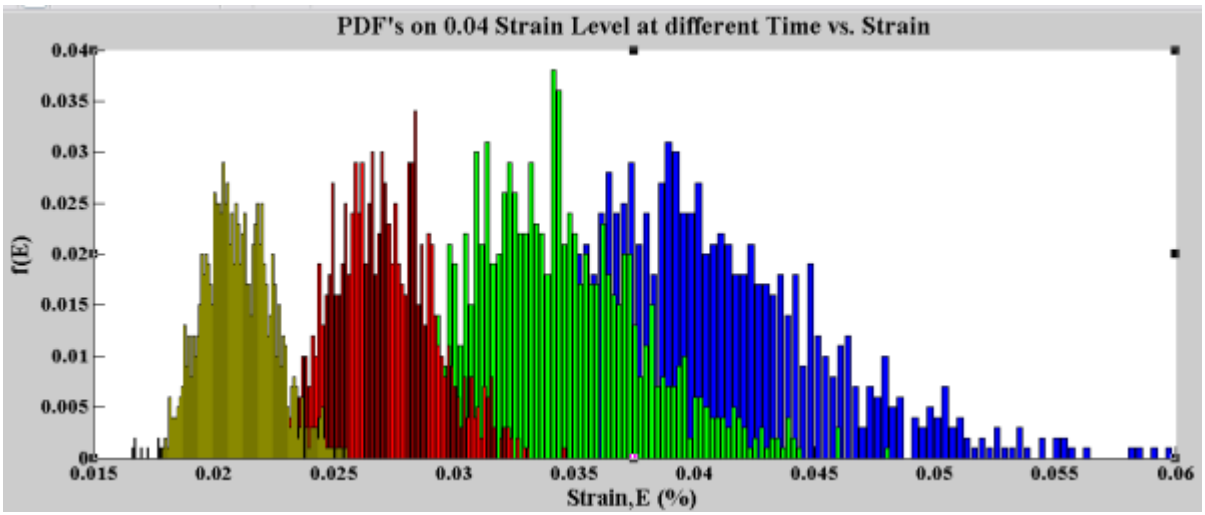


**Figure 6.7: Lognormal pdfs calculated with MATLAB code for 0.04 % strain level (practical strain limit in service) for X-70 carbon steel**

Figure 6.8 shows the cumulative distribution of the exceedance at different times above 0.04% strain level for X-70 carbon steel, calculated by MATLAB code.

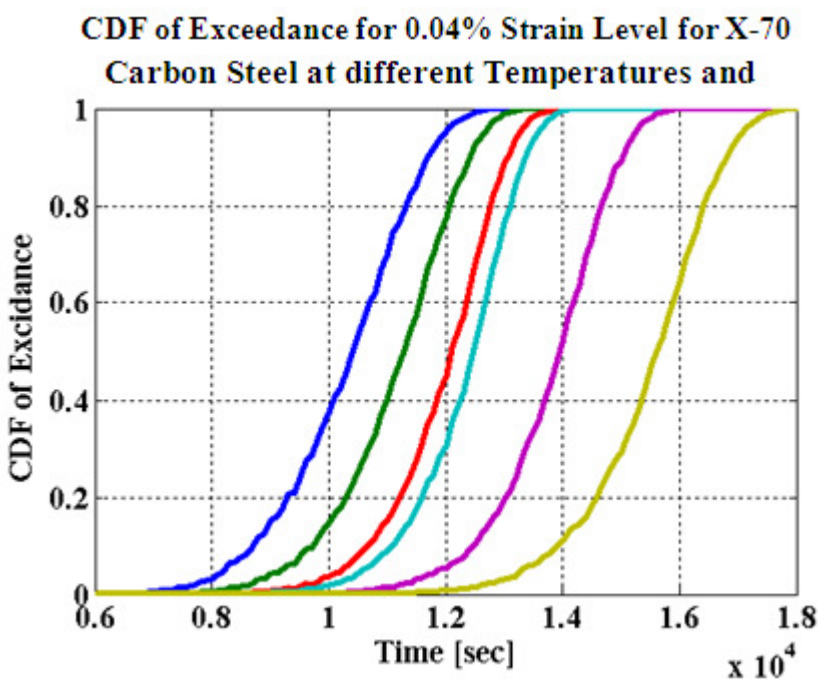


**Figure 6.8: Lognormal cumulative distributions calculated by Weibull++ for 0.04 % strain level (practical strain limit in service) for X-70 carbon steel between 450°C and 500°C**

EXCEL and Weibull++ program were used to calculate the probability of excidance ($P_E$) at different times. Again, the proposed empirical model was used to evaluate the corresponding experimental data. Figure 6.9 shows the related graph.

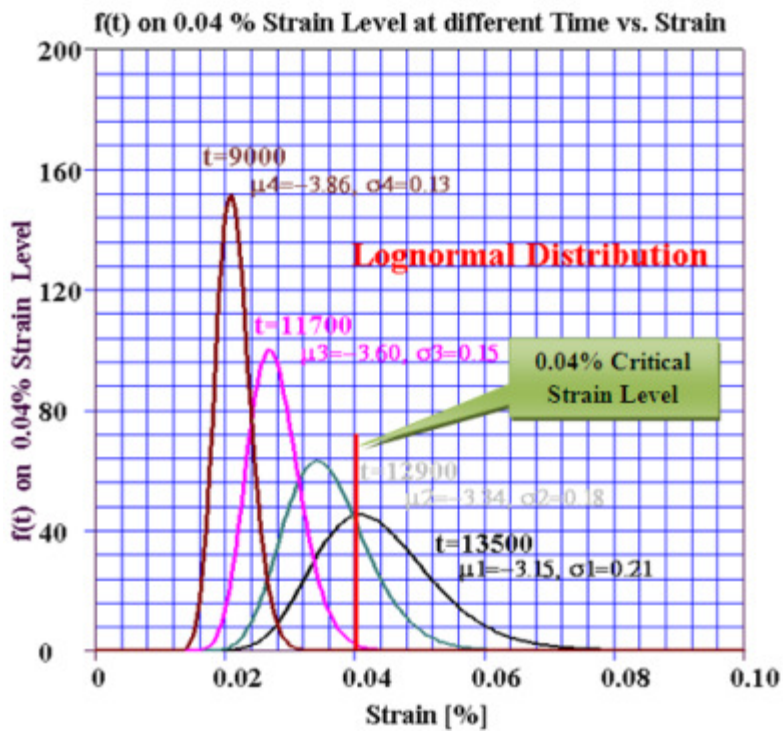


**Figure 6.9: Lognormal pdfs calculated by EXCEL, and drawn by Weibull++ for 0.04 % strain level for X-70 carbon steel**

Table 6.1 shows the probability of exceedance ($P_E$) calculated according to:

$$P_E = 1 - P(\varepsilon > 0.04) = 1 - \int_0^{\varepsilon=0.04} f(\varepsilon)d\varepsilon \tag{6.21}$$

at 0.04 strain level for different times.

**Table 6.1: Probability and probability of exceedance on the 0.04 Strain level at different times**

| Time [hrs] | P | $P_E$ |
|---|---|---|
| 13500 | o.5434 | 0.4566 |
| 12900 | 0.9571 | 0.0429 |
| 11700 | ~1 | $4.5x10^{-8}$ |
| 9000 | 1 | 0 |

According to the values given in Table 6.1, more than 40% degradation of X-70 carbon steel occurs before 13500 hrs. Therefore, the inspection time should be chosen between operation times t=11700 and t=12900 hrs.

# 7. Conclusion

The most important degradation mechanisms in structures such as piping used in the nuclear, chemical and petroleum industries are attributed to creep and creep-corrosion. Creep is one of the most serious high temperature damage mechanisms. To investigate the pipeline health, risk and reliability, it is highly important to model creep and creep-corrosion phenomenon to characterize the observed deformation and fracture with respect to time.

After classification of sixty-two creep equations in two simple groups of power law and exponential models, this thesis developed a simple probabilistic PoF model to describe the degradation of X-70 carbon steel and Al-7075-T6 structures. The physical parameters in this probabilistic model are applied stress, and temperature. Experimental studies and model updating support this study.

A proposed empirical model was developed and it was compared with the mostly used and acceptable models from phenomenological and statistical points of view. This model that based on a power law approach for the primary creep part and a combination of power law and exponential approach for the secondary and tertiary part of the creep curve captures the whole creep curve appropriately. Besides, we found the stress and temperature dependencies of our model.

In the next step, the proposed probabilistic empirical model was validated by experimental data taken from Al-7075-T6 and X-70 carbon steel samples. The details of experimental designs of chambers for corrosion, creep-corrosion, corrosion-fatigue, stress-corrosion cracking (SCC) (both on CT and dog-boned steel and Aluminum samples), and a high

temperature (1200 $^{0}$C) furnace for creep and creep-corrosion (gas pressure) furnace both for CT and dog-boned samples have been provided.

Furthermore, the uncertainties of the probabilistic models as well as their parameters were estimated by WinBUGS program based on Bayesian inference.

Finally, practical applications of the probabilistic model to estimate the activation energy of creep process were provided, and two case studies to estimate the remaining life of a super heater tube, and probability of exceedance of failures at 0.04% strain level for X-70 carbon steel were given.

The proposed probabilistic model is simple consisting of only two parameters (represented by probability density functions). Linear temperature and stress dependency of exponent parameters n, and m are presented here for the first time. In the case study, the empirical model offered proper assessment and reasonably predicted the expected remaining life of the pipeline.

## Appendix A. Creep Models Summarized from 1898 to 2007 According to the Year of their Publishing.

**1- Kelvin- Voigt ( visco-plastic creep) model [1898].[1]**

$$\sigma(t) = E \cdot \varepsilon(t) + \eta \cdot \frac{d\varepsilon}{dt}$$

$$\boldsymbol{\varepsilon(t) = \frac{\sigma_0}{E}[1 - \exp(-(E/\eta) \cdot t)]}, \qquad with\ \frac{\eta}{E} = t_r = Retardation\ time$$

where $\varepsilon$ is strain, t is time, η is the viscosity, σ is the stress, and E is the elastic modulus

**2- Phillips model [1905], [2]**

$$\varepsilon = \alpha \cdot \log(t) + C, \qquad or \quad \varepsilon = \varepsilon_0 + \log(1 + t),\ or\ \ \varepsilon = \varepsilon_0 + A\log(1 + B \cdot t)$$

where $\alpha$, B and C are constants.

**3- Anderade 1/3 model [1910-1914], [3]**

$$\varepsilon = A[1 + B(t/t_0)^{\frac{1}{3}}] \cdot \exp\,(-k \cdot t)$$

where k, A, and B are a constants.

**4- Prandtl model [1928], [4]**

$$\varepsilon = B \cdot \sinh\,(\frac{\sigma}{c})$$

where B, and C care constants.

**5- Norton model [1929], [5]**

$$\dot{\varepsilon}_{tmin} = A \cdot \sigma^n \cdot \exp\,(Q_A/RT)$$

where $\dot{\varepsilon}_{tmin}$is the minimum strain rate, $Q_A$ is the activation energy of the creep process, R is the gas constant, and T is the temperature in Kelvin.

**6- Modified Norton model [1929-1935], [6]**

$$\dot{\varepsilon}_{tmin} = A \cdot \sigma^n \exp\,(Q_A/RT) + B \cdot \sigma^n \exp\,(Q_B/RT)$$

where A, B, and n are constants, R is the gas constant, $Q_A$ , and $Q_B$ are activation energies, $\dot{\varepsilon}_{tmin}$ is the minimum strain rate, and T is the absolute temperature in Kelvin.

**7-Bailey-model [1935], [7]**

$$\varepsilon = A \cdot t^n, \;\; \frac{1}{3} \leq n \leq \frac{1}{2}$$

where A, and n are constants

**8- Norton-Bailey model [1929-1935, 2003]**

$$\varepsilon_f = A \cdot \sigma^n \cdot t^p$$

where $\varepsilon_f$ is the final strain, and n and p are constants.

**9- Weaver model [1936], [8]**

$$\varepsilon_f = A \cdot \log(t) + B \cdot t + C$$

where A, B, and C are constants.

**10- Soderberg model [1936], [9]**

$$\varepsilon = A + B \cdot t - C \cdot \exp(-D \cdot t)$$

where A, B, C, and D are constants.

**11- Freudenthal model [1936], [10]**

$$\varepsilon = \frac{A \cdot t}{1 + B \cdot t}$$

where A, and B are constants.

**12- Nadai model [1938], [11]**

$$\dot{\varepsilon}_s = \dot{\varepsilon}_0 \cdot \sinh\left(\frac{\sigma}{\sigma_0}\right) \cdot \exp\left(-\frac{\Delta H}{RT}\right)$$

where $\Delta H$ is the activation enthalpy of the creep

**13- Lacombe-model [1947], [12]**

$$\varepsilon = A + B \cdot (t/t_0)^m + C \cdot (t/t_0)^n$$

where A, B, C, *m*, and *n* are constants.

**14- Nadai - McVetty model [1943], [13-15]**

$$\varepsilon = \varepsilon_0 \cdot \sinh\left(\frac{\sigma}{\sigma_0}\right) + (v_0 \cdot \sinh\left(\frac{\sigma}{\sigma_1}\right)) \cdot t$$

where $v_0$ and $\sigma_i$ with i= 0, and 1, are constants.

**15- McHenry model [1943], [16]**

$$\varepsilon = A[1 - \exp(-B \cdot t)] + C[1 - \exp(-D \cdot t)]]$$

where A, B, C, and D are constants.

**16- Cottrell-Ayetkin model [1947], [17]**

$$\varepsilon = A + B \cdot t^{1/3} + C \cdot t$$

where A, B, and C are constants.

**17- Mott and Nabarro model [1948], [18]**

$$\boldsymbol{\varepsilon = A \cdot [\log(1 + B \cdot t)]^{2/3}}$$

where A, and B are constants.

**18- Wyatt model [1953], [19]**

$$\varepsilon_f = A \cdot \log(t) + B \cdot t^n + C \cdot t \ , \ \ n = 1/3$$

where A, B, C, and n are constants.

**19-Manson-Haferd-Grounes (MHG) model [1953], [20, 21]**

$$t_c = \exp(T \cdot F(\varepsilon, \sigma) + C)$$

$$F(\varepsilon, \sigma) = a_0 + a_1 \cdot \log(\sigma^2) + a_2 \cdot \log(\varepsilon^3)$$

where $a_i$, and C are constants.

**20- Orr- Sherby -Dorn-models [1953], [22]**

$$\dot{\varepsilon} = f(s) \cdot \sigma^n \cdot \exp\left(-\frac{Q_A}{RT}\right),\ s = structure\ parameters$$

where n is a constant, R is the gas constant, $Q_A$ is the activation energy, T is the absolute temperature in Kelvin

**21- Graham-Walles model [1955], [23]**

$$\varepsilon_f = a_1 \cdot t^{1/3} + a_2 \cdot t + a_3 \cdot t^3$$

$$\dot{\varepsilon}_f = \sum_1^3 A_i \cdot \exp\left(-K_i / T\right) \cdot \sigma^{n_i} \cdot \varepsilon^{n_i}$$

where $K_i$ and $a_i$ , $A_i$, and $n_i$ are material parameter

**22- Bailey-Norton model [1954]**

$$\varepsilon^c = C_0 \cdot \sigma^{(C_1)} \cdot t^{(C_2)} \cdot \exp\left(-\frac{C_T}{T}\right), \qquad C_1 > 1\ and\ \ 0 < C_2 \leq 1$$

$$\varepsilon^c = A + B \cdot \sinh\left[C \cdot \left(\frac{t}{t_0}\right)^{\frac{1}{3}}\right]$$

where A, B, C and $C_i$ with i=0, 1, and 2 are constants, and $C_T$ is a material constant dependent on temperature

**23-Weertman model [1955], [24]**

$$\boldsymbol{\dot{\varepsilon} = A \cdot \sigma^{\alpha} \cdot \exp\left(-\frac{Q_A}{kT}\right)}$$

where A, α are constants, k= Boltzmann constant, $Q_A$=activation energy, T=Temperature

**24- Classical Strain Hardening model [1953????], [25]**

$$\dot{\varepsilon}_f = A \cdot \exp\left(-\frac{K}{T}\right) \cdot \varepsilon^{-s} \cdot \left(\frac{\sigma}{\sigma_0}\right)^r \quad , \quad \sigma = \sigma_0 \cdot \exp\,(\omega \cdot \varepsilon)$$

$$s = a_1 + b_1 \cdot T + c_1 \cdot \sigma + d_1 \cdot \sigma \cdot T$$

$$r = a_2 + b_2 \cdot T + c_2 \cdot \sigma + d_2 \cdot \sigma \cdot T$$

$$\omega = a_3 + b_3 \cdot T + c_3 \cdot \sigma + d_3 \cdot \sigma \cdot T$$

where $A, a_i, b_i, c_i, and\ d_i are\ constants$

**25-Dorn to Laks to Hollomon model [1946-54], [26,27]**

$$\dot{\varepsilon}_s = A \cdot (\frac{\sigma}{\sigma_0})^{n(T)} \cdot \exp\,(-\frac{\Delta H}{RT})$$

where A is a constant, ΔH is the activation enthalpy, and n(T) is a material parameter dependent on temperature.

**26- Pao-Martin model [1957], [28]**

$$\varepsilon^c = A(1 - \exp(-Bt)) + C \cdot t$$

where A, B, and C are constants.

**27- Parker model [1958], [29]**

$$\boldsymbol{\varepsilon = A + B \cdot \sinh\,(C \cdot t^{\frac{1}{3}})}$$

where A, B, and C are material parameters

**28- Jenkins-model [1962], [30]**

$$\varepsilon = A \cdot \sigma + B \cdot \sigma^2$$

where A, and B are constants.

**29- Conway-Mullikin model, Polynomial form [1962], [31]**

$$\varepsilon = A + B \cdot t^{1/3} + C \cdot t^{2/3} + D \cdot t, \;\; or\; \varepsilon = A + B \cdot t^{m} + C \cdot t^{n} + D \cdot t^{\,p}$$

where A, B, C, D, m, n, and p are constants.

**30- Li model [1963], [32]**

$$\varepsilon = \varepsilon_0 + \frac{\dot{\varepsilon}_s}{A} \cdot \ln\,[1 + \frac{\dot{\varepsilon}_i - \dot{\varepsilon}_s}{\dot{\varepsilon}_s} \cdot (1 - \exp(-A \cdot t)] + \dot{\varepsilon}_s \cdot t$$

where A is a constant, and $\dot{\varepsilon}$- are initial and secondary strain rates.

**31- Li-Akulov-model [1963-1964], [32, 33, 34]**

$$\varepsilon_f = \frac{\dot{\varepsilon_{f_{min}}}}{A} \ln\left(1 + \frac{\dot{\varepsilon}_i - \dot{\varepsilon}_{f_{min}}}{\dot{\varepsilon}_{f_{min}}}(1 - \exp(-At))\right) + \dot{\varepsilon}_s \cdot t + \varepsilon_T(\exp(t/t_t) - 1)$$

where A is a constant, and $\dot{\varepsilon}_i, \dot{\varepsilon}_{fmin}, \dot{\varepsilon}_s, and\; \dot{\varepsilon}_T$ are different strain rates.

**32- Garofalo-model [1965], [35]**

$$\boldsymbol{\varepsilon = \varepsilon_0[1 - \exp(-A \cdot t)] + \dot{\varepsilon}_{f_{min}} \cdot t}$$

where A is a constant, ε=strain, $\varepsilon_0$=initial strain, $\dot{\varepsilon}_{f_{min}}$is the minimum strain rate

**33- Modified Nadai (by Conway) model [1967], [36]**

$$\boldsymbol{\dot{\varepsilon}_s = A \cdot \sinh(\alpha \cdot \frac{\sigma}{RT})^n \cdot \exp\,(-\frac{\Delta H}{RT})}$$

where A, and α are constants

**34- Harmathy (H-model) [1967], [37]**

$$\dot{\varepsilon} = b_1 \cdot coth^2(b_2 \cdot \varepsilon)$$

$$b_1 = c_1 \cdot \exp\left(c_2 \cdot \ln(\sigma) - \frac{c_5}{T}\right), \qquad \sigma < \sigma_t \; with \;\; \sigma_t = transitionstress$$

$$b_1 = c_6 \cdot \exp\left(c_1 \cdot \ln(\sigma) - \frac{c_5}{T}\right), \qquad \sigma > \sigma_t \; with \;\; \sigma_t = transitionstress$$

$$b_2 = 1/(c_3 \cdot \sigma^{c_4})$$

where $b_i, c_i \; are \; constants.$

**35- Fairbairn-model, Polynomial, [1967], [38]**

$$\varepsilon = A \cdot \sigma^n \cdot (t^2 + 2t)^p$$

where A, *n*, and *p* are constants

**36- RCC_MR- model [1970], [39]**

$$\varepsilon_f = C_1 \cdot \sigma^{n_1} \cdot t^{c_2} \qquad for \;\; t \leq t_{f_p}$$

$$\varepsilon_f = C_1 \cdot \sigma^{n_1} \cdot {t_{fp}}^{c_2} + 100 \cdot C \cdot \sigma^n \cdot (t - t_{fp}) \qquad for \;\; t > t_{f_p}$$

where C, $C_1$, $C_2$, n, $n_1$=f(T) and $t_{fp}$=f(σ, T)

**37- Davis model [NASTRAN]-NAsa-STRuctural-ANalysis-Finite element Program [1976], [40]**

$$Ln(\varepsilon_{ijCr}) = A + B \cdot T + C \cdot \sigma^2 + D \cdot \ln(\sigma) + E \cdot \ln(t) + \cdots$$

where A, B, C, D, and E are constants

**38-Leckie and Hayhurst model (ABAQUS-Finite Element-Modeling) [1977], [41, 42]**

$$\dot{\boldsymbol{\varepsilon}}^c = \frac{3}{2} \cdot \frac{\dot{\varepsilon}_0}{\sigma_0}\left[1 + \left(\frac{\sigma_{vM}}{\sigma_0}\right)^{n-1}\right] \cdot \boldsymbol{\sigma},$$

$$with \; \dot{\boldsymbol{\varepsilon}}^c \; and \; \boldsymbol{\sigma} \;\; as \; Tensors, \sigma_{vM} = Von \; Mises \; equivalent \; stress$$

**39- Sandström, Kondyr model [1979], [43]**

$$\dot{\varepsilon}_f = \dot{\varepsilon}_0 \cdot \exp\,(\Omega \cdot \varepsilon)$$

where $\Omega$ is a material parameter.

**40- Moles-Westwood- Residual Life Time model [1982]. [44, 45]**

$$t_{nr} = \frac{1}{K'} \cdot \left\{1 - [1 + K' \cdot (n-1) \cdot t_r]^{1/(1-n)}\right\}$$

where $t_{nr}$ is rupture life in service under wall-thinning conditions $K'$ is wall-thinning rate [$hr^{-1}$], and equal to $K' = ((\frac{w_i - w_f}{w_i})/t_{op})$ with $w_i$, $w_f$ and $t_{op}$ as initial, final wall thickness and operational time [hr], and n=4-8, for ferritic steel tube, is the stress sensitivity (Norton law exponent) and $t_r$ is the time to rupture of a tube without wall thinning.

$t_r$ can be estimated by Larson Miller Parameters or other related parameters.

Remaining life time $t_{res} = t_{nr} - t_{op}$

**41- Evans and Wilshire-(Theta-Projection)-model [1985], [46]**

$$\boldsymbol{\varepsilon_f = \theta_1[1 - \exp(-\theta_2 \cdot t)] + \theta_3[\exp(\theta_4 \cdot t) - 1]]}$$

$$\boldsymbol{\log(\theta_i) = a_i + b_i \cdot T + c_i \cdot \sigma + d_i \cdot \sigma \cdot T}$$

$$\boldsymbol{\varepsilon_f = A + B \cdot T + C \cdot \sigma + D \cdot \sigma \cdot T}$$

where $\theta_i$, $a_i$ …. *are material parameters.*

**42- Johnson-Cook-model [1985], [47-48]**

$$\varepsilon_f = [A + B \cdot \exp\,(C \cdot \sigma'] \cdot [1 + D \cdot \ln\,(\dot{\varepsilon}')] \cdot [1 + E \cdot T']$$

$$\sigma', \dot{\varepsilon}' \; and \; T' \; as \;\; incremental \; parameters$$

**43- The Johnson–Cook (JC) model** relation for the flow stress ($\sigma_y$) **[1983-1985], [47-48]**

$$\sigma_y(\varepsilon_P, \dot{\varepsilon}_P, T) = [A + B(\varepsilon_P)^n]\{1 + C \cdot ln(\dot{\varepsilon}_P{}^*)][1 - (T^*)^m]$$

where $\varepsilon_P$ is the equivalent plastic strain, $\dot{\varepsilon}_P$ is the plastic strain-rate,

and $A$, $B$, $C$, $n$, $m$are material constants.

The normalized strain-rate and temperature in the above equation are defined as

$$\dot{\varepsilon}_P{}^* := \frac{\dot{\varepsilon}_P}{\dot{\varepsilon}_{P_0}} \quad and \;\; T^* = \frac{(T - T_0)}{(T_m - T_0)}$$

where $\dot{\varepsilon}_{P_0}$is the effective plastic strain-rate of the quasi-static test used

to determine the yield and hardening parameters A,B and n.

**44- Modified Theta-model [1985], [49]**

$$\varepsilon_f = \theta_1[1 - \exp(-\theta_2 \cdot t)] + \theta_m \cdot t + \theta_3[\exp(\theta_4 \cdot t) - 1]]$$

$$\theta_m = A \cdot \sigma^n \cdot \exp\,(-Q_A/RT)$$

where $\theta_i$ are material parameters dependent on stress, temperature and yield of materials.

**45- Rabotnov-Kackanov-model [1986], [50-52]**

$$\dot{\varepsilon_f} = \frac{h_1 \cdot \sigma^n}{(1 - \omega)} \qquad \dot{\omega} = \frac{\dot{k}_1 \cdot \sigma^\nu}{(1 - \omega)^\zeta}$$

$$\varepsilon_c = \varepsilon_R \left[1 - \left(1 - \frac{t}{t_R}\right)^{\frac{1}{\lambda}}\right], \lambda = \frac{\varepsilon_R}{\dot{\varepsilon}_0 t_R}$$

where $h_1$, $k_1$, and $\omega$ are material parameters and n, $\nu$, $\zeta$, and $\lambda$ are constants.

**46- Maruyama-model (simplified Theta-model) [1990], [54]**

$$\varepsilon = \varepsilon_0 + A \cdot [1 - \exp(-\alpha \cdot t)] + B \cdot [\exp(\alpha \cdot t) - 1]]$$

where α is a material parameter dependent on stress, temperature and yield of materials

**47-Brinkman, Booker and Ding-model [1991], [55]**

$$\varepsilon^* = \exp[\beta \cdot (t^* - 1)] \cdot (t^*)^{\alpha}, \qquad \varepsilon^* and\ t^*\ are\ \ normalized\ strain\ and\ time$$

where $\alpha\ and\ \beta\ are\ constants.$

**48- Bolton model and Mech.E (CSWP) model [1994], [56, 57]**

$$R_{u/t/T} = (A + B/\varepsilon - C \cdot \varepsilon^2) \cdot R_{\varepsilon/t/T} + D + E/\varepsilon + F/\varepsilon^2 - G \cdot \varepsilon^2$$

where $R_{u/t/T}$ is the strength ratio of tensile to compressive strength ($\sigma_t/\sigma_c$).

$$\varepsilon_f(\sigma) = \varepsilon \cdot (\frac{R_{u/t/T}}{R_{\varepsilon/t/T}} - 1)/(\frac{R_{u/t/T}}{\sigma} - 1)$$

**49- Bartsch-model [1986-1995], [58, 59]**

$$\varepsilon_f = A \cdot \sigma \cdot \exp\,(-Q_{A_1}/RT) \cdot \exp(-B \cdot \sigma) \cdot t^p + C \cdot \sigma \cdot \exp\,(-Q_{A_2}/RT) \cdot \exp(-D \cdot \sigma) \cdot t$$

where A, B, C, D and $p$ are constants, R is the gas constant, $Q_{A_1}$ , and $Q_{A_2}$ are activation energies, and T is the absolute temperature in Kelvin.

**50- Omega-model (Prager model) [1995], [60]**

$$\varepsilon = -\frac{1}{\Omega_p} \cdot \ln(t_r - t) + \frac{1}{\Omega_p} \cdot \ln\left[\frac{1}{\dot{\varepsilon}_0 \Omega_p}\right], or\ \ \varepsilon = \dot{\varepsilon}_0 \cdot \exp\left(\Omega_p \cdot\ \varepsilon\ \right), or$$

$$\dot{\varepsilon_f} = \frac{\dot{\epsilon}_{f_{min}}}{1 - \dot{\epsilon}_{f_{min}} \cdot \Omega \cdot t}, and\ \ \Omega = A_\Omega \cdot \sigma^{-n_\Omega} \cdot \exp\,(\frac{Q}{RT})$$

where $A_\Omega$, $n_\Omega$, and $\Omega_p$ are constants, ε=strain, $\dot{\varepsilon}_f$=final strain rate, $\dot{\varepsilon}_{f_{min}}$is the minimum strain

rate , Ω= ∂lnε/∂ε. Omega defines the rate at which strain rate accelerates as a result of creep strain.

**51- BJF (Jones and Bagley)-model [1995-1996], [61]**

$$\epsilon_f = A[1 - \exp(-t)]^{\beta} + Bt$$

$$t = (\sigma/A_1)^n \cdot \exp\,(-Q/RT)$$

$$\text{or} \quad t = \int (\sigma_{eff}/A_1)^n \cdot \exp\,(-Q/RT)\,dt$$

$$\sigma_{eff} = \frac{\sigma}{1-\omega} \quad and \quad \dot{\omega} = B \cdot (\frac{\sigma}{1-\omega})^m$$

where A,B, $A_1$, β, n, and m are constants, ω is a damage parameter between 0, and 1, and $\sigma_{eff}$ is the effective stress.

**52- Dyson and McLean-model [1998-2000], [62]**

$$\varepsilon_f = \epsilon_0' \cdot (1 + D_d) \cdot \exp\,(-Q/RT) \cdot \sinh\left(\frac{\sigma(1-H)}{\sigma_0(1-D_p)(1-\omega)}\right)$$

where $\varepsilon_f$ and $\epsilon_0'$ are the equivalent minimum creep strain rate and the reference creep strain rate; $\sigma$ and $\sigma_0$ are the equivalent stress and the reference stress, respectively; $T$ is the temperature; $Q$ is the creep activation energy. $H$ is the hardening parameter, $D_d$ is the damage parameter caused by multiplication of mobile dislocations, $D_p$ is the damage parameter caused by particle coarsening and $\omega$ is the damage parameter caused by the cavity nucleation and growth.

**53- Robotnov- Hayhorst- Dunne- Hyde: Creep in structural members,**

**Continuum Damage Mechanics, Constitutive Equations [CDMCE], [1969-1998,…],**

**[63-67]**

$$\dot{\varepsilon} = A \cdot \left(\frac{\sigma}{1-\omega}\right)^{n} \cdot t^{m}, and\ \ \dot{\omega} = B \cdot \frac{\sigma^{\chi}}{(1-\omega)^{\phi}} \cdot t^{m}$$

The uniaxial parameters A, n,ϕ **,** B, χ and m shown in above equations can be determined by fitting a group of creep test strain curves for different stress levels at fixed temperature to the following theoretical strain equation.

$$\varepsilon = \frac{A \cdot \sigma^{(n-\chi)}}{B \cdot (\phi + 1 - n)} \cdot \left\{1 - \left[1 - \frac{B \cdot (1-\phi)\sigma^{\chi} \cdot t^{(1+m)}}{1+m}\right]^{((1-n)/(\phi+1))}\right\}$$

$$or\ \varepsilon = \frac{A \cdot \sigma^{n} \cdot {t_f}^{(1+m)}}{(1+m) \cdot [(1 - n/(\phi+1)]} \cdot \left\{1 - \left[1 - \left(\frac{t}{t_r}\right)^{(1+m)}\right]^{((1-n)/(\phi+1))}\right\}$$

$$with\ t_r\ as\ the\ time\ to\ rupture, and\ \varepsilon_f = \frac{A \cdot \sigma^{n} \cdot {t_f}^{(1+m)}}{(1+m) \cdot [(1 - n/(\phi+1)]}$$

**54- Modified Garofalo-model (Granacher et.al.) [2001], [68]**

$$\epsilon_f = \dot{\varepsilon}_f \cdot [1 - \exp\left(-A \cdot (t/t_{12})^{u}\right) + \dot{\varepsilon}_{t_{min}} \cdot t + B \cdot (t/t_{23})^{f}]$$

where A, B, $u$, and $f$ are constants, $\dot{\varepsilon}_{t_{min}}$ minimum creep rate, $t_{ij}$ are transition times between different creep stages.

**55- Modified Omega-model (Merckling) [2002], [69]**

$$\epsilon_f = \left(\frac{1}{\Omega} - \frac{1}{2C_{tr}}\right) \cdot (-\ln(t_u - t) + \ln(t_u)) + C_{tr}(1 - \exp(m_{tr} \cdot t))$$

where $t_u$ is the observed time to rupture, $C_{tr}$and $m_{tr}$ and $\Omega$ are material constants.

**56- Altstadt-model, ANSYS-Finite element code [2003], [70, 71]**

$$\dot{\varepsilon} = A \cdot \sigma^{\alpha} \cdot \varepsilon^{\beta} \cdot \exp\left(-\frac{B}{T}\right)$$

where A, B, α, and β are constants.

**57- Baker-cane-model (Baker and O'Donnell) [2003], [72]**

$$\epsilon_f = A \cdot t^m + \epsilon_p + \phi \cdot \varepsilon_s + \varepsilon_s(\boldsymbol{\lambda} - \phi) \cdot \left[ I - \frac{\frac{t}{t_u} - \phi}{1 - \phi} \right]^{\frac{1-\phi}{\lambda-\phi}}$$

$$I = \varepsilon_u / \varepsilon_s \ , \ \ \varepsilon_s = \dot{\varepsilon}_m \cdot t_u \ \ and \ \ \phi = t_p / t_u$$

where ϕ, λ are material parameters, $t_u$ is the observed rupture time.

**58- MHG-model [2004], [73]**

$$t_{\varepsilon} = \exp(TF(\varepsilon, \sigma) + C)$$

where F(ε, σ)-function is freely selected from multi-linear combinations of σ and ε with an optimized value of C

**59- Extended Omega model-Clech [2004], [74, 75]**

$$\dot{\varepsilon} = a \cdot \exp(-A \cdot \varepsilon) + b \cdot \exp(\Omega \cdot \varepsilon)$$

where a, b, A, and Ω are material parameters.

**60-Modified Sandstroem Φ model for primary and Ω model for tertiary creep [2004], [76]**

$$\varepsilon = \phi_1 \cdot \varepsilon^{-\phi_2} + \Omega_3 \cdot \exp\left(\varepsilon \cdot \Omega_4\right)$$

$\Phi_1$, $\Phi_2$, $\Omega_3$ and $\Omega_4$ are constants that are fitted to the creep curve.

**61- Continuum Damage Mechanics (CDM)-based constitutive equation-model [2005], [77, 78]**

$$\dot{\varepsilon} = A \cdot sinh\left[\frac{B\sigma(1-H)}{(1-\Phi)(1-\omega)}\right]$$

$$\dot{H} = \frac{h\dot{\varepsilon}}{\sigma}(1-\frac{H}{H^*})$$

$$\dot{\Phi} = \frac{K_c}{3}(1-\Phi)^4$$

$$\dot{\omega} = C \cdot \dot{\varepsilon}$$

where A, B, C, h, $H^*$ and $K_c$ are material constants to be determined after the data fitting.

**62- Holmström- Auerkari- Holdsworth (Logistic Creep Strain Prediction model), (LCSP), [2006-2007], [79, 80]**

$$\boldsymbol{log(t_\varepsilon) = \frac{log(\alpha t_r) + \beta}{1 + \left(\frac{log(\varepsilon^{cr}}{x_0}\right)^p} - \beta}$$

$$\boldsymbol{x_0(\sigma, T) = A + B \cdot log(\sigma) + C/(T + 273)}$$

$$\boldsymbol{p(\sigma, T) = D + E \cdot log(\sigma) + F/(T + 273)}$$

where $t_r$ is the time to rupture from a creep rupture model to a given strain, and $x_0$, $p$, and $\beta$ are fitting factors defining the curve shape and α ~1.

Figure A.1 helps to understand the parameters used in the above sixty-two different creep models [81].

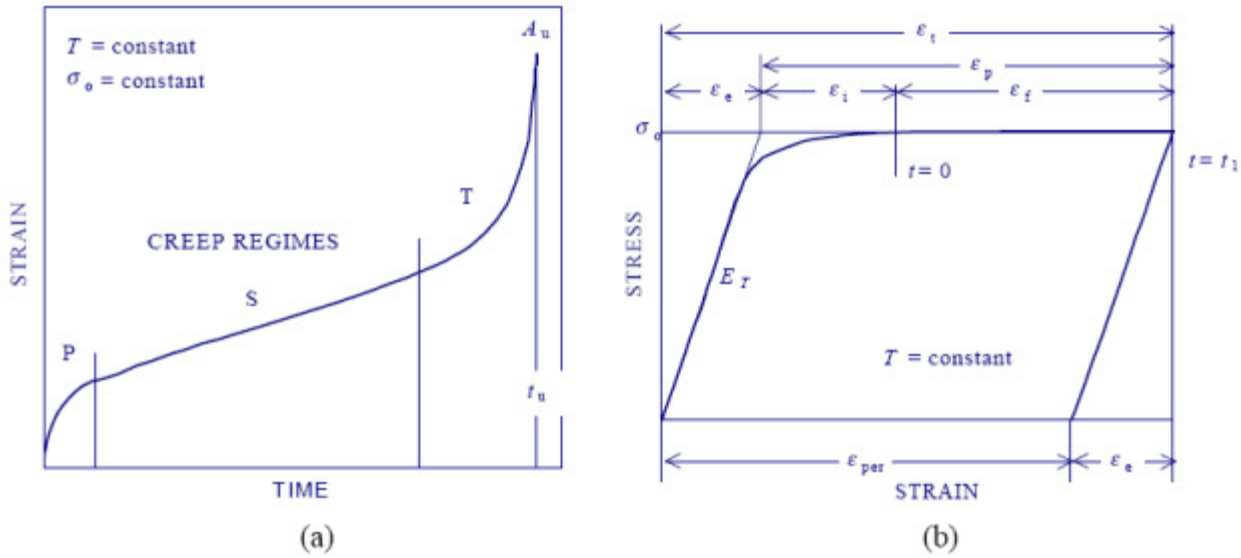


**Figure A.1: Schematic presentation of three parts of the creep curve (a), and strains generated during the loading in a creep test [81]**

As it is seen in the Figure A.1, the total strain $\varepsilon_t$ is the sum of elastic strain $\varepsilon_e$, and plastic strain $\varepsilon_p$ (or permanent strain $\varepsilon_{per}$). The plastic strain itself is the sum of instantaneous plastic strain $\varepsilon_i$ and final plastic strain $\varepsilon_f$.

## Appendix B. References to Creep Models


1- **Kelvin- Voigt** creep model, *cube.case.edu/EMAC403/EAMC403_Mechanical%20**Models**.**pdf***

2- **Phillips,F**,; The Slow stretch in India rubber, Glass and metal wire when subjected to a constant pull, Phil. Mag.9,513,**1905**

3- **Anderade**, E.N. da C.; TheViscous flow in metals and allied phenomena, Proc. Roy. Soc., A84,1, 1910; A90, 329, **1914**

4- **Prandtl, L**. ; Proceedings of the first international conference on applied mechanics, Delft, The Netherlands, p.43, **1924**

5- **Norton, F.H**. ; Creep of steel at high temperatures, McGraw-Hill Book Co. Inc. **1929**

6- **Modified Norton model:**

7- **Bailey,R.W**. The utilization of creep test data in engineering de sign, Proc. I. Mech. E.**131, 1935,…. Norton bailey**, in Robinson, D. N., Binienda, W. K., and Ruggles, M. B. ~2003 ‘‘Creep of polymer matrix composites. I: Norton/Bailey creep law for transverse isotropy.’’ *J. Eng. Mech.,* 129, 3, 310–317**,[2003]**

8- **Weaver,S.H**.; The creep curve and stability of steels at constant stress and temperature, Transe. ASME,58, 745, **1936**

9- **Soderberg,** C.R. ; The interpretation of creep tests for machine design, Trans. ASME,58, 735, **1936**

10- **Freudenthal,A. M., ;** Theory of wide-span arches in concrete and reinforced concrete, International Association Bridge and Structural Engineers 4, 249, **1936**

11- **Nadai, A**.; The influence of time upon creep. The Hyperbolic Sine creep law, Stephan Timoshenko Anniversary Volume, Macmillan Company, New York, **1938**

12- **De Lacombe,** J.; A method of representing creep curves, Rev. Metal. 36, 178, **1939**

13- **McVetty, P.G.** ; Creep of metals at elevated temperatures- The hyperbolic Sine relation between stress and creep rate, Trans. ASME, 65, 761, **1943**

14- **Nadai, A. and McVetty**, P.G. ; Hyperbolic Sine chart for estimating working stresses of alloys at elevated temperatures, Proc. ASTM, 43, 735, **1943**

15- **Davis, D.S.** ; Empirical equations and nomography, McGraw-Hill, **1943**

16- **McHenry, D. ;**A new aspect of creep in concrete and its application to design, Proc. ASTM 43, 1069, **1943**

17- **Cottrell, A. H. and Aytekin, V. ;** Andrade's creep law and the flow of Zinc crystals, Nature, 160,328, **1947**

18- **Mott,N.F. and Nabarro.F. R. N.;** Dislocation theory qnd transient creep, Report of the conference on the strength of solids, 46, The Physical society (London) **1948**

19- **Wyatt,O. H**. ; Transient creep in pure metals, Proc. Phys. Soc. London, B, 66, 459, **1953**

20- **Grounes, M.**; A Reaction rate treatment of the extrapolation methods in creep testing. J. Basic Eng.,Series D, Trans. ASME **1969**

21- **Manson, s. S. and Haferd, A.M**.; A linear time-Temperature relation for extrapolation of creep and stress-rupture data, NACA TN 2890, March **[1953]**

22- **Orr, R.L., Sherby, O.D. and Dorn**, J.E. ; Correlations of rupture data for metals at elevated temperatures, Trans. ASM, 46, 113, **1954**

23- **Graham, A. and Walles,** K.F.A. ; NGTE Reports Nos.R.100(1952), R.137 (1953), R.189 and R.190 (1956); J. Iron and steel Inst.179,105, **[1955]**

24- **Weertman, J**. ; Theory of steady-state creep based on dislocation climb, Journal of Applied Physics, Vol. 26, 1213,**1955**

25- ***Classical work hardening model*** *in : ECCC, Recommendation and guidance for the assessment of creep strain and creep strength data,www.ommi.co.uk/etd/eccc/advancedcreep/V5PIbi2x.**pdf***

26- **Laks,H.,Wiseman,C. D., Sherby, O.D. and Dorn, J. E**. ; Effect of stress on creep at high temperatures, J. App. Mech. 24, 207, **1957**

27- **Hollomon, J. H.** ; The problem of fracture, Welding Journal, Am. Welding Soc., Vol. 25, 534s,**1946**

28- **Pao, Y. H. and Marin,** J., "Analytical theory of creep deformation of materials", ASME Trans., Journal of Applied Mechanics, Vol. 20, No. 2, pp. 245-252, **1957**

29- **Parker, E.R**.; Modern concepts of flow and fracture, Trans. ASM, 50, 52, **1958**

30- **Jenkins, G. M. and** Williamson, G. K., ; Irradiation Creep in Graphite**,** www.osti.gov/bridge/servlets/purl/4639694-tdr3Oa/4639694.pdf

31- **Conway, j. B. and Mullikin**, M.J. ; An evaluation of various first stage creep equations, presented at October 1962 meeting of AIME, Detroit Michigan, **1962**

32- **Li, J.C.M.** ; A dislocation mechanism of transient creep, Acta Met 11,1269, **1963**

33- **AKULOV, N. S**. 'On dislocation kinetics', *Acta metall.* 12, 1195, **1964**

34- **AKULOV, N. S**. 'The statistical theory of dislocations', *Phil. Mag.* 9, 767,**1964**

35- **GAROFALO,** F. Fundamental of creep and creep-rupture in metals. 16 (Macmillan),**1965.**

36- **Modified Nadai (by Conway) model in:** Conway, J.B. Numerical methods for creep and rupture analysis, Grodon and Breach, New York, **1967**

37- **Harmathy, T. Z.;** "Deflection and Failure of Steel-Supported Floors and Beams in Fire," ASTM Special Technical Publication, No. 422, **1967.**

38- **Fairbairn,** J. ; Journal mechanical engineering science, Vol.9, 2, **1967**

39- **RCC-MR-model in**: Norbeto, N. & Merckling, G.; 'Use of Omega and ISO methods for the analysis of creep strain data', ISB, WG/31, 12/9/02, **2002** and [17-]

40- **Devis, J**. W. Cramer, B. A. ; Prediction and verification of creep behavior I metallic materials and componentsfor space shuttle thermal protection system, NASA, CR- 2685, **1976**

41- **F.A. Leckie, F. A. and D.R. Hayhurst, D. R**.; *Constitutive equations for creep rupture.* Acta Metall. vol.25 (**1977**), p. 1059

42- **ABAQUS** Finite Element Code, Hibbett, Karlsson and Sorensen Inc., Providence, RI, USA.

43- **Sandström R, Kondyr A**.; A model for tertiary creep in Mo- and CrMo-steels. In: Proceedings of third international conference on mechanical behaviour of materials, Cambridge, **1979**

44- **Moles, M. D. C. and Westwood, H. J.; "** Residual life estimation of high temperature superheater and reheater tubing," CER RP, 78-66,Final report of OntarioHydor Research Dev., Toronto, for the Canadian Electrical Assn., Montreal, Mar. 1982, p 67-82

45- **Viswanathan, R.;** "Damage mechanisms and life assessment of high temperature components, ASM International, Metal Park, Ohio 44073, 1989

46- **R.W. Evans and B. Wilshire,** Creep of metals and alloys, Institute of Metals (**1985**).

47- Johnson, G.R.; Cook, W.H. (1983), "A constitutive model and data for metals subjected to large strains, high strain rates and high", 1983

48- **Johnson,G. R.,Cook**, W.H. ; Fracture characteristics of three metals subjected to various strain rates, temperatures and pressures, Eng. Fracture Mechanics, 21(1), p 31-48, **1985**

49- **Modified Theta model** in: R.W. Evans and B. Wilshire, Creep of metals and alloys, Institute of Metals (**1985**).

50- **Rabotnov,** Y.N. ; Some problems of the theory of creep, NACA., TM, 1353, **1953**

**51- Rabotnov,** Y. N. ; On the equation of state of creep, ASME/ASTM/IMechE Proceedings Conference on creep, Inst. Mech. E., New York/London, **1963**

**52- Kachanov,** L. M. ; The theory of creep (ed. A. J. Kennedy), National Lending Library, Boston Spa, UK, **1967**

**53- Kachanov, L. M.,** ; Introduction to Continuum Damage Mechanics, Nijhoff, Dordrecht.**1987**

**54- Maruyama**, K. et al. ; Long-term creep curve prediction based on the modified θ projection concept. J. Pressure Vessel Technol., 112, **1990**

**55- Brinkman, C.R.; Booker, M.K.; and Ding, J.L.:** Creep and Creep-Rupture Behavior of Alloy 718. Proceedings of the International Symposium on the Metallurgy and Applications of Superalloys 718, 625, and Various Derivatives, Minerals, Metals & Materials Society, Warrendale, PA, **1991.**

**56- (CSWP)-model** in: Townley, C. H. A., et al., ; ''High Temperature Design Data for Ferritic Pressure Vessel Steels,'' Creep of Steels Working Party (CSWP), Inst. Mech. Eng., J. Mech. Eng., London. **1991**

**57- Bolton JL**. Design considerations for high temperature bolting. In: Strang A, editor. Proceedings of conference on performance of bolting materials in high temperature plant applications, York, 16–17/6/94, p. 1–14, **1994**

**58- Bartsch, H.,** ; 'A new creep equation for ferritic and martensitic steels' *SteelResearch*, **66**(9), 384-388, **1995**

**59- Bartsch-model** in: Holdsworth, S.R., 2002, 'Creep strain assessment using Bartsch and Bolton model equations', Alstom Power, WG1/32, 12/9/02**,[2002]**

60- **Prager**, M. 'Development of the MPC **Omega method** for life assessment in the creep range', ASME J. Pressure Vessel Technology, **1995**, **117**, May, 95-103.

61- **BJF-model: Jones**, D.I.G, French, R.M. and Bagley, R.L.; "A Renewal Theory of Inelastic Thermo-Mechanical Behavior of Metal Alloys"; ASME AD-Vol. 50, Fatigue and Fracture at Elevated Temperatures, A. Nagar and S. Mall, ed.; Book No. H01013-**1995**

62- **McLean, M. and B. F. Dyson**, B. J. ; Modeling the Effects of Damage and Microstructural Evolution on the Creep Behavior of Engineering Alloys, J. Eng. Mater. Technol.Vol.122, Issue 3, 273, July **(2000)**

63- **Rabotnov, *Y.* N.,** "Creep problems in structural members", English translation by F. A. Leckie,North Holland, Amsterdam, (1969).

64- **Hayhurst, D. R.,** "Creep continuum damage mechanics: A unifying theme in high temperature design ", High Temperature Structure Design, ESIS 12, Edited by L. H. Larsson, Mechanical Engineering Publications, London, (1992), 3 17-334.

65- **Dunne, F. P. E.,** Othman, A. M., Hall, F. R. and Hayhurst, D. R., "Representation of uniaxial creep curves using continuum damage mechanics", Int. J. of Mech. Sci., 32, 11, (1990), 945-957.

66- **Hyde, T. H., ;** "Constitutive equations for creep of metals", Proc. XXV AIAS International Conference of Materials Engineering, Gallipoli, Leece, (1996).

67- **Hyde,T. H. Sun, W. and Tang, A.;** Determination of material constants in creep continuum damage constitutive equations, UDC: 539.376, 620.1, 'Strain ', August I998

68- **Modified Garofalo model in: Granacher J**, Möhlig H, Schwienheer M, Berger C. Creep equation for high temperature material. In: Proceedings of seventh international conference on creep and fatigue at elevated temperatures (Creep 7), 3–8 June, NRIM, Tsukuba, p. 609–16, **2001**

69- **Modified Omega model** in: **Merckling** G. Metodi di calcolo a confronto per la previsione dellulteriore esercibilità in regime di scorrimento viscoso. In: Proceedings of conference on fitness for service, Giornata di Studio CESI-CONCERT, Milan, 28 November, **2002.**

70- **Altstadt, E**. ; Extension of ANSYS –creep plasticity and damage simulation capabilities,Forschungscentrum Rossendorf Dresden, **2003**

71- **ANSYS** Finite Element Code, Swanson Analysis Systems Inc., Houston, PA, USA.

72- **Baker and Cane model**: Baker AJ, O'Donnell MP. R5 high temperature structural integrity assessment of a cracked dissimilar metal weld vessel test. In: Proceedings of second international conference on integrity of high temperature welds, 10–12 November **2003**, London.

73- **MHG model:** Holmström S, Auerkari P. Prediction of creep strain and creep strength of ferritic steels for power plant applications. In: Proceedings of Baltica conference on life management and maintenance for power plants, VTT Symposium 234, 8–10 June, Espoo, **[2004]**

74- **Clech, J.-P.,** "An obstacle-controlled creep model for Sn-Pb and Sn-based lead-free solders", Proceedings (CD-ROM), SMTA International Conference (SMTAI'04), Chicago, IL., September 26-30, **2004** (available for download at: http://www.jpclech.com).

75- **J.-P. Clech:** Proc. Conf. on 'Electronic components and technology',Orlando, FL, USA, May–June **2005**, 1261–1271.

76- **Wu, R. Sandström, R. Seitisleam,** F. J. Eng. Mater. Technol., Vol. 126, pp. 87-94, 2004

77- **(CSWP)-model** in: Townley, C. H. A., et al., ; ''High Temperature Design Data for Ferritic Pressure Vessel Steels,'' Creep of Steels Working Party (CSWP), Inst. Mech. Eng., J. Mech. Eng., London. 1991, and **2005**

78- **Continuum Damage Mechanics (CDM)-based constitutive equation-model, [from 1985-2011], in:** Zhang ,W. ; "Review of damage mechanic", *Continuum damage mechanics (CDM)* Levy A., A physically *based constitutive equation* for creep-damaging solids ... *www.springerlink.com/index/P582140L5H666658.**pdf*** (2011)

79- **Holmström, S., and Auerkari, P.;** "Robust Prediction of Full Creep Curves From Minimal Data and Time to Rupture," Energy Mater: Mater. Sci.Eng. Energy Syst., **1**, pp. 249–255, **2006**

80- **Holmström, S., Auerkari, P., Holdsworth S.** Predicting creep strain response from rupture data and robust creep curve model. International Conference on Life Management and Maintenance for Power Plants. Helsinki-Stockholm-Helsinki, 12-14 June 2007. Vol 1.**2007**

81- **Holdsworth S.R., Merckling G.;** ECCC developments in the assessment of creep-rupture data. In: Proceedings of sixth international Charles Parsons Conference on engineering issues in turbine machinery, power plant and renewables, Trinity College, Dublin, 16–18 September, **2003**.

## Appendix C. MATLAB-Program for 7075-T6 Creep (Stress Dependency)

```
clear all;

 number = 20;

%T=648;

%n=0.426;

%m=2.473;

m=1.055;

p=0.0000034;

Ef=0.3;

 mesh=100;

 t=[0:10000/number:500000];

 hold on;

 for i = 1: length(t)

%A(i)=lognrnd(-9.48, 0.06);

%B(i)=lognrnd(-35.647, 0.11);

A(i)=lognrnd(-12.02375, 0.06);

B(i)=lognrnd(-39.367, 0.11);

s6=6.88;   %added

s1=7.88;
```

```
s2=8.86;

s5=10.535;   %added

s3=12.21;

s4=13.7;

E6(i)=A(i)*exp(0.3299*s6)* t(i)^(0.0085*s6+0.454) +  B(i)*(s6^9.5531)* t(i)^m* exp(2e-6*exp(0.1898*s6)*t(i));

E1(i)=A(i)*exp(0.3299*s1)* t(i)^(0.0085*s1+0.454) +  B(i)*(s1^9.5531)* t(i)^m* exp(2e-6*exp(0.1898*s1)*t(i)) ;

E2(i)=A(i)*exp(0.3299*s2)* t(i)^(0.0085*s2+0.454) +  B(i)*(s2^9.5531)* t(i)^m* exp(2e-6*exp(0.1898*s2)*t(i)) ;

E5(i)=A(i)*exp(0.3299*s5)* t(i)^(0.0085*s5+0.454) +  B(i)*(s5^9.5531)* t(i)^m* exp(2e-6*exp(0.1898*s5)*t(i));

E3(i)=A(i)*exp(0.3299*s3)* t(i)^(0.0085*s3+0.454) + B(i)*(s3^9.5531)* t(i)^m* exp(2e-6*exp(0.1898*s3)*t(i)) ;

E4(i)=A(i)*exp(0.3299*s4)* t(i)^(0.0085*s4+0.454) + B(i)*(s4^9.5531)* t(i)^m* exp(2e-6*exp(0.1898*s4)*t(i)) ;

end

axis([0  500000 0  0.7]);

xlabel('time[sec]');

ylabel('Creep strain E[%]');
```

```
title('Creep strain vs. time');

grid(gca,'minor')

plot(t, E1, 'b',t, E2, 'g', t, E3, 'r', t, E4, 'm', t, E5, 'c', t, E6, 'y');
```

Figure below shows a schematic result of this program.

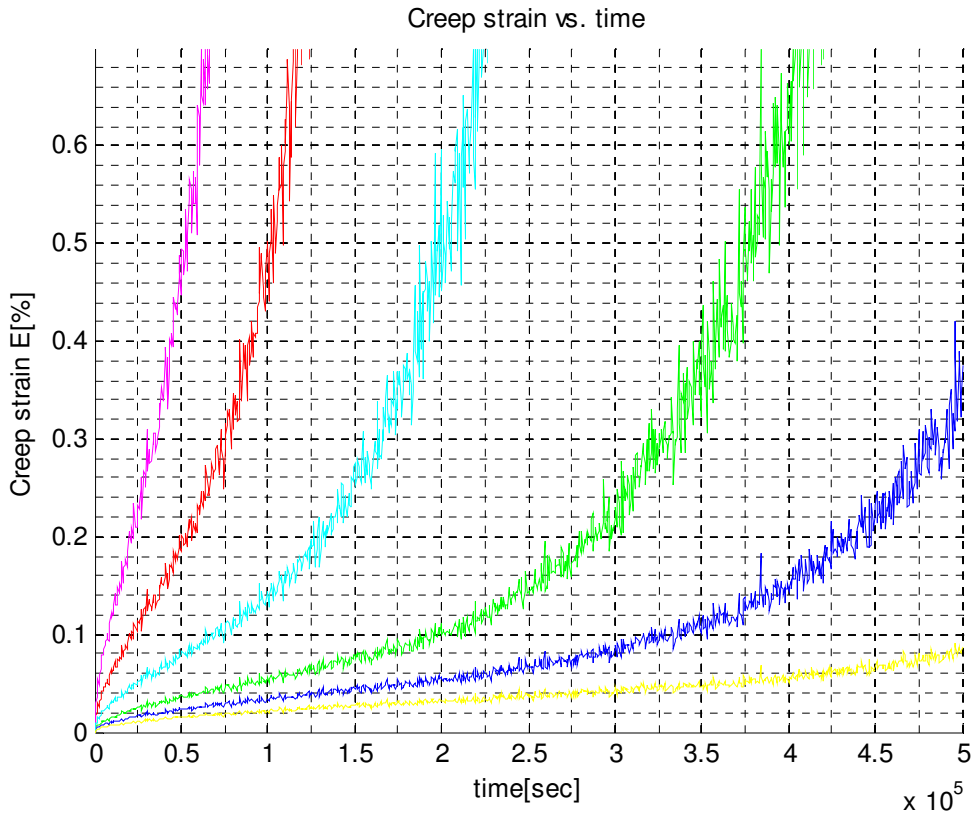


**Figure C1: MATLAB-picture from the above program for stress dependency of Al-7075-T6**

**Appendix D. MATLAB-Program for Creep of X-70 Carbon Steel (Stress and Temperature dependency)**

```
clear all;

number =500;

ns1= (-0.008);

Ea= (-269000);

R=8.31446;

a1= 0.0003;

b1= 0.000045;

c1= 0.39303;

d1= -0.013;

a2= 0.0006;

b2= 0.0001;

c2= 1.4784;

p1=8.015E-5;

p2= 0.006;

T (7)= 683;

T (1)= 691;

T (2)= 710;

T (3)= 723;
```

```
T (4)= 736;

T (5)= 743;

T (6)= 753;

 S (7)= 123;

 S (1)= 133;

 S (2)= 258;

 S (3)= 346;

 S (4)= 426;

 S (5)= 465;

 S (6)= 495;

 mesh =100;

t= [0:10000/number:15000];

for  i2=1:1

hold on;

for i=1:length(t)

    A(i)=lognrnd(38.4706, 0.11);

   %A(i)=lognstat(38.4706, 0.11);

    B(i)=lognrnd(-17.94011, 0.12);

   %B(i)=lognstat(-17.94011, 0.12);
```

```
Beta17= (a1*T(7)) + (b1*S(7))+c1;

Beta11= (a1*T(1)) + (b1*S(1))+c1;

Beta12= (a1*T(2)) + (b1*S(2))+c1;

Beta13= (a1*T(3)) + (b1*S(3))+c1;

Beta14= (a1*T(4)) + (b1*S(4))+c1;

Beta15= (a1*T(5)) + (b1*S(5))+c1;

Beta16= (a1*T(6)) + (b1*S(6))+c1;

Beta27= (-a2*T(7))+ (-b2*S(7))+c2;

Beta21= (-a2*T(1))+ (-b2*S(1))+c2;

Beta22= (-a2*T(2))+ (-b2*S(2))+c2;

Beta23= (-a2*T(3))+ (-b2*S(3))+c2;

Beta24= (-a2*T(4))+ (-b2*S(4))+c2;

Beta25= (-a2*T(5))+ (-b2*S(5))+c2;

Beta26= (-a2*T(6))+ (-b2*S(6))+c2;

E7(i)=A(i)*exp(ns1*S(7))*exp(Ea/(R*T(7)))*t(i)^(Beta17) + B(i)*exp(d1*S(7))*t(i)^(Beta27)
*exp(p1*exp(p2*S(7))*t(i));

E1(i)=A(i)*exp(ns1*S(1))*exp(Ea/(R*T(1)))*t(i)^(Beta11) + B(i)*exp(d1*S(1))*t(i)^(Beta21)
*exp(p1*exp(p2*S(1))*t(i));

E2(i)=A(i)*exp(ns1*S(2))*exp(Ea/(R*T(2)))*t(i)^(Beta12) + B(i)*exp(d1*S(2))*t(i)^(Beta22)
*exp(p1*exp(p2*S(2))*t(i));
```

```
    E3(i)=A(i)*exp(ns1*S(3))*exp(Ea/(R*T(3)))*t(i)^(Beta13) + B(i)*exp(d1*S(3))*t(i)^(Beta23)
*exp(p1*exp(p2*S(3))*t(i));

    E4(i)=A(i)*exp(ns1*S(4))*exp(Ea/(R*T(4)))*t(i)^(Beta14) + B(i)*exp(d1*S(4))*t(i)^(Beta24)
*exp(p1*exp(p2*S(4))*t(i));

    E5(i)=A(i)*exp(ns1*S(5))*exp(Ea/(R*T(5)))*t(i)^(Beta15) + B(i)*exp(d1*S(5))*t(i)^(Beta25)
*exp(p1*exp(p2*S(5))*t(i));

    E6(i)=A(i)*exp(ns1*S(6))*exp(Ea/(R*T(6)))*t(i)^(Beta16) + B(i)*exp(d1*S(6))*t(i)^(Beta21)
*exp(p1*exp(p2*S(6))*t(i));

    end

  end

  axis([0 15000 0 0.07]);

  xlabel('time');

  ylabel('Creep strain, E(mm)');

  title('Creep strain "E" vs. Time "t"');

   %plot(t, E1,'b', t, E2, 'r',t, E3, 'g',t, E4,'k',t, E5,'k',t, E6,'k',t, E7,'r',t, E8,'g',t, E9,'g',t, E10,'r');

   plot(t, E7,'k',t, E1,'b', t, E2, 'g',t, E3, 'r',t, E4,'k',t, E5,'b',t, E6,'k');

  %plot(t, E1,'b');

  % hold off
```

Figure below shows the result for the temperature and stress dependency of X-70 carbon steel from MATLAB program.

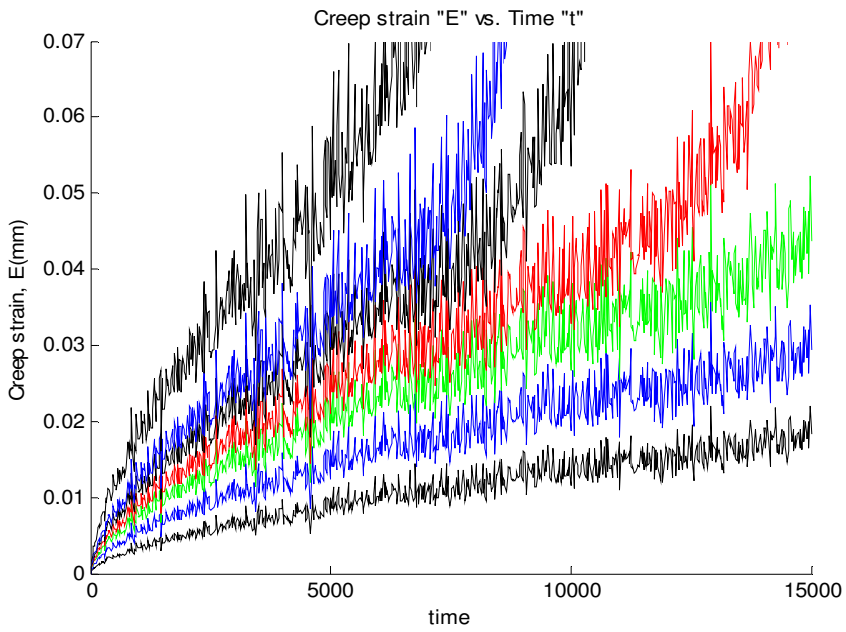


**Figure D1: MATLAB-picture from the above program for Temperature and stress dependency of X-70 carbon steel**

## Appendix E. Example of a WinBUGS- Program for Creep of materials

```
Model {
A~dunif(0, 30)
B~dunif(-150,0)
s2~dunif (0, 100)
ns1~dlnorm (-4.92, 1.60637E6)
nt1<-17078.6798
d1~dlnorm (-1.489, 10000)
p1~dlnorm (-30, 10000)
p2~dlnorm (-3.34, 5.6689E6)
        C <- 1000000
                        for(i in 1:267){
                            zeros[i] <- 0
m[i]<- (exp(A)*pow(x[i,3],-ns1)*exp(-nt1/x[i,4])*pow(x[i,2],
(0.2119*exp(0.0023*x[i,3])))+exp(B)*exp(d1*x[i,3])*pow(x[i,2],
(0.1943*exp(0.004*x[i,3])))*exp(p1*exp(p2*x[i,3])*x[i,2]))
L[i]<-exp(-0.5*pow((log(x[i,1]) -log(
m[i]))/s2,2))/(s2*2.50663*(x[i,1]))
                                phi[i]<- -log(L[i])+C
                            zeros[i] ~ dpois(phi[i])
          }
                        }
```

## Appendix F. Example of a WinBUGS Program for Non-Linear Regression Model of Creep of Materials

```
Model {

n~dunif(0,0.7)
m~dlnorm(0.4567, 100)
c~dlnorm(-26.04, 100)
p~dlnorm(-5.918,100)
#a<-0.0013

s~dunif(0,100)

        C <- 1000
                        for (i in 1:N){
                            zeros [i] <- 0

          L[i]<-exp(-0.5*pow((x[i,2]-(0.00003*exp(7.0744*n))*pow(x[i,1],n)-
c*pow(x[i,1],m)*exp(p*x[i,1]))/s,2))/(pow((2*3.141592654),0.5)*s)

                            ghr[i]<-(-1)*log(L[i])+C
                            zeros[i]~dpois(ghr[i])
                        }
                          tau<-1/pow(s,2)
                          e~dnorm(0,tau)
                          for (j in 1:10){
                          y0[j]<-
(0.00003*exp(7.0744*n))*pow(x0[j],n)+c*pow(x0[j],m)*exp(p*x0[j])+e
                        }

                        }
```

## Appendix G. Akaike Information Criterion

Akaike [ch.2, 17] found a formal relationship between information theory that was based on the relative entropy and the maximum likelihood (ML) of the statistical theory. Akaike combined ML, least square and model selection under a unified theoretical framework under the name of Akaike's information criterion (AIC).

$$AIC = -2\ln\left(\mathrm{L}(\hat{\theta}|\mathrm{data})\right) + 2K \tag{G1}$$

where $\ln\left(\mathrm{L}(\hat{\theta}|\mathrm{data})\right)$ is the value of the maximum loglikelihood over the unknown parameters ($\hat{\theta}$), given the data and the model, and K is the number of model parameters.

In the special case of least-square estimation with normally distributed errors, AIC is described by:

$$AIC = n\log(\hat{\sigma}) + 2K, \quad with\ \hat{\sigma}^2 = \frac{\sum \hat{e}_i{}^2}{n} \tag{G2}$$

where $\hat{e}_i$ are the estimated residuals from the fitted model.

### AG1. Classification or Ranking the models

Akaike's approach allows identifying the best model in a group of models and allows ranking the rest of the models easily. It is possible to rescale AIC values with a parameter like $\Delta_i$ such that the model with the minimum information criterion has a value of 0 (zero), i.e.

$$\Delta_i = AIC - \min\,(AIC) \tag{G3}$$

The $\Delta_{i,}$ values are easy to interpret and allow a quick comparison and ranking of models. The smaller the $\Delta_{i,}$ the better is the fitted model. It is generally important to know which model is the second best (the ranking) with respect to the best model. According to this description a

ranking procedure was created.

Models having

- $\Delta_i \leq 2$ Substantial Support
- $4 \leq \Delta_i \leq 7$ Limited Support
- $\Delta_i > 10$ No support by the data

Akaike [ch.2, 17], derived later (1981) the expression $\exp\left(-\frac{\Delta_i}{2}\right)$ which gives the likelihood of the model given the data: $L(g_i|data)$.

$$L(g_i|data = y) = \exp\left(-\frac{\Delta_i}{2}\right) \tag{G4}$$

It is often useful to normalize these likelihoods. Akaike gave the following weight parameters for comparing models with one another:

$$w_i = \frac{\exp\left(-\frac{\Delta_i}{2}\right)}{\sum_{r=1}^{N} \exp\left(-\frac{\Delta_r}{2}\right)} \tag{G5}$$

$w_{i,}$ is the Akaike weight and provides a relative weight of evidence for each model [ch.2, 17].

# Appendix H. First Page of Published Papers

ELSEVIER

Available online at www.sciencedirect.com

ScienceDirect

Procedia Engineering 10 (2011) 1930–1935

Engineering Procedia

ICM11

## Reliability Analysis for Degradation Effects of Pitting Corrosion in Carbon Steel Pipes

M. Nuhi[a], T. Abu Seer[b], A. M. Al Tamimi[a], M. Modarres[*a], A. Seibi[b]

[a]Center for Risk and Reliability, Department of Mechanical Engineering, University of Maryland, College Park 20742, US
[b]Mechanical Engineering Department of Petroleum Institute, Abu Dhabi, UAE

**Abstract**

Corrosion is a major cause of failure in some metals with adverse effects on reliability of components and structures made from such metals. For example in carbon steel pipes various forms of localized corrosion, pitting corrosion, and stress corrosion cracking (SCC) cause sudden and catastrophic failures due to the absence of any external sign of damage in the system. Studying the growth of pit depth and pit densities at different temperatures and stress conditions with respect to time is critical in monitoring the localized corrosion damage and preventing the system downtime. A new probabilistic physics-of-failure (PPOF) model is developed to determine the temperature and stress dependencies of pit depth growth with respect to time. In doing so, microscopic methods are used to determine the pit depths produced on X-70 carbon steel samples subjected to accelerated corrosion tests. The pit depths and densities are measured in unstressed and stressed samples exposed to a solution of Sodium thiosulfate and water at different times and temperatures to ascertain the temperature and stress dependencies of pit depths that propagate during the pitting corrosion process. The stress and temperature dependency of the new model follows the exponential law (Arrhenius law), which allows estimating the activation energy of pitting corrosion process. Moreover, the pit size and intensity under different temperatures and stress conditions, estimated at different times, appear to follow the lognormal distribution. The uncertainty associated with the proposed models due to scattering of pit data and also the autocorrelation among such data are accounted for.

© 2011 Published by Elsevier Ltd. Selection and peer-review under responsibility of ICM11

Keywords: Pitting Corrosion; Pit Depth; Lognormal Distribution; Reliability; Uncertainty Analysis; Autocorrelation; Bayesian inference.

Reliability Engineering and System Safety 96 (2011) 1601–1610

Contents lists available at SciVerse ScienceDirect

Reliability Engineering and System Safety

journal homepage: www.elsevier.com/locate/ress

# A probabilistic physics-of-failure model for prognostic health management of structures subject to pitting and corrosion-fatigue

M. Chookah[1], M. Nuhi, M. Modarres*

*Department of Mechanical Engineering, University of Maryland-College Park, Glenn L. Martin Hall, College Park, MD 20742, USA*

ARTICLE INFO

*Article history:*
Received 31 December 2010
Received in revised form
30 June 2011
Accepted 15 July 2011
Available online 16 August 2011

*Keywords:*
Pitting
Fatigue crack growth
Corrosion-fatigue
Probabilistic modeling

ABSTRACT

A combined probabilistic physics-of-failure-based model for pitting and corrosion-fatigue degradation mechanisms is proposed to estimate the reliability of structures and to perform prognosis and health management. A mechanistic superposition model for corrosion-fatigue mechanism was used as a benchmark model to propose the simple model. The proposed model describes the degradation of the structures as a function of physical and critical environmental stresses, such as amplitude and frequency of mechanical loads (for example caused by the internal piping pressure) and the concentration of corrosive chemical agents. The parameters of the proposed model are represented by the probability density functions and estimated through a Bayesian approach based on the data taken from the experiments performed as part of this research. For demonstrating applications, the proposed model provides prognostic information about the reliability of aging of structures and is helpful in developing inspection and replacement strategies.

© 2011 Elsevier Ltd. All rights reserved.

## 1. Background and motivation

Structures such as pipes and steam generator tubes in power plants and oil pipelines subject to changing loads and corrosive agents are susceptible to degradation over the span of their service lives. Corrosion (especially chloride and $H_2S$ corrosion) is one of the most common degradation mechanisms, but other critical mechanisms, such as stress corrosion cracking (SCC) and creep, are also important. The rate of degradation is influenced by many factors, such as piping material, characteristics of the fluid, process conditions, geometry and location. Based on these factors, a best estimate for the service life (reliability) can be calculated. This estimate serves as a target guideline for prognosis and health management (PHM), preventive maintenance and replacement practices. After a long period of service, however, this estimate requires re-evaluation due to new evidence observed from monitoring conditions of the structure.

A number of deterministic models have been proposed to estimate the reliability of pipes. Among these models is the ASME B31G code [1], which is the most widely used method for the assessment of pipe corrosion [2]. However, these models are highly conservative and unable to estimate the true life and health of the structure. In addition to the limitations embedded in these deterministic models are the problems associated with inspection techniques and tools that may be inadequate and inaccurate.

The research summarized in this paper proposes and compares a simple empirical probabilistic model developed using information from well-established mechanistic models for pitting-corrosion and corrosion-fatigue. The parameters of the proposed empirical model are estimated through a formal Bayesian inference from data obtained from pitting and corrosion-fatigue experimental tests. Uncertainties about the structure of the model itself and parameters of the model are characterized. The proposed model can capture wide ranges of structural materials [2–10] and accounts for variability in material and size. The existing probabilistic models sufficiently address the corrosion and fatigue mechanisms individually, but are inadequate to capture mechanisms that synergistically interact such as corrosion-fatigue. Further, the mechanistic models have far too many parameters and are too complex for routine reliability and life estimation practices, especially for routine use in the field. The proposed model alleviates these shortcomings.

Admitting the fact that capturing all degradation mechanisms would be a challenging task, the new model addresses two of the most important mechanisms that synergistically interact: pitting-corrosion and corrosion-enhanced fatigue crack growth. This paper first reviews the literature in pitting and corrosion-fatigue and then prepares a simulation technique to inform the empirical model development process. It describes a procedure for estimating the parameters of the proposed model. Finally, it discusses the

* Corresponding author.
*E-mail address:* modarres@umd.edu (M. Modarres).
[1] Current address: Emirates Nuclear Energy Corporation, Abu Dhabi, United Arab Emirates.

0951-8320/$ - see front matter © 2011 Elsevier Ltd. All rights reserved.
doi:10.1016/j.ress.2011.07.007

## Reference to Chapter 1


1. Roesler, J. et al, "Mechanical Behaviour of Engineering Materials", Springer, Berlin, Heidelberg New York, 2007.
2. Viswanathan, R., "Damage Mechanisms and Life Assessment of High-Temperature Components". Metals Park, Ohio: ASM International, 1989.
3. Neubauer, B.; Wedel, U., "Restlife Estimation of Creeping Components by Means of Replicas", in ASME International Conference on Advances in Life Prediction Methods, Eds. D.A. Woodford, J.R. Whitehead, ASME, New York, 1983
4. http://www.mech.uq.edu.au/courses/mmme2104/chap11/maintenance.htm
5. Creep and high temperature failures, users.encs.concordia.ca/~mmedraj/.../lecture%2012%20 creep.pdf.
6. D.R.H. Jones "Creep failures of overheated boiler, superheater and reformer tubes", Engineering Failure Analysis", 11, 873–893, 2004
7. Ashby, M.F. "A First Report on Deformation-Mechanism Maps", Acta Met., v. 20, p. 887-897, 1972.
8. Mohamed, F.A.; Langdon, T.G. "Deformation Mechanism Maps: Their Use in Predicting of Creep Behavior", J. Eng. Matls. and Technol., v. 98, p. 125-130, 1976.
9. Frost, H. J., & Ashby, M. F., "Deformation-Mechanism Maps: The Plasticity and Creep of Metals and Ceramics", pp. 1-5, 20-29, Oxford: Pergamon Press, 1982
10. Yousefiani, Ahmadali, Farghallia. Mohamed, and Earthma, James. C. N; "Creep Rupture Mechanisms in Annealed and Overheated 7075 Al under Multiaxial Stress States", Metallurgical and Materials Transactions A , Vol. 31A, Nov. 2000

11. Pedersen, K. O., Børvik , T., Hopperstad, O. S.; "Fracture mechanisms of aluminium alloy AA7075-T651 under various loading conditions", Materials and Design 32, 97–107, 2011

12. Zou Hong-hui, "Effects of microstructure on creep behavior of Mg-5%Zn-2%Al(-2%Y) alloy", Trans. Nonferrous Met. Soc. China 18, 2008

13. Kelvin- Voigt creep model, *cube.case.edu/EMAC403/EAMC403_Mechanical%20**Models.pdf***

14. Holmström, S., Auerkari, P., Holdsworth S. "Predicting creep strain response from rupture data and robust creep curve model", International Conference on Life Management and Maintenance for Power Plants. Helsinki-Stockholm-Helsinki, 12-14 June 2007. Vol. 1., 2007

15. M. Evans, "Predicting times to low strain for a 1CrMoV rotor steel using a 6-theta projection technique", Journal of Materials Science, **35,** 2937 – 2948, 2000

16. Garofalo, F. "Fundamental of creep and creep-rupture in metals", 16 (Macmillan), 1965

17. Evans, R.W., and Wilshire, B.; "Creep of metals and alloys", Institute of Metals 1985

18. Sawada, K. et.al."Analysis of long-term creep curves by constitutive equations". Material science and engineering A 510-511, 190-194, 2009

19. For references given in the Table 1.2, see Appendix B.

**Reference to Chapter 2**


1. Norton, F.H. ; "Creep of steel at high temperatures", McGraw-Hill Book Co. Inc. 1929
2. Sawada, K. et. al."Analysis of long-term creep curves by constitutive equations".Material Science and Engineering A 510-511,190-194, 2009
3. Maruyama, K. and H. Oikawa. Tetsu-to-Hagane, **73**, pp. 26–33, 1987
4. Holdsworth. S., Mater. High Temp., **21**, pp. 25–32, 2004
5. GAROFALO, F. Fundamental of creep and creep-rupture in metals. 16 (Macmillan), 1965.
6. Wilshire. B. and Burt, H., "A unified theoretical and practical approach to creep and creep fracture", Materials science and engineering,p. 3-12, 2005
7. Dyson, B. F., ISI J International, Vol. 30, No, lO, pp. 802-81, 1990
8. Graham, A. and Walles, K.F.A. ; NGTE Reports Nos.R.100, 1952, R.137, 1953, R.189 and R.190, 1956; J. Iron and steel Inst.179,105, 1955
9. Feher, A., et.al. In FVW/FVHT, Stahl-Zentrum Duessseldorf, Germany 28. N0v. 2008
10. Maruyama, K. and Oikawa, H., Trans. ASME, J. Press. Vess.Technol. 109, 142, 1990
11. Maruyama, K. and Oikawa, H., J. Jpn. Inst. Met. 55, 189, 1991.
12. Kachanov, L. M. ; "The theory of creep", (ed. A. J. Kennedy), National Lending Library, Boston Spa, UK, 1967
13. Penny, R.K., and Marriott, D. L.; "Design for creep", Chapman & Hall, 1971
14. Rabotnov, Y. N., "Creep problems in structural members", English translation by F. A. Leckie, North Holland, Amsterdam, 1969.
15. Evans, M.,"Predicting times to low strain for a 1CrMoV rotor steel using a 6-$\mu$ projection technique", Journal of Materials Science, **35,** 2937–2948, 2000

16. Bailey, R. W., "Steam piping for high pressure and high temperature", A Archive: Proceeding of the Institution of Mechanical Engineers, 1847-1982, (vol. 1-196), vol. 164, pp.324-350, 1951

*17.* Burnham, K. P. and Anderson, D. R.," Model selection and multimodel inference, A practical Information-theoretic Approach, Springer, 2002

18. Zhao, Bin, et.al. "Experiment and simulation of creep damage for duralumin alloy 2A12", Material Science and Engineering A 513-514, 91-95, 2009

19. Lin, J., Kowalewski, Z. L. and Cao, J., Int. J. Mech. Sci. **47**, pp. 1038–1058, 2005, Article | PDF (322 K) | View Record in Scopus | Cited By in Scopus (6)

20. Kachanov, L. M., *Izv. AN SSSR, OTN* **8**, pp. 26–31, 1958

21. Kachanov, L. M., "The Theory of Creep", British Library, Boston Sp, Wetnerley, 1960

22. Rabotnov, Y. N., "Creep Problems in Structural Members", Amsterdam, North-Holland 1969

23. Huang, R., Turbine Technol. **43**, pp. 9–13, 2001

24. Evans, R.W., and Wilshire, B. "Creep of Metals and Alloys", The Institute of Metals, London, 1985

25. Evans, R. W. and Wilshire, B., "Introduction to Creep", The Institute of Materials, London 1993

26. Burt, H. and Wilshire, B., Metall. Mater. Trans. A **35A** , pp. 1691–1701, 2004

27. Burt, H. and Wilshire, B., *Metall. Mater. Trans. A* **36A** (2005), pp. 1219–1227, 2005

28. Zhao, Bin., et.al."Experiment and simulation of creep damage for duralumin alloy 2A12, Materials Science and Engineering A 513-514, 91-96, 2009

29. Ling, X., Zheng. Y. Y. and You, Y. J., Int. J. Pressure Vessels Piping **84** (2007), pp. 304–309, 2007 **Article** | PDF (339 K) | View Record in Scopus | Cited By in Scopus (8)

30. Azarkhail, M., Ontiveros, V., Modarres. M., "A Bayesian Framework for Model Uncertainty Consideration in Fire Simulation Codes." 17 th. International Conference on Nuclear Engineering, Brussels, 2009

31. Azarkhail, M. and Modarres, M., "A Novel Bayesian Framework for Uncertainty Management in Physics-Based Reliability Models", ASME International Mechanical Engineering Congress and Exposition, November 11-15, Seattle, Washington, USA., 2007

**Reference to Chapter 3**

1. Metal Handbook,(ASTM), Jeffery C. Gibeling "Creep deformation of Metals, polymers, ceramics, and composites".vol.8, Metal testing and evaluation p363-382, 2000
2. Metal Handbook,(ASTM),Howard R. Voorhees, "Assessment and use of Creep-Rupture properties", vol. 8, Metal testing and evaluation p383-397, 2000
3. Penny, R.K., and Marriott, D.L., "Design for Creep", Chapman & Hall, London. 1971
4. Norton, F.H., "The Creep of Steel at High Temperatures"; McGraw-Hill, London, 1929
5. Johnson, A.E. et. Al. Multi-axial creep strain/complex stress/time relations for metallic alloys with some applications to structures, in ASME/ASTM/I Mech. E, Proceedings Conference on creep, Inst. Mech. E., New York/London
6. Dorn, J.E. "Some fundamental experiments on high temperature creep,J.Mech.Phys.Solids,3, 1955

7. Soderberg, C.R. The interpretation of creep tests for machine design Trans. ASME,58, 1936

8. McVetty, P.G. “Working stresses for high temperature service”, Mech. Eng.,56,1934

9. Garofalo, F. “Fundamentals of creep and creep rupture in metals”, Mac Millan, New York. 1965

10. Evans, R. W. and Wilshire, B.” Introduction to creep”, “The institute of materials,1993

11. R.W. Evans and B. Wilshire, “Creep of Metals and Alloys” (London: The Institute of Metals, pp. 203–243, 1985

12. Levi de Oliveira, Bueno, “ Effect of oxidation on creep Data: Part 2- A procedure for Assessing the effect of oxidation on Constant Stress or Constant load Creep curves using the Theta-Projection Concept”, ECCC Creep Conference,12-14,September,London.p890-899, 2005

13. Klenk, A. et.al., “Experimental and Numerical Investigations on Creep Damage Evolution”, Key Eng. Mats., Vols. 171-174, pp.25-34, Trans. Tech. Publications, Switzerland, 2000

14. ABU-Haiba, M. S., et.al., “ Creep deformation and monotonic stress-strain behavior of Haynes Alloy 556 at elevated temperature”, Journal of material science 37, 2899-2907, 2002

15. Hyde, T.H. “Creep of materials and structures, Mechanical Engineering Publications, London, 1994

16. Metal Handbook,(ASTM),Howard R. Voorhees, “Assessment and use of Creep-Rupture properties”, vol. 8, Metal testing and evaluation p383-397, 2000

17. Dorn, J.E. “Some fundamental experiments on high temperature creep. J. Mech. Phys. Solids, 3, 1955
18. R.W. Evans and B. Wilshire,” Introduction to creep”, The institute of materials,1993
19. Evans, R.W. and Wilshire, B. “Creep of Metals and Alloys”, London: The Institute of Metals, pp. 203–243, 1985
20. R.W.Bailey, “Steam piping for high pressure and high temperature”, A Archive: Proceeding of the institution of mechanical Engineers, 1847-1982, (vol. 1-196), vol. 164, 1951, pp.324-350, 1951
21. Klenk, A. et al.,”Experimental and Numerical Investigation on Creep Damage Evolution”, Key Engineering Materials, Trans. Tech. Publications, vol. 171-174, pp25-34, 2000
22. M.Malchin and Lupinc, “Modeling the high temperature creep behavior of a new single crystal Nickel based superalloy” Key Engineering Materials, Trans. Tech. Publications, vol. 171-174, pp245-252, 2000
23. F.R.N.Nabarro and H.L. de Villiers, “The Physics of Creep”, Taylor & Francis Publisher, 1995, pp. 32-33. Metal Handbook,(ASTM), Jeffery C. Gibeling “Creep deformation of Metals, polymers, ceramics, and composites”.vol.8, Metal testing and evaluation p363-382, 2000

**References to Chapter 4**

1. Schuren, Jay, ; Aluminum 7075 Microstructure and Current Research through the use of In- situ X-ray Diffraction, ftp://ftp.ccmr.cornell.edu/tmp/410/MS&E%20410/.../Schuren.pdf

**References to Chapter 5**


1. Brooks, S. P. "Markov Chain Monte Carlo Method and its Application,"The statistician, Royal Statistical Society, Vol. 47, No. 1, pp. 69-100, 1998

2. Spiegelhalter, D., Thomas, A., Best, N., and Lunn, D., WinBUGS 1.4 Manual, 2003

3. Azarkhail, M., and Modarres, M. "A Novel Bayesian Framework for Uncertainty Management in Physics-Based Reliability Models," *Proceedings of IMEC2007*, 2007 ASME International Mechanical Engineering Congress and Exposition, Seattle, Washington, USA, 2007

4. Azarkhail, M., and Modarres, M. "Markov Chain Monte Carlo Simulation for Estimating Accelerated Life Model Parameters," *Annual Reliability and Maintainability Symposium (RAMS) Proceedings*, Orlando, FL, USA, 2007


**References to Chapter 6**


1. Monkman, F.C. and Grant, N.J. "An empirical relationship between rupture life and minimum creep rate in creep-rupture tests", Proc. ASTM,56,593, 1956

2. Conway, J.B. ; "Numerical methods for creep and rupture analysis", Gordon and Beach, Science Publisher, New York, 1967

3. LEE, D.Y., PARK, J.G. and CHO, D.H.; "High-temperature properties of dispersion-strengthened 7075-T6 aluminum alloy", Journal of Materials Science Letters **16,** 158–160, 1997

4. Burt, H. and Wilshire, B. ; "Theoretical and Practical Implications of Creep Curve Shape Analyses for 7010 and 7075", Metallurgical and Materials Transactions A, Vol. 37A, March, 2006—1005

5. Garofalo, F. Whitemore, R.W. et.al.; "Creep and creep-rupture relationships in an austenitic stainless steel", Trans. AIME 221, 310, 1961.

6. Larson,F.R. and Miller,J. ; "A time-temperature relationship for rupture and creep stresses", Trans. ASME, 74, 765,1952

7. Dorn, J. E. ; "Some fundamental experiments on high temperature creep", J. Mech. Phys. Solids, 3, 1955

8. Syn, C.K. et al. *;* " Stress-Strain Rate Relations in Ultra High Carbon Steels Deformed in the Ferrite Range of Temperature", UCRL-JC-151884February 20,2003 Thermec 2003 International Conference on Processing and Manufacturing of Advanced Materials; Leganes, Madrid, Spain, July 7-1 1, 2003

9. Moles, M. D. C. and Westwood, H. J.; " Residual life estimation of high temperature superheater and reheater tubing," CER RP, 78-66,Final report of OntarioHydor Research Dev., Toronto, for the Canadian Electrical Assn., Montreal, Mar., p 67-82, 1982

10. Viswanathan, R.; "Damage mechanisms and life assessment of high temperature components, ASM International, Metal Park, Ohio 44073, 1989

11. Wardle, T. J.; Creep-rupture assessment of superheater tubes using nondestructive oxide thickness measurements, ICOLM (International Conference on Life Management and Life Extension of Power Plant), Xi'an, P.R. China, May 2000

12. Remaining life assessment of refinery furnace tubes using Omega Simulations, www.aiche-chicago.org/symposium06/wilks.**pdf**